Fall 2001

Automated myocardial infarction diagnosis from ECG

Chen Zhou
Louisiana Tech University

INFORMATION TO USERS

This manuscript has been reproduced from the microfilm master. UMI films the text directly from the original or copy submitted. Thus, some thesis and dissertation copies are in typewriter face, while others may be from any type of computer printer.

The quality of this reproduction is dependent upon the quality of the copy submitted. Broken or indistinct print, colored or poor quality illustrations and photographs, print bleedthrough, substandard margins, and improper alignment can adversely affect reproduction.

In the unlikely event that the author did not send UMI a complete manuscript and there are missing pages, these will be noted. Also, if unauthorized copyright material had to be removed, a note will indicate the deletion.

Oversize materials (e.g., maps, drawings, charts) are reproduced by sectioning the original, beginning at the upper left-hand corner and continuing from left to right in equal sections with small overlaps.

Photographs included in the original manuscript have been reproduced xerographically in this copy. Higher quality 6" x 9" black and white photographic prints are available for any photographs or illustrations appearing in this copy for an additional charge. Contact UMI directly to order.

ProQuest Information and Learning
300 North Zeeb Road, Ann Arbor, MI 48106-1346 USA
800-521-0600

NOTE TO USERS

This reproduction is the best copy available.

UMI®

AUTOMATED MYOCARDIAL INFARCTION DIAGNOSIS FROM ECG

by

Chen Zhou, B. E.

A Dissertation Presented in Partial Fulfillment
of the Requirements for the Degree
Doctor of Philosophy

COLLEGE OF ENGINEERING AND SCIENCE

LOUISIANA TECH UNIVERSITY

November 2001

LOUISIANA TECH UNIVERSITY

THE GRADUATE SCHOOL

October 19, 2001
Date

We hereby recommend that the dissertation prepared under our supervision by Chen Zhou entitled Automated Myocardial Infarction Diagnosis from ECG be accepted in partial fulfillment of the requirements for the Degree of Doctor of Philosophy

Stan Napper
Supervisor of Dissertation Research

Stan Napper
Head of Department

Biomedical Engineering
Department

Recommendation concurred in:

Advisory Committee

Approved:
Director of Graduate Studies

Approved:
Dean of the Graduate School

Dean of the College

GS Form 13
(1/00)

ABSTRACT

In the present dissertation, an automated neural network-based ECG diagnosing system was designed to detect the presence of myocardial infarction based on the hypothesis that an artificial neural network-based ECG interpretation system may improve the clinical myocardial infarction. 137 patients were included. Among them 122 had myocardial infarction, but the remaining 15 were normal. The sensitivity and the specificity of present system were 92.2% and 50.7% respectively. The sensitivity was consistent with relevant research. The relatively low specificity results from the rippling of the low pass filtering. We can conclude that neural network-based system is a promising aid for the myocardial infarction diagnosis.

TABLE OF CONTENTS

LIST OF TABLES

CONTENTS **PAGES**

LIST OF FIGURES

CONTENTS **PAGES**

ACKNOWLEDGMENTS

I must first acknowledge my parents, Xinrong Zhou and Zuying Yang. Through all of my pursuits, educational and otherwise, I was constantly reassured by their love, patience, support, and encouragement, especially through difficult times.

I must certainly acknowledge my committee. I am grateful to Dr. Stan Napper for being my advisor for the past four years. I also want to thank Dr. Edwin Alexander, Dr. Huaijin Gu, Dr. Paul Hale, and Dr. Steven Jones for providing valuable suggestions and support in the preparation of this dissertation.

I also want to say thanks to the cardiologists, Rong Dong and Chunying Yang, in the Beijing Hospital, for their cooperation and support.

I also want to extend my gratitude to those who provide guidance and assistance during these years. Thanks to Dr. Zou for his advice on signal processing, and thanks to Dr. Srikanth for his guidance in my research. Finally, I thank all my friends for their love and support.

CHAPTER 1

INTRODUCTION

1.1 Research Need

Heart diseases are the leading killers of Americans today. Over 60 million Americans have one or more heart diseases. In 1993, more than 950,000 people died from them--over 42 percent of all deaths in the United States [American Heart Association News Letter, 1999]. But many of them could be healed, especially if we could detect the diseases at early stage. The electrocardiogram (ECG) is the most common and most successful diagnostic method to detect early pathological changes of the heart. For several decades, computerized ECG interpretation has been used by clinicians and cardiologists as a much needed supplement [Willems et al., 1990].

Unfortunately, because of the mechanism of ECG and the recording methods, there are many difficulties in interpreting ECG output. Because an ECG is the recorded potential difference at the body surface, any movement of sensors or anything influencing the electrical signals will alter the shape of the wave. Also since the physiological structures of humans vary, different people have different shapes of ECG. Therefore, the wave shape of the same disease may have many different versions. For some diseases, the clinical symptoms are seen in the ECG only when the disease is first apparent, whereas many cardiac diseases develop over a long time, e.g., myocardial infarction. It may take

one month to one year to make a diagnosis for such disease. Sometimes, patients are told to carry a Holter ambulatory monitor, which can record their ECG for about 24 hours. During 24 hours, the number of ECG waves will be over 100,000. It is unreasonable to expect cardiologists to read all the waves and make a diagnosis in 30 minutes.

The appearance and the development of computers and automated interpretation greatly changes the lives of people. They also have changed clinical diagnosis significantly. Twenty-five years ago, the ECG was among the first biomedical signals to be processed by computers. Today, people are still trying to find more efficient computer applications for ECG processing. Mainly, there are two kinds of applications: one is off-line interpretation of the ECG, and the other is dynamic on-line analysis. In the former application, ECG waves are examined by computers for anomalies of shape, size, and rate, and the diagnosis is then given. Some software will also give statements about the possible physiological state which would cause such anomalies. The latter is most often used in the ICU to detect vital cardiac rhythm disturbances.

Currently there are many integrated commercial ECG analysis systems, especially Holter analysis [Srikanth, 2000], to help cardiologists make a diagnosis. After several decades of development, the major brands of the current generation of ECG interpretation systems include some components of artificial neural networks to improve the performance [GE Medical Systems, 2000]. However, very few of them provide the function of detecting myocardial infarction.

Some ECG waves cannot be recognized by linear classifiers [Srikanth, 2000]. An artificial neural network is a non-linear pattern classifier [Baxt, 1992a; Baxt and Skora, 1996]. It may detect the multi-dimensional relationships in patterns, which are not

apparent to humans, and may show the more important predicators, which were ignored before [Baxt, 1992; Baxt *et al*, 1995]. Also, due to their structure, artificial neural networks have a strong ability for self-generalization and noise-resistance, making them ideal for ECG pattern recognition.

This dissertation focuses on the attempts of designing an artificial neural network based automated Holter ECG analysis system for early detection of myocardial infarction.

1.2 ECG Interpretation System Development--Overview

The earliest ECG interpretation system can be dated back to the 1960's. At that time, there were no digitized signal recordings. And since the 1970's, although struggling with the analog to digital converter and very limited storage, the effort of computerized ECG analysis continues [Van Bemmel et al., 1990]. The main approaches of pattern recognition in the early ECG diagnosis systems were syntactic and statistical. Haisty et al. developed a quite popular system in 1972, applying statistical methods [Haisty et al., 1972]. Another main methodology is the syntactic approach [Willems, 1990]. However, due to the non-linearly separable nature of ECG signals, both statistical and syntactic methodologies proved limited [Macfarlane and Lawrie, 1974].

In the 1980's, with the development of VLSI technology and the surge of personal computers, the sizes of systems became much smaller than before [Van Bemmel, 1990]. Besides the techniques mentioned before, since the late 1980's the use of artificial neural networks has been the most popular methodology in pattern recognition. And there are reports that the result of artifical neural networks are better than those of the human cardiologists [Baxt, 1992b; Heden et al., 1997; Srikanth, 2000]. The inherent structure of artificial neural networks offers good adaptiveness and robustness, and quite ideal for

classification problems like ECG recognition. The limitation of artificial neural network applications is that the field must be narrow, and some field knowledge must be provided [Bishop, 1995]. Almost all the systems incorporating artificial neural network components have used expert systems. Expert systems have two major parts: knowledge base and inference engine. The knowledge base is the container of knowledge and heuristics derived from human experts, and the inference engine is the software and logic to identify the proper answer for the input question.

All computerized ECG interpretation systems include several components: (i) ECG signal acquisition, (ii) ECG signal pre-processing, (iii) Feature extraction, and (iv) Pattern classification. The first step often does not receive enough attention; but this step is the beginning of analysis and any error or noise introduced at this step will be accumulated in the following steps. The second step is relatively standard. The latest so-called intelligent systems can detect the interpolation of sensors, and the removal of the 50 or 60 Hz noise (for Japan and U.S.A., it is 60 Hz; for China, 50 Hz), and other items [Van Bemmel, 1990]. Very few methods for step 3 and step 4 are disclosed in either research journals or other publication [Srikanth, 2000].

Almost all commercial systems do not detect myocardial infarction and the research literature published on myocardial infarction detection is even more limited. Several reasons contribute to this dearth, including lack of digitized ECG signals records and morphological evolution in the whole development of myocardial infarction. Unlike electro-organic arrhythmias easier to describe by certain parameters, myocardial infarction mainly involves morphology changes difficult to describe by fixed parameters.

1.3 Hypothesis and Objective

The hypothesis of the proposed dissertation is that an artificial neural network-based ECG interpretation system may improve clinical diagnosis of myocardial infarction, especially early detection of myocardial infarction.

An artificial neural network is a gross abstraction of its counterpart in animals. It tries to capture the structural characteristics of brain processing, hoping to have similar processing abilities of brains. Basically, it is a group of interconnected units which perform simple mathematical functions [Bishop, 1995]. All the units work in parallel. In a different way from traditional computer processing, information in a neural network is stored in the weights, which are the connection strength between units. If some of the units are damaged or interfered with by noise, the whole network still can output the right result. Another characteristic of artificial neural networks is self-generalization, which can detect complicated relationships between patterns that may be ignored by humans. Self-generation is of great importance for pattern recognition, which involves many parameters. Artificial neural networks can be non-linear classifiers if the mathematical functions performed by each unit are carefully designed [Bishop, 1995].

The current criteria to define myocardial infarction include information from clinical tests, patient history, and ECG. None of them serves as an absolute predictor [Goldman, 1988]. Those criteria, especially use of the ECG parameters, differ from country to country. The whole set of criteria may include 20 parameters [Baxt, 1991; Baxt, 1992a; Heden et al, 1997]. Since ECG pattern recognition is non-linear, any purely rule-based system or system using only statistical clutter or regression analysis will not

be promising [Srikanth, 2000]. Also, due to the noise introduced during ECG recording, myocardial infarction, especially early detection, remains a challenge.

Artificial neural networks have found broad applications in medicine, including ECG interpretation [Hudson et al., 1988;Marconi et al., 1988; Smith et al., 1988; Salto et al., 1988; Yoon et al., 1989; Bounds et al., 1990; Kaufman et al., 1990; Hiraiwa et al., 1990; Clos et al., 1990; Baxt, 1991; Baxt, 1992a; Baxt and White, 1995; Baxt et al., 1996; Eberhart et al., 1991; Heden et al., 1997; Goldman et al., 1988]. Some publications [Baxt 1992; Heden et al., 1997; Yoon et al., 1989; Bounds et al., 1990] show that accuracy of artificial neural networks can be substantially better than physicians'. The research projects in San Diego, CA, and in Lund, Sweden, demonstrated that the performance of artificial neural networks to detect early myocardial infarction in emergency department is above 90%, much better than that of physicians [Baxt, 1992a, Heden et al., 1997], and even better than a commonly used rule-based medicine system [Heden et al., 1997].

Based on the findings above, we hypothesize that an artificial neural network based ECG interpretation system may improve clinical myocardial infarction detection, especially early myocardial infarction.

The system in this dissertation includes these sub-systems:

- Signal Pre-processing Block
- Wave Detection Block, which implement QRS complex detection, T wave detection and fiducial point estimation.
- Feature Extraction Block
- Classification Block

The objective of the present thesis is to present an integrated automated ECG diagnosing system which can be used for clinical Holter data, with the capacity to expand to multi-lead ECG interpretation systems and to be included in other ECG interpretation systems which do not detect myocardial infarction. Also, we would compare the accuracy of this system with that of experienced cardiologists. Artificial neural networks with feed forward connections and associative networks will be pattern classifiers. Routine ECG data from lead V1 and lead V5 are used for the study. All the data were annotated by two experienced cardiologists.

CHAPTER 2

BACKGROUND

2.1 Anatomy and physiology of Heart

The normal heart is a strong, muscular pump, a little larger than a fist. It pumps blood continuously through the circulatory system. The heart is actually two separated pumps: "a right heart that pumps blood through lungs and a left heart that pumps blood through peripheral organs." [Guyton and Hall, 1996] Each of these two hearts has two chambers: an atrium and a ventricle, so the heart has four chambers. The upper two are the right and left atria; the lower two, the right an left ventricles (see Figure 2.1). Principally, the atrium works as the weak primer pump for the ventricle, helping to move the blood into the ventricle. The ventricle is the source of main force that pushes the blood through the circulation [Guyton and Hall, 1996].

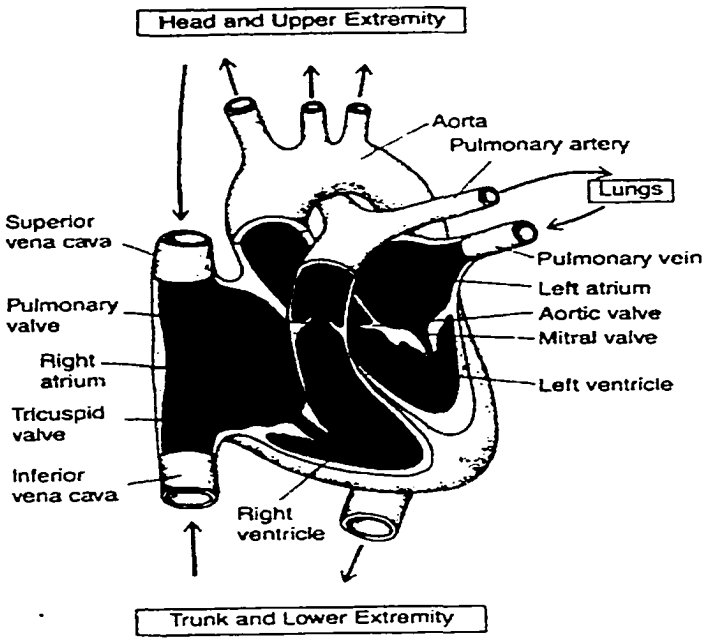

Figure 2.1 Heart Structure

2.1.1 Cardiac Muscle

There are three major types of cardiac muscle: atrial muscle, ventricular muscle, and specialized excitatory and conductive muscle fibers. The first two types of muscle are similar to the skeletal muscle except that the duration of contraction is much longer.

For the heart to function properly, the chambers must beat in an organized manner. This sequence is governed by the electrical impulse. This kind of activity results from the electrochemical properties of the specialized excitatory and conductive system, as shown in Figure 2.2. These systems exhibit rhythmicity and varying rates of conduction.

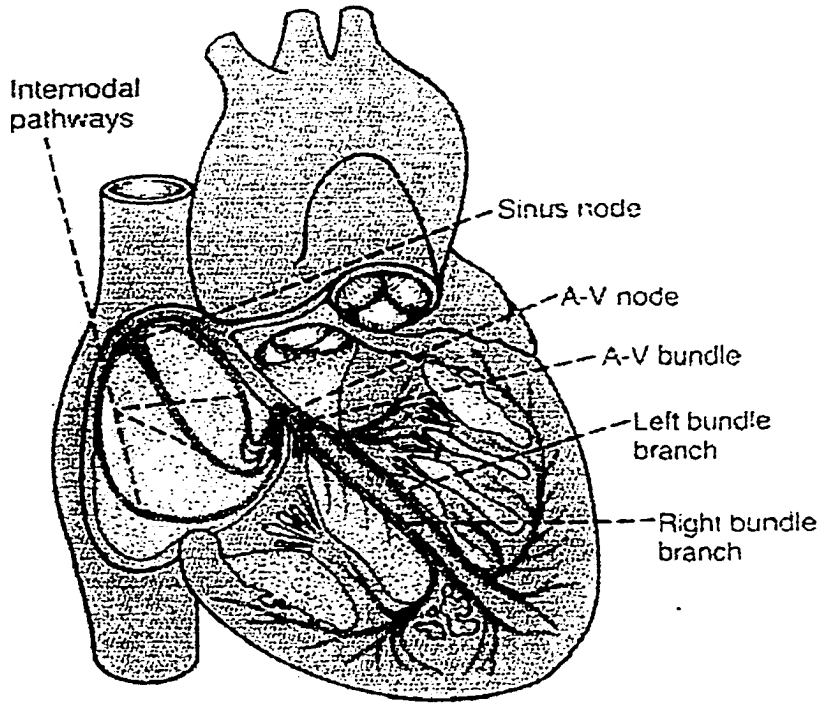

Figure 2.2 Excitation System

2.1.2 Specialized Excitatory and Conductive System

Many cardiac fibers have the ability to excite themselves. The process causes automatic rhythmical discharge and contraction. This special system not only has the ability to generate rhythmical impulses to cause rhythmical contraction of the heart muscle, but also can conduct these impulses rapidly throughout the heart. These cells include the sinoatrial node, specialized atrial tissues, the atrioventricular node and the His-Purkinje system [Conn and Horwitz, 1971; Brest et al., 1968].

2.1.2.1 Sinoatrial node. The SA node is a small, flattened, ellipsoid strip of specialized muscle whose fibers have almost no contractile filaments. The sinus fibers connect directly with the atrial fibers so that the action potential initiating from sinus node will spread very soon into the atria. Usually this node controls the rate of the entire heart.

Compared with the ventricular muscle fiber, the potential of the sinus nodal fiber has a negativity of only -55 to -60 millivolt, much less than -85 to -90 millivolts, because of the fact that the cell membranes of the sinus fibers are naturally leaky to the sodium ions. Figure 2.3 [Guyton and Hall, 1996] shows both the action potentials of the sinus nodal fiber and the ventricular muscle fiber. The resting membrane potential of the sinus nodal fiber increases slowly until it reaches the threshold for action potential.

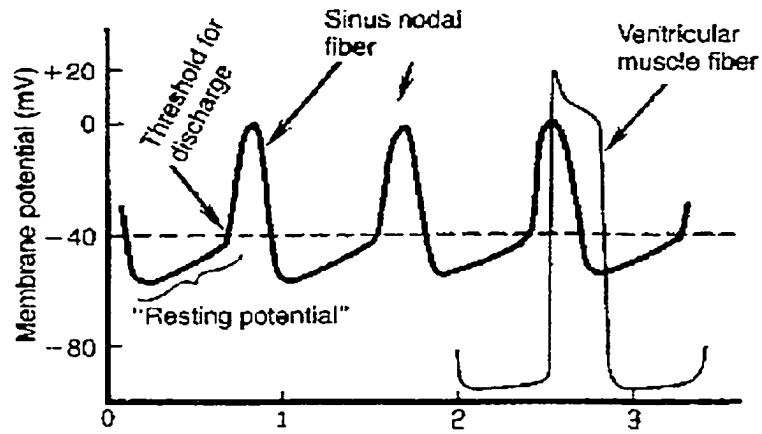

Figure 2.3 Membrane Potential of Sinus Nodal Fiber and Ventricular Muscle Fiber

2.1.2.2 Specialized Atrial Tissues. The tissues include two parts: automatic atrial cells outside the sinoatrial node, and cells in specialized atrial conducting tracts. The cells in the conducting tracts have a number of specialized conduction fibers mixed with the atrial muscle, such that the conduction speed in these tracts is faster. Again, these tracts can be divided into two parts: internodal, which passes through the anterior walls of the atria to the left atrium, and interatrial, which is made of three small bundles: anterior, middle and posterior, curving through the atrial walls and ending in the atrioventricular node.

2.1.2.3 Atrioventricular Node

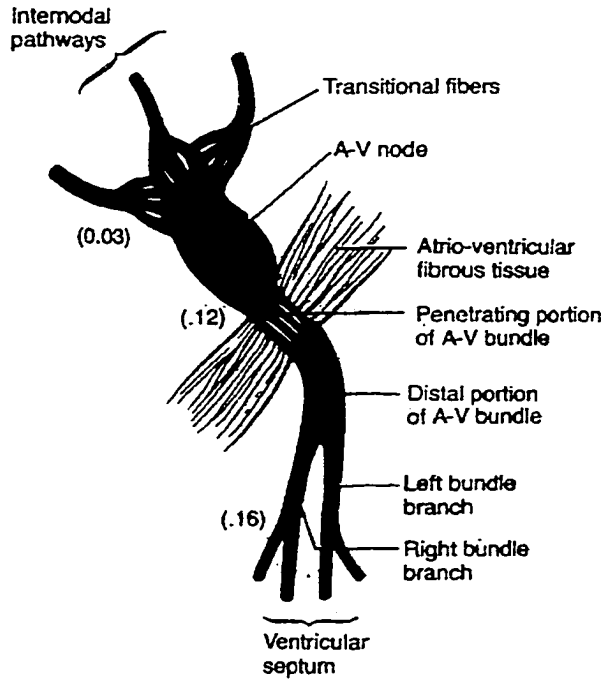

Figure 2.4 Organization of the A-V Node

Figure 2.4 [Guyton and Hall, 1996] shows the organization of the A-V node. The numbers in the figure represents the time taken for the impulse originating from the sinus node to travel to that point. It takes 0.03 second for the sinus node impulse to travel to the A-V node. Then there is a delay of 0.09 second in the A-V node. Then the impulses enter the penetrating portion of the A-V bundle, where the final delay of 0.04 second occurs. The delay in the A-V node and its adjacent conductive fibers allow time for the atria to empty their contents into the ventricles before ventricular contraction begins. The major causes of the slow conduction in these parts are the low voltage to drive the ions and the high resistance to the movement of the ions.

2.1.2.4 His-Purkinje System. The Purkinje fibers originate from the A-V node and travel through the A-V bundle into the ventricles They are very large fibers, even larger than the normal ventricular muscle fibers. Their conduction velocity is 1.5 to 40 cm per

second, much higher than that of the usual cardiac muscle fiber, making the cardiac impulse transmit almost immediately through out the whole ventricular system. There are four parts of the Purkinje system:

1. Common bundle
2. Bundle branches
3. Subendocardial Purkinje fibers
4. Intramyocardial Purkinje fibers

The impulse rate generated by each is different. From top to bottom in the list above, the rate varies from quickest to slowest (under normal conditions). The quicker pacemaker will suppress the impulse of the slower ones. Thus, the normal heartbeat begins from sinus node, then to A-V node, then to the His bundle.

2.2 Electrical Activities of Cardiac Cells and ECG

2.2.1 Membrane Potential and Excitable Cells

There are electrical potentials across the membrane of almost all cells of the body. Some cells, such as nerve and muscle cells, are able to generate electrochemical impulses at the membrane themselves. These cells are called excitable cells. If no signals are transmitting on the membrane, the electrical potential difference across the membrane is called the resting membrane potential. For big nerves, the resting membrane potential is around -90 millivolts. For most cardiac cells, the potential difference across the resting membrane is -85 millivolts to -90 millivolts.

2.2.2 Source of the Membrane Potential

The main source of membrane potential is the concentration difference of charged ions across the membrane. Sodium channels, potassium channels, potassium-sodium leakage channels, sodium-potassium pumps and others. All contribute to membrane potential.

2.2.3 The Propagation of Action Potentials

The propagation of the action potential results from the fact that an action potential usually excites adjacent parts of the membrane. Figure 2.5 [Guyton and Hall, 1996] shows the mechanism of it. As demonstrated in Figure 2.5, the action potential will propagate in both directions until it reaches the end of the fiber.

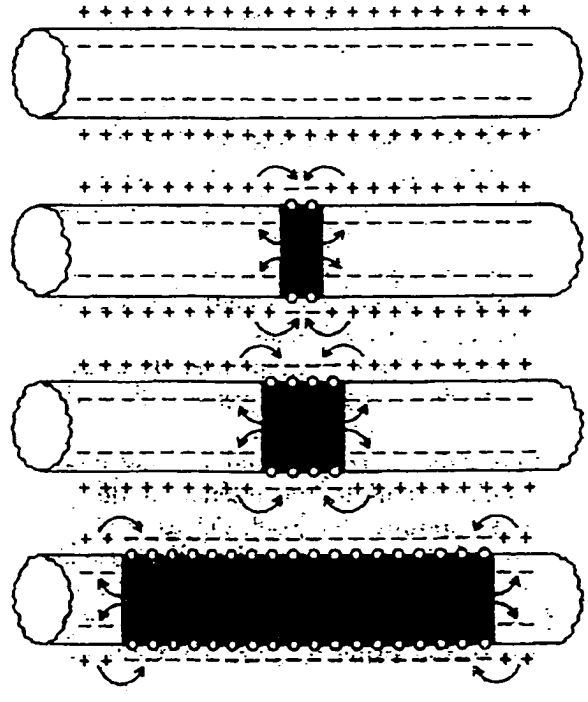

Figure 2.5 The Propagation of Action Potential

2.2.4 The Normal Cardiac Cycle and the ECG

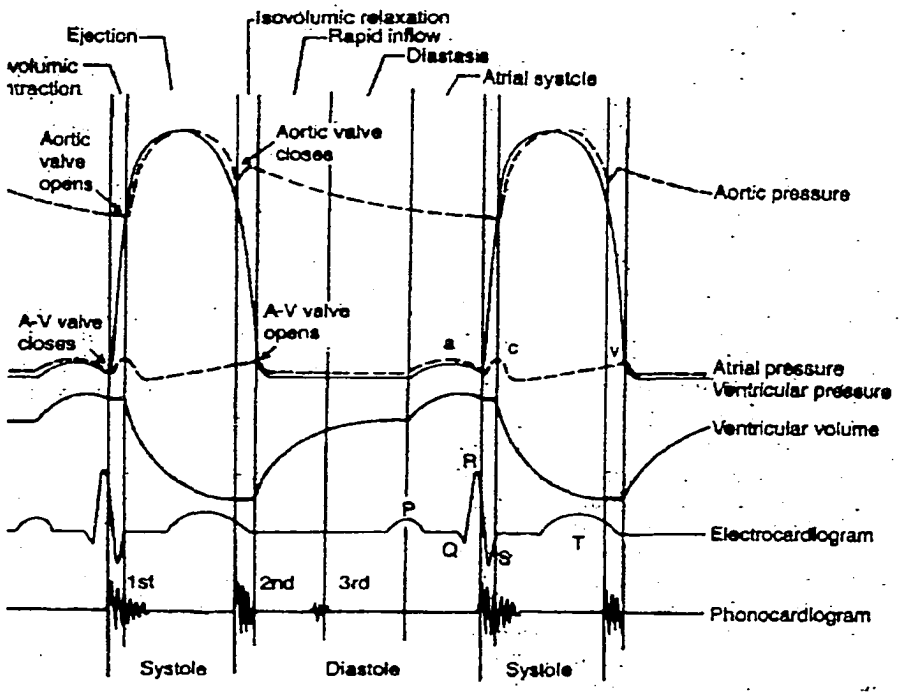

Figure 2.6 The Relationship between Normal Cardiac Cycle and the ECG.

Figure 2.6 [Guyton and Hall, 1996] shows the relationship between normal cardiac cycle and the ECG. The cardiac cycle is defined as the electrical, chemical, and physical events that occur from the beginning of one heart beat to the beginning of the next [Guyton and Hall, 1996].

In a normal cardiac cycle, the pressure of the aorta, ventricles, and atria changes, and so does the volume. Each normal heartbeat begins from the sinus node, which spontaneously depolarizes 60 to 100 times per minute [Chung, 1989]. Then the wave travels along the internodal conductive paths and atrial myocardium at a speed of 800 mm to 1000 mm per second, making atria depolarize and contract. Then at the A-V node, the speed drops to 200 mm per second. The A-V node has two functions: one is to delay the depolarization wave from the atria, ensuring the optimum filling of the ventricles; the other is to prevent any premature atrial electrical activity from entering the ventricular

conduction system [Lazzara, 1979]. Then the wave travels along the bundle of His, then the bundle branches, then through the Purkinje fibers, and then at last cause the ventricles to depolarize and contract by traveling through the ventricular myocardium.

"As the cardiac impulses passes through the heart, electrical currents spread into the tissues surrounding the heart, and a small portion of these spreads all the way to the surface of the body. If electrodes are placed on the skin on opposite sides of the heart, electrical potentials generated by these currents can be recorded; the recording is known as an ECG" [Guyton and Hall, 1996]. The ECG cannot represent completely the cardiac events in the cardiac cycles. It records only the potential changes between two electrodes on the body surface. It is a one-dimensional projection of the moving dipole on the axis between the electrodes [Katz, 1977].

From Figure 2.6, we can see that the first wave of the ECG is the P wave, which reflects the time required to depolarize the whole atria. The depolarization wave generated by the sinus node is too small to detect. Between the P wave and the QRS complex, the ECG remains on the baseline, indicating that there is no potential change between electrodes on the body surface. During this time, the depolarization wave is being propagated though the AV node, His bundle, the bundle branches and the Purkinje fibers. Due to the small masses involved, no evidence is shown on the ECG.

The QRS wave demonstrates how the depolarization wave passes through the ventricular myocardium. Because the mass involved in the propagation is more than that in the conduction in the atria, the amplitude of the QRS complex is bigger than that of the P wave. Due to the fast conduction speed, the QRS duration is shorter than that of the P wave.

The QRS complex reflects phase 0 and phase 1 of the cardiac action potential. The baseline region between the QRS complex and T wave reflects phase 2, when all the ventricles are depolarized. The T wave is generated by the repolarization of the ventricles. It reflects the later part of phase 2 and phase 3. The duration of T wave is greater than the QRS complex since there is no conduction pathway to synchronize the propagation. Sometimes, a small U wave can be seen. It is believed that it is related to the repolarizaton of the Purkinje fibers [Katz, 1977].

2.2.5 The Leads

A lead consists of 2 wires and 3 electrodes which form a complete circuit. Due to the different combinations of the electrode positions for recording on the body surface, there are many different leads. Table 2.1 shows the most commonly used 12 leads in clinical examination.

Table 2.1 Electrode Positions of 12 Leads

	Leads	Positive Electrode	Negative Electrode
Bipolar	I	Left Arm	Right Arm
Bipolar	II	Left Leg	Right Arm
Bipolar	III	Left Leg	Left Arm
Unipolar Limb Lead	aVR	Right Arm	Central Terminal
Unipolar Limb Lead	aVL	Left Arm	Central Terminal
Unipolar Limb Lead	aVF	Left Leg	Central Terminal
Precordial Lead	VI	Right of Sternum in 4^{th} ICS	Central Terminal
Precordial Lead	V2	Left of Sternum in 4^{th} ICS	Central Terminal
Precordial Lead	V3	Midway between V2 and V4	Central Terminal
Precordial Lead	V4	Midclavicular Line in 5^{th} ICS	Central Terminal
Precordial Lead	V5	Midway between V4 and V6	Central Terminal
Precordial Lead	V6	Lateral Chest in 5^{th} ICS	Central Terminal

2.2.6 Depolarization Waves and Repolarization Waves

Figure 2.7 [Guyton and Hall, 1996] shows two kinds of waves: depolarization waves and repolarization waves. Suppose the left electrode is connected to the negative end of the meter, and the right electrode is connected to the positive end of the meter. When the current direction is in the direction from the left electrode to the right electrode, the potential recorded is positive (Figure 2.7 A and B). In the opposite direction, the wave recorded will be negative Figure 2.7 C and D).

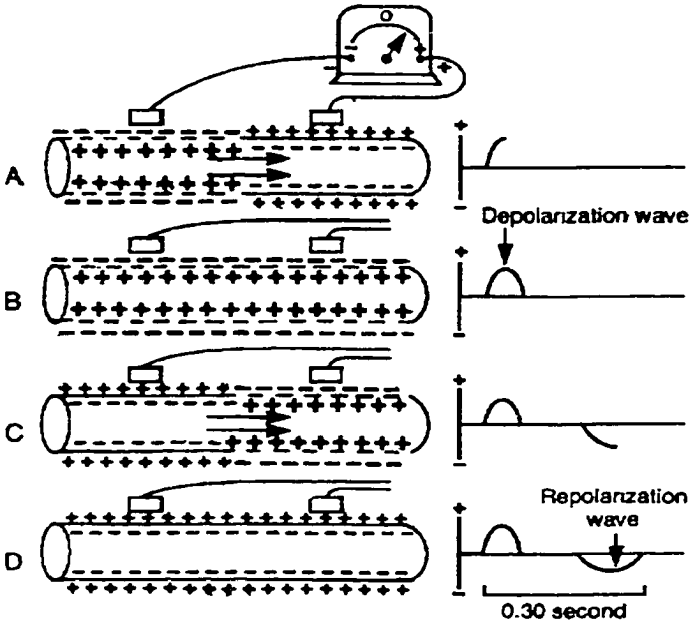

Figure 2.7 Depolarization Waves and Repolarization Waves

2.3 Myocardial Infarction (MI)

2.3.1 Definition of MI

"Immediately after an acute coronary occlusion, blood flow ceases in the coronary vessels beyond the occlusion except for small amounts of collateral flow from surrounding vessels. The area of muscle that has either zero flow or so little flow that it cannot sustain cardiac muscle function is said to be infarcted. The overall process is called a myocardial infarction." [Guyton and Hall, 1996]

2.3.2 Mechanism of MI

MI results from shortage of blood supply to a region of heart and which is not restored in an appropriate period of time. The common sequence of injurious events of MI begins with subendocardial or transmural ischemia, followed by necrosis, and eventual fibrosis (scarring). [Guyton et al., 1996] "Rupture of an atherosclerotic plaque followed by acute coronary thrombosis is the usual mechanism of acute MI."

2.3.3 Physiological Changes

During myocardial infarction, the heart cells die after a certain period of time of insufficient blood supply. The sarcoplasm in the muscles are damaged and the fluid in the sarcoplasm leaks into blood circulation. The fluid in the sarcoplasm contains large quantities of protein enzymes [Guyton and Hall, 1996]. Further, when the myocardium is damaged, the components of myocardium are released into blood. So after several hours, the concentration of these markers in the blood begins to increase and will last for several hours to several days [Kennedy et al., 1997]. These markers include myoglobin, creatine kinase (CK) and its cardiac-specific isoenzyme (CK-MB), lactate dehydrogenase (LDH), troponin-T, and troponin-I [Murphy et al., 1999; Ebell et al., 2000a; Ebell et al., 2000b; Jurlander et al., 2000; de Winter et al., 2000].

Myoglobin is a heme protein found in all striated muscle fibers, which accounts for about 2% of both skeletal and cardiac tissue mass. It is the earliest marker among these because it has a smaller molecular weight. The serum concentration of it will increase 2 hours after the onset of the symptoms and reaches the peak serum level in 3 to 15 hours, and has maximal diagnostic accuracy for the diagnosis of myocardial infarction at 5 hours after the onset of the symptoms. According to the research of de Winter et al., at 5

hours, sensitivity was 87% and specificity was 97% using a myoglobin cutoff value of 90 ug/L [de Winter et al., 2000]. The problem associated with myoglobin is that if the patient has skeletal muscle disease or damage, or neuromuscular disorders, strenuous exercise, renal failure, intramuscular injections, and cardiac bypass surgery, the serum concentration of it is also high [Kennedy et al., 1996, Murphy et al., 1999].

Abnormally elevated serum levels of CK-MB is one criterion establish by the World Health Organization to diagnose myocardial infarction [de Winter et al., 1995]. Usually CK or LDH is used together with CK-MB, since without CK-MB, CK or LDH lacks specificity. The highest accuracy for acute myocardial infarction diagnosis was identified by the threshold concentration. For CK-MB, it is 5 ug/L [Jurlander et al., 2000]. It increases about 4 hours after the onset of the symptoms and remains elevated for around 24 hours, which is a disadvantage. It is a very sensitive early indicator of AMI. When serum level doubles with serial samples obtained every 2 hours, it is a highly sensitive indicator of AMI [Murphy et al., 1999].

Troponin T and troponin I are 2 components of the cardiac troponin complex, a basic component of the myocardium. Through its role in the transmission of intracelluar calcium into the actin-myosin interaction, the troponin complex is involved in the contraction of myocardial muscle. The structures of troponin T and I in cardiac muscle are different from those of skeletal muscle. These differences can be used to distinguish the cardiac cells from skeletal cells [Alonsozana et al., 1996]. When myocardial ischemia occurs, the cell membranes become more permeable, and intracellular components such as cardiac troponin leak into the interstitium and into the intravascular space [Brown et al., 1997]. The serum level of troponin T begins to increase 3 to 5 hours after myocardial

injury occurs and remains elevated for 14 to 21 days [Antman et al., 1996; Wong, 1996; Brown et al., 1997]. The cardiac troponin I levels begin to increase 3 hours after myocardial ischemia begins, peak at 14 to 18 hours, and remain elevated for 5 to 7 days [Wong, 1996; Malr et al., 1996]. Murphy et al. showed that assays for troponin T had a sensitivity of up to 100% for myocardial damage within 4 to 6 hours after myocardial infarction, and assays for troponin I had a sensitivity of up to 100% by 6 hours [Malr et al., 1996]. The problem with troponin T and I is that the sensitivity of them is so dependent on the number of hours from the onset of chest pain [Ebell et al., 2000a].

2.3.4 The ECG Changes

For several decades, the ECG has been established as the cornerstone for early diagnosis of acute myocardial infarction [Yusuf et al., 1984; Timmis, 1990]. The changes of ECG waves in the course of myocardial infarction are the common predictors of myocardial infarction, especially the early detection of acute myocardial infarction.

During repolarization in ST-T segments in standard ECGs, ischemic changes can be observed best. Maybe because of a slight reduction of potassium in the intracellular areas, phase 3 of the action potential slows during ischemia. When the subepicardium is ischemic, the subendocardial polarizes earlier, reversing the normal direction of repolarization and producing an inverted T wave. In subendocardial ischemia, a tall and upright T wave with prolonged QT interval is the typical change. Ischemia can lead to pseudo normalization of chronically inverted T wave. Ischemia may cause the T wave to become more peaked or deep, more symmetrical, or have a sharper ST-T angle [Breslow et al., 1986]

New ST deviation may demonstrate more severe ischemia than that causing only the T wave changes. Since the U-P baseline is difficult to measure, P-Q segment is often used as the baseline although it may be lower than the U-P segment. ST deviation can be measured at the J point or up to 80 milliseconds after it. An ST segment that is isoelectric for 80 milliseconds or more is one of the earliest signs of ischemia. Ischemia will lead to a sharp ST-T junction, which can be seen best in lead V5. Upward sloping ST depression signifies ischemia. Horizontal depression and concave upward sagging depression of the ST-T segment are signs of ischemia. The downward sloping depression has the highest specifity for ischemia. When there is severe ischemia, there may be inversion of the early part of the T wave. With even more severe ischemia, the T wave will be inverted completely. The diagnosis accuracy of new 1-mm ST depression for the detection of ischemia may be hampered by persistent ST deviation [Weiner, 1981]. In the standard 12-lead ECG, ST elevation is considered more likely to be associated with injury leading to myocardial infarction, while ST depression is considered more likely to be associated with reversible myocardial ischemia [Kornreich et al., 1993]. Some factors lead to nonischemic ST deviation. Usually the ST deviation caused by these factors is fixed, and no heart rate variations are associated.

When a coronary artery is occluded, firstly the R wave amplitude will decrease. The decrease will last about one minute. After several minutes, the conduction in the ischemic area slows. It leads to a longer period of depolarization and causes the R wave amplitude increase. The time when the R amplitude begins to increase varies, depending on the presence of collateral [Michaelides, et al., 1990].

If MI results from total coronary occlusion, which causes more homogeneous tissue damage, a wave pattern will be seen. A non Q-wave MI pattern, evolving ST-T changes over time without the formation of pathologic Q waves, reflects MI's resulting from subtotal occlusion, which causes more heterogeneous tissue damage. Two-thirds of MI's presenting to emergency rooms evolve a non-Q wave.

2.3.5 Stages of Recovery from Acute MI

When the area of ischemia is small, there may be little or no death to myocardial muscle cells. When the area of ischemia is large, within 1 to 3 hours of no blood supply, some of the fibers in the center die. Immediately around the dead cell area is the nonfunctional area, which is possible to return to normal if it gets blood supply in time. Around the nonfunctional area is an area that contracts more weakly than normal [Guyton and Hall, 1996].

2.3.6 Location of MI

"Most MIs are located in the left ventricle. In the setting of a proximal right coronary artery occlusion, however, up to 50% may also have a component of right ventricular infarction as well. Right-sided chest leads are necessary to recognize right ventricular MI."[AHA, 1999].

Table 2.2 shows how to detect the location of MI from ECGs of different leads. The "+" means in that lead, ECG waves show the dead cell type Q wave, ST segment elevation and inverted T wave. The "-" means the appearance of high R wave, ST segment, and deviation from normal T wave.

Table 2.2 Location of Myocardial Infarction

	V1	V2	V3	V4	V5	V6	V7	I	II	III	aVL	aVF
Interior Frontier Wall	+	+	+					+				
Frontier Wall			+	+	+			+			+	
Frontier Side Wall					+	+	+	+			+	
Pan-Frontier Wall	+	+	+	+	+			-	+	+	+	
Lower Wall								-	+	+	-	+
Lower Interior Wall	+	+	+					-	+	+	-	+
Lower Side Wall					+	+	+	+	-	-	-	+
Back Side Wall											+	-
Back Wall						+	+					

2.3.7 Measurements of ECG in Each MI Stage

Stage 1: High and sharp T wave, prolonged Q-T interval

Stage 2: Elevated S-T segment, high and sharp T wave and prolonged Q-T interval

Stage 3: Elevated S-T segment develops to monophasic curve

Stage 4: Elevated S-T segment and inverted T wave

2.3.8 Research on MI Detection

For many years, the detection of myocardial infarction has remained challenging because it is a disease of low incidence, yet a very high price has to be paid for its misdiagnosis. Acute myocardial infarction was one of the earliest applications of artificial neural networks. The following Table 2.3 shows the major research projects using artificial neural networks to diagnosis of chest pain and to analysis of ECGs. Almost all

of them show that sensitivities and specificities of the artificial neural network results were better than those of human experts ($P<0.05$).

Table 2.3 Projects Utilizing Artificial Neural Networks to Diagnosis of Chest Pain and to Analysis of ECGs

Major Researchers	Application	Result
Hart & Wyatt [Hart et al., 1989]	Chest pain, classified as high, low, or risk of being cardiac origin	Sensitivity: 73% Specificity: 68% For new cases
Baxt [Baxt, 1990]	Acute Coronary Occlusion	Sensitivity: 92% Specificity: 96%
Harrison, Marshall & Kennedy [Harrison et al., 1991]	Heart Attacks	Sensitivity: 88% Specificity: 88% Accuracy: 88%
Baxt [Baxt, 1991]	Chest pain presenting to emergency room	Sensitivity: 97% Specificity: 96%
Baxt & Skora [Baxt et al, 1996]	Extend the research in 1990 and 1991 to over 1000 patients	Sensitivity: >95% Specificity: >95%
Edenbrandt [Edenbrandt et al., 1993]	Anterior myocardial infarction, (AMI) Inferior myocardial infarction (IMI)	Sensitivity: 73% Specificity: 68%
Hu [Hu et al., 1993]	Healed AMI (HAMI), Healed IMI (HIMI)	Sensitivity: 63% Specificity: 97%
Bortolan & Willems [Bortolan et al., 1993]	Ventricular hypotrophy and myocardial infarction	See table 2.4
Devine & Macfarlane [Devine et al., 1993]	Ventricular strain	Sensitivity: 97% Specificity: 88%
Heden [Heden et al., 1994]	Healed AMI Healed IMI	Sensitivity: 81% Specificity: 97.5%
Heden [Heden et al., 1996]	Healed myocardial infarction	Sensitivity: 81.4% Specificity: 94.8%
Kennedy [Kennedy et al., 1997]	Acute myocardial infarction	Sensitivity: 91.2% Specificity: 90.2%
Heden [Heden et al, 1997]	Acute myocardial infarction	Sensitivity: 97% Specificity: 88%

Table 2.4 Testing Result of 3253 ECGs by Artificial Neural Network [Bortolan et al., 1993]

Category	Sensitivity	Specificity
Normal	90.2%	92.5%
Left-Ventricular Hypertrophy	59.3%	98.2%
Right-Ventricular Hypertrophy	31.2%	98.9%
Biventricular Hypertrophy	84.4%	89.0%
Anterior Myocardial Infarction	51.6%	97.8%
Inferior Myocardial Infarction	86.3%	91.1%
Combined Myocardial Infarction	47.1%	95.3%

In the field of computer-aided myocardial infarction, no one can ignore the paper of Goldman [Goldman et al., 1988]. In that paper, he presented the result of a project which lasted for around 10 years, involving 6 hospitals and 8601 patients. With careful selection of potentially eligible patients, strict method design and rigorous statistical analysis, this multi-center research set the foundation of later diagnosis criteria of MI, the combination of patient history, clinical examinations and ECG measurement, which were selected from about 50 potential predictors. These criteria have been used in most of the emergency rooms in America. His result showed that the computer protocol had a significantly higher specificity (74% vs. 71%) in predicting the absence of infarction than physicians deciding whether to admit patients to the Coronary Care Unit (CCU) and that it had a similar sensitivity in detecting the presence of infarction (88.0% vs. 87.8%). This result greatly encouraged subsequent research on computer-aided MI detection [table 2.3].

Among the projects listed in Table 2.3, three groups of researchers worked continuously in this field and showed promising results. The leaders are Baxt [Baxt, 1990; Baxt, 1991; Baxt, 1992a; Baxt, 1992b; Baxt, 1994; Baxt et al., 1995; Baxt et al., 1996], Harrison, Marshall & Kennedy [Harrison et al., 1991 & Kenney et al., 1997], and Heden

and Edenbrandt [Edenbrandt et al., 1993; Heden et al., 1994; Heden et al., 1996; Heden et al., 1997].

When he was in the Dept. Of Emergency and Medicine, University of California, San Diego Medical Center, Baxt published a series of papers on the study of a neural network trained to identify the presence of MI [Baxt, 1990; Baxt, 1991; Baxt, 1992a; Baxt, 1992b; Baxt, 1994; Baxt et al., 1995; Baxt et al., 1996]. The clinical data were collected from the patients presenting to the Emergency Dept. with the main claim of anterior chest pain. The number of patients expanded from about 300 to 1070 in 1996. The first goal was "to validate prospectively the use of an artificial neural network to identify myocardial infarction in patients presenting to an emergency department with anterior chest pain." A three layered artificial neural network was designed based on the computer protocol of Goldman [Goldman et al., 1988]. The artificial neural network was trained by the back propagation algorithm [Rumelhart et al., 1985 and Rumelhart et al., 1986]. The data used by the network were collected by the physicians who treated the patient. The physicians were medical residents in postgraduate years 2 and 3 and emergency department attending faculty physicians. Once the data were input in the pre-designed form with 22 items, no attempt was made to change the data. Then the physicians made their decision whether the patient had a myocardial infarction. These decisions were also recorded for later comparison. The final diagnosis was established by subsequent review of patient records and follow-up phone interviews. Any patient who could not be followed was dropped from this research. This process was blind to the initial data entry. After statistical analysis, 20 out of 22 variables were selected to form the final design of the artificial neural network. Half of the data set was used for training

the network and another half, never exposed to the network, was used for testing the network. Of the total 331 patients, 36 patients had had myocardial infarction, 63 had crescendo angina, and the remaining 194 patients had noncardiac etiologies. The physician correctly diagnosed 28 out of 36 patients with myocardial infarction, yielding a sensitivity of 77.7% and correctly diagnosed 250 patients without myocardial infarction for a specificity of 84.7%. The artificial neural network correctly diagnosed 35 out of 36 patients with myocardial infarction for a sensitivity of 97.2% and incorrectly diagnosed 11 patients without myocardial infarction for a specificity of 96.2% [Baxt, 1990 and Baxt, 1991]. He pointed out that the prospective validation of establishing the use of artificial neural network as an aid to the clinical diagnosis of myocardial infarction required that the network be tested on many patients and multi-center studies. In the following research, he analyzed the influence of each variable on the result of the artificial neural network and found that the presence of ECG findings--as well as the presence of rales, syncope, jugular venous distension, response to trinitroglycerin, and nausea and vomiting--are the major predictive sources [Baxt, 1992b]. Surprisingly, some factors--such as age, sex, history of hypertension, diabetes mellitus, and angina, which were thought be strong indicators of myocardial infarction--had weak or even negative impact on the diagnosis of myocardial infarction [Baxt, 1992b]. Since it is divergent from the traditional medical school teaching, he did further statistical analysis and got the implication that the network may be doing the diagnosis by identifying relationships between inputted information, indicating his methods are not different from accepted teaching [Baxt, 1994] and it was not the result of random sampling variation [Baxt et al., 1995]. One problem associated with artificial neural network methods is that, once the trained artificial neural network

yields optimal result in either detection rate (sensitivity) or false alarm rate (specificity), any increase in one is always at the cost of the decrease of the other. So, two networks were trained on patients with different likelihoods of myocardial infarction. During testing, the input was analyzed by both networks, one for absence of myocardial infarction and the other for presence of myocardial infarction. If the result of the network for absence of myocardial infarction is under the empirical threshold, the result of it would be the diagnostic output, or the result of the network for the presence of myocardial infarction would be the output. Baxt compared the results of these networks with the single network. Both identified 39 out of 40 patients with myocardial infarction, yielding the detection rate of 97.5%. The dual networks wrongly identified 5 out of 301 patients without myocardial infarction; while the single network wrongly identified 19 of 301. The false alarm rate of the dual networks was significantly lower than that of the single network [Baxt, 1992a]. To further validate the potential of artificial neural networks as an aid to clinical diagnosis of myocardial infarction, Baxt extended the previous research. The network was tested on 1070 patients. The result again showed both the specificity (96.0% vs. 81.1 %) and the sensitivity (96.0% vs. 73.3%) of the network is significantly higher than those of the physicians [Baxt et al. 1996].

There are, however, several weaknesses in Baxt's research: (1) the physicians were just medical residents in postgraduate years 2 and 3 and emergency department attending faculty physicians. He did not mention the portion of medical residents in the whole research. At least, we can say their average performance of the medical residents can not be as good as that of the cardiologists who have been in practice for more than 10 years. (2) The data collected for artificial neural networks training and testing were based on the

observation of different physicians. There were both intra-observer variability and inter-observer variability. (3) As he pointed out, the data were collected from one hospital. The portability of the artificial neural network can not be tested.

Another center of research on ECG interpretation is in Europe. One group working continuously on artificial neural network application in myocardial infarction detection is the group led by Heden and Edenbrandt [Heden et al., 1994; Heden et al., 1996; Heden et al., 1997]. In 1994, they published their results [Heden et al., 1994]. This research was a joint program between the Dept. of Clinical Physiology, Lund University in Sweden and the Dept. of Medicine, Section of Cardiology, Wake Forest University Medical Center in North Carolina. They explored the sensitivity and specificity relationships of healed myocardial infarction. They compared their results with the conventional interpretation program, the widely used Glasgow program [Macfarlane et al., 1989] developed at the Glasgow Royal Infirmary, instead of the human experts. The study population were the patients who had undergone diagnostic cardiac catheterization at the North Carolina Baptist Hospital, Winston-Salem, North Carolina from 1981 to 1986. The total number of patients was 1107: 479 were in the normal group, 272 with anterior myocardial infarction , and 356 had inferior myocardial infarction. The data were collected by a computerized electrocardiograph recorder. Measurements of durations and amplitudes of the QRS complexes and ST-T segments were performed by custom software. The following parameters were measured from leads V2, V3, V4, II, III and aVF: Q, R, and S amplitudes, Q and S durations, and 5 amplitudes within the ST-T segment regularly spaced between, not including ST junction and the end of the T wave. Four different, two layered feed forward neural networks were used, two for anterior myocardial infarction

and the other two for interior myocardial infarction. All were trained by back propagation algorithm. For those two networks used for anterior myocardial infarction, one was used for the classification of the presence of anterior myocardial infarction, and the other was for the classification of no presence of anterior myocardial infarction (the same for those two networks for interior myocardial infarction). The measurements from lead V2, V3, and V4 were used by the anterior myocardial infarction networks and those from lead II, III, aVF were used by the interior myocardial infarction networks. For those networks trained to classify no presence of myocardial infarction, the measurements of QRS complexes would be the only inputs. For the other two networks for the detection of the presence of myocardial infarction, besides those 5 measurements from QRS complexes, 5 more measurements from ST-T segments were used. Two thirds of the data were used for training and the rest for testing. The results of the networks without inputs of ST-T segments were not significantly different from the result of the conventional criteria. The network trained with ST-T segments for the classification of anterior myocardial infarction showed higher sensitivity for all specificities in the range of 90% to 100%. The conventional criteria showed a sensitivity and specificity of 68% and 97.5%, respectively. For the interior myocardial infarction classification, the conventional criteria showed a sensitivity and specificity of 65.5% and 95%, respectively. The network using both QRS and ST-T measurements showed a sensitivity of 78% for the same specificity [Heden et al., 1994]. In their paper published in 1996, they extended the initial research to the comparison of the performance between the artificial neural networks and the experienced electrocardiographer. Since conventional ECG interpretation programs presented verbal statements, such as "possible", or "probable", they transferred the

numeric artificial neural network outputs into 5 verbal statements by introducing several thresholds. These 5 statements were: I: definitely no anterior myocardial infarction II: probably no anterior myocardial infarction; III: possibly anterior myocardial infarction; IV: probably anterior myocardial infarction; V: definitely anterior myocardial infarction. The outputs of artificial neural networks were between 0 and 1, with 0 standing for "definitely no anterior myocardial infarction " and 1 standing for "definite anterior myocardial infarction ". A total of 1664 subjects were included in the study, 351 healthy volunteers and 1313 patients with a history of chest pain. All the patients had undergone diagnostic cardiac catheterization at the North Carolina Baptist Hospital, Winston-Salem, North Carolina. The signal preprocessing part was the same as the initial research. The same measurements were made [Heden, et al., 1994]. The neural networks were the same as those in the previous research. A K-fold cross validation procedure was used. The data set was randomly divided into K equal parts. Each of the K different parts of the data was used once as a test set, while the remaining (K-1) parts were used for training. Threefold cross validation was used to decide when to terminate learning in order to avoid "over-training" and eightfold cross validation was used to train the network and assess the networks' performance. The eightfold cross validation was repeated 10 times. The result of the electrocardiographer showed a sensitivity and specificity of 74.4% and 94.8%, respectively. The sensitivity of the networks was 81.4% at a specificity of 94.8%, significant higher than that of the electrocardiographer. The agreement between the classification of the electrocardiographer and the networks was 77.0%, a difference of one class or less was 93.9% and a difference of two classes was 98.1 %, showing a high level of agreement. They also pointed out that the training data set is barely enough for

their networks. A larger data set would improve the performance. And also the presence of some ECGs with uncommon features, too different from the training set, also caused misclassification [Heden et al., 1996]. In 1997, Heden et al. published a paper reporting their attempt to use an artificial neural network to detect acute myocardial infarction. Just as did Baxt, they realized the importance of early detection of acute myocardial infarction in the emergency department and tried to improve the correct detection rate with the aid of the artificial neural networks. They compared the results of the artificial neural networks with those of conventional rule-based criteria and of an experienced cardiologist. There were two conventional criteria: A and B. The cardiologist is the head of the coronary care unit. Conventional A were as follows: ST-segment elevation > 1 mm in two or more adjacent extremity leads or > 2 mm in two or more adjacent precordial leads. Conventional criteria B was from [Macfarlane, 1989] In his paper [Heden et al., 1997], there was no specific description of the conventional B. A total of 1120 ECGs from patients with acute myocardial infarction and 10452 control ECGs were studied. All the ECGs were recorded by Siemens-Elema AB at the University Hospital in Lund, Sweden, from July 1990 to June 1995. Only ST-T measurements were used as the inputs to the network. These measurements are ST-J amplitude, ST slope, ST amplitude 2/8, ST amplitude 3/8, positive T amplitude, and negative T amplitude. The artificial neural network used was a 2 layer perceptron, trained by the Langevin extension of the back propagation algorithm [Rognvaldsson, 1994]. Again, a threefold cross validation procedure was used for learning and repeated three times. The performance of the artifical neural network was better than that of the conventional criteria as well as that of the cardiologist. The sensitivity of the neural networks was 18.3% higher than that of

criterion A (47.1% vs. 28.8%) and 15.5% higher than that of criterion B (46.2% vs. 30.7%) compared at a specificity of 95.4%. Compared at a specificity of 86.3%, the sensitivity of the networks was 10.5% higher than that of the cardiologist (65.9% vs. 55.4%). One finding in this research showed that the cardiologist was better at finding ECGs with clear-cut change of acute infarction. One possible explanation is that a cardiologist is trained to focus on symptoms and clear-cut ECG changes that qualify the patient for thrombolytic treatment. Another finding for criterion A is that the sensitivity is only 28.8%, but much higher (68%) in the study by Lee and his coworkers [Lee et al., 1994]. It suggested that the subjects studied must be different. Heden's research included all ECGs recorded in the emergency department unless there was severe technical deficiencies, while in Lee's research, only patients with chest pain were included. Heden also pointed out that the input is only a part of the information for the diagnosis of myocardial infarction [Heden et al., 1997].

Another group in Europe working on artificial intelligent applications in myocardial infarction is from the United Kingdom. Harrison et al. published their research of artificial neural network application in heart attacks in 1991 [Harrison et al., 1991], showing a quite promising result (see Table 2.3). Six years later, they published their work on acute myocardial infarction diagnosis in emergency department by artificial neural networks [Kennedy et al., 1997]. Their research focused on multi-center testing. They compared the results of artificial neural networks with serum myoglobin measurements. In emergency departments, the factor of time for myocardial infarction is crucial. "For patients with large transmural anterior myocardial infarction, the prompt administration of thrombolytic therapy decreases mortality by some 30 - 50% and also

preserves long-term cardiac function." [Kennedy et al., 1997]. But if they were administered inappropriately, the drugs for thrombolytic therapy may be dangerous--e.g., to patients with dissecting aortic aneurysm or gastrointestinal haemorrhage. Kennedy et al. compared the specificity of some biochemical markers for myocardial infarction detection. Currently the most commonly used biochemical marker is CK-MB, the cardiac-specific isoenzyme of creatine kinase(CK). CK-MB increases about 4 h after the onset of symptoms and remains elevated for approximately 24 h. Another specific marker is cardiac troponin T, whose circulating concentration increases within 4 h of onset. It would remain elevated for 7 days and was also positive in some patients with unstable angina, reflecting the minor degree of myocardial necrosis which took place in these patients. The marker selected by Kennedy et al. was myoglobin, a 17 kDa oxygen carrying haem protein found in skeletal and cardiac muscle. Although it lacked the specificity of the above markers, its concentration increased within 3 h of the onset of acute myocardial infarction. Myoglobin can be measured quickly and is the earliest and most useful marker of emerging myocardial damage, in the absence of skeletal muscle disease or damage. Since they took between 8 and 12 h after the onset of symptoms for them to become reliably positive, the real benefit of measuring the most commonly used markers is limited. It means that the early diagnosis of AMI relies mainly on clinical data and electrocardiographic information. A total of 290 patients with non-traumatic chest pain from the Dept. of Medicine, Northern General Hospital, Sheffield, were involved in the training and validating phases. The training stage included 90 patients and the validation stage included the remaining 200. Similar to the methods of Baxt, the physician would record the clinical and ECG variables at the time of presentation. The

final diagnosis was based on clinical follow-up, cardiac enzyme studies and sequential ECG recordings. The diagnosis was assigned independently by a panel of three experienced clinicians. In the prospective testing stage, 89 from those 290 patients satisfied the entry requirement (provisional diagnosis of ischaemic heart disease, presenting within 4 h, and lacking diagnostic ECGs changes of AMI), and the remaining 91 subjects in the testing phase were from the Accident and Emergency Dept., Royal Infirmary of Edinburgh. Again, the clinical history, ECG findings and opinions of the duty casualty officers were recorded. Myoglobin was measured using an immunturbidimetric assay (Behring Diagnostics) in the Dept. of Clinical Chemistry, Western General Hospital, Edinburgh. The neural network again was a 2 layered perceptron, with 53 inputs, including clinical history, symptoms, and ECG measurements. Linear discriminant analysis was implemented also. The result is shown in Table 2.5

Table 2.5 Research Results of Kennedy et al.

.Stage (patient number)	ANN Specificity	ANN Sensitivity	Linear Discrimant Specificity	Linear Discrimant Sensitivity
Validation (200)	90.2%	91.2%	82.6%	77.9%
Testing(89)	86.6%	77.3%	82.1%	59.0%
Testing(91)	80.0%	52.4%	76.9%	28.5%

Then, the results of the artificial neural networks were compared with myoglobin measurements. 86 of the 91 patients from Royal Infirmary of Edinburgh were included since the opinions of the admitting doctors were not recorded in 5 cases. Among these patients, 21 had acute myocardial infarction, 47 had angina, and the rest 18 had other diseases. Table 2.6 shows the results of combined strategies. In each column, if any of the measurement was positive for acute myocardial infarction, acute myocardial infarction was diagnosed.

Table 2.6 Combination of Clinical Opinion, Artificial Neural Network and Myoglobin [Kennedy et al. 1997]

	Doctor/ANN	Doctor/ANN+myoglobin	Doctor/ANN+3h myoglobin
AMI (n=21)	Positive 12 Uncertain 3 Negative 6	Positive 15 Uncertain 2 Negative 4	Positive 20 Uncertain 0 Negative 1
Angina (n=47)	Positive 17 Uncertain 15 Negative 15	Positive 19 Uncertain 14 Negative 14	Positive 19 Uncertain 14 Negative 14
Others (n=18)	Positive 3 Uncertain 5 Negative 10	Positivie3 Uncertain 5 Negative 10	Positive 3 Uncertain 5 Negative 10

Their results conformed with those of Baxt [Baxt, 1990; Baxt, 1991; Baxt, 1992a; Baxt, 1992b; Baxt, 1994; Baxt et al., 1995; Baxt et al., 1996]. The trained artificial neural network was promising for the acute myocardial infarction detection and was superior to linear discriminant analysis. In the testing phase, the patients included were particularly difficult to diagnose. Kennedy et al. showed that the trained artificial neural network was at least as accurate as the admitting doctors. And he pointed out as the statistical algorithms, which decreased in accuracy when the algorithm was used in a different center to that in which it was developed, the artificial neural network showed a good portability [Kennedy et al., 1997], meaning the network showed good results in different locations.

Before the wide use of the artificial neural network (see the definition in section 2.8) for myocardial infarction detection, the statistical methods and decision rules were the major classification methods. From 1985 to 1991, clinical doctors from nine countries in Europe undertook a large international study to compare the performance of nine electrocardiographic computer programs with that of eight cardiologists in interpreting

ECGs in 1220 clinically validated cases of various cardiac disorders [Willems et al., 1991]. The data were collected in five European centers. These data included 7 groups of pathological ECGs: control patients, patients with left ventricular hypertrophy, patients with right ventricular hypertrophy, patients with biventricular hypertrophy, patients with anterior myocardial infarction, patients with inferior myocardial infarction, patients with combined myocardial infarction, and patients with combined infarction and hypertrophy. The nine computer programs were Marquette Electronics, Hannover, Hewlett-Packard, Medis, Nagoya, Glasgow, Padova, Means, and Leuven. Among them, the programs developed in Hanover and Leuven use a statistical approach to classification. All others apply heuristic or deterministic rules. Table 2.7 and Table 2.8 showed the sensitivities of eight cardiologists and nine computer programs in identifying myocardial infarction. The participating cardiologists were deans of ECG in the hospitals. Their average performance is better than the average of common physicians. The average sensitivity of these programs was significantly lower than the that of the cardiologists (67.1% vs. 77.6%) [Willems et al., 1991]. In all of the research discussed in this section, the artificial neural networks had much higher sensitivities than the cardiologists. Also it was noted that the results of Hannover and Leuven were better than the rest.

Table 2.7 Results of Programs

Programs	Sensitivity
Marquette Electronics	69.7%
Hannover	79.0%
Hewlett- Packard	64.5%
Medis	62.5%
Nagoya	63.7%
Glasgow	67.7%
Padova	47.1%
Means	67.2%
Leuven	82.1%

Table 2.8 Results of Cardiologists

Cardiologist	Sensitivity
1	84.5%
2	78.1%
3	78.9%
4	78.7%
5	79.1%
6	69.3%
7	68.6%
8	83.5%

For the results of the cardiologists, none of the cardiologists' names were revealed.

The major statistical methods used for MI detection were: logistic regression [Pozen et al., 1994, Pahlm and Sornmo., 1990; Kennedy et al., 1996], recursive partition analysis [Goldman et al, 1988, Pahlm et al., 1990], and Bayesian method [Jonsbu et al, 1993]. The following table (Table 2.9) shows the results of several projects using statistical methods.

Table 2.9 Research Results using Statistical Methods

Major Researchers	Methods	Results
Pozen [Pozen et al., 1984]	Logistic Regression	Sensitivity:94.5%, Specificity:78. 1 %
Goldman [Goldman et al, 1988]	Recursive Partition Analysis	Sensitivity:88% Specificity: 74%
Pahlm [Pahlm et al., 1990]	Recursive Partition Analysis	Sensitivity:75%(best) Specificity:97% (best)
Pahlm [Pahlm et al., 1990]	Logistic Regression	Sensitivity:74% Specificity: 96%
Jonsbu [Jonsbu et al, 1993]	Bayesian Method	Accuracy:84%(No information about Sensitivity and Specificity)
Kennedy [Kennedy et al., 1996]	Logistic Regression	Sensitivity:87.3% Specificity: 80.4%

The results in Table 2.9 are not as good as those in Table 2.3. There are also some problems associated with the statistical methods. (1) The best performance of models was possible only if the models were specifically derived for use in a given center, using the

most predictive factors for patients presenting to that hospital. The performance degraded greatly at other centers [Kennedy et al., 1996]. (2) When Bayesian method was used, it was assumed that there was no dependence among the variables, which was obviously untrue [Jonsbu et al, 1993]. This unrealistic assumption results in incorrect significance of the predictors with dependence. (3) Generally speaking, the logistic regression and the recursive partition method are linear classifiers. Until now, no one is very clear about the nature of MI classification. If it is not linear separable, surely these methods cannot get the best performance. And usually these methods will achieve the best performance when at least 15-20 variables are included [Pozen et al., 1984, Goldman et al, 1988; Pahlm et al., 1990; Jonsbu et al, 1993; Kennedy et al., 1996]. Some even used 53 variables. The more variables included in the model, the higher dimension it is and the more difficult to construct the hyperplane to separate them. So even if it is linear separable, to achieve the good result is difficult. (4) These methods also required a large data set to derive the model for a good performance. Insufficient data surely will lead to poor classification result [Jonsbu et al., 1993; Kennedy et al., 1996]

Another method broadly used since the early 1970's is based on heuristic rules. The problem of this method was the same as the recursive partition and the logistic regression methods. They all are linear classifiers. And if the problem is not linear separable, the dynamic ranges of these classifiers are limited, which means that the increase of the sensitivity must be at the cost of the specificity [Elghazzawi and Geheb., 1997]

2.4 Pattern Recognition

2.4.1 Definition

Pattern recognition is the construction of algorithms capable of processing the range of input patterns of interest to yield a set of output patterns such that the occurrence of each input causes a uniquely identifiable output pattern to occur. It is essentially a decoding process in which discriminations are made. In simpler cases, tree methods of serial segmentation find value. Ideally, such measures enable one to divide remaining patterns at each decision node into two disjoint patterns, similar in principle to the basis for binary decoding. Another approach makes use of as many measures as possible that appear to be related to the desired discriminations. A search is then made for an appropriate differential weighting of these measures so as to obtain maximal spacing between patterns. This approach is sometimes referred to as factor analysis.

In this dissertation, we define pattern recognition as the process of assigning unknown objects to the category it belongs to based on the available information about these objects.

2.4.2 Some Basic Terms in Pattern Recognition

A classifier is used to classify the unknown objects. We make classifiers based on the learning set. Mathematically, we can represent a classifier as a mapping S: X, where xFn is a vector of n features. Many commonly used classifier functions, will be introduced in the following section. Another important concept in pattern recognition is the error of the classifier, defined as

(Number of wrongly classified objects / Total Number of objects) x100%

In this case, the sum of type A classified as type B and type B classified as type A is

the number of wrongly classified objects. Several reasons contribute to error. One is class overlap. Some values of features appear in more than one class. If the probability density function of these features overlap also, no classifier is able to classify without error.

The final aspect of pattern recognition is rejection, which means the system refuses to classify an input if the values of features are in a certain range. In this way, we can reduce the error since the error of rejecting is less then the error of wrong classification.

2.4.2.1 Common Classifiers.

(1) Linear Classifiers

Linear Classifiers are a set of classifiers implementing linear functions. They can be divided by a line in a two-dimensional feature space or a plane in a three-dimensional space or a hyperspace. Classifier function S(X) can return a value either 0 or 1. X is an unknown object. If S(X)=0, which means X belongs to group A; if S(X)=1, which stands for group B.

(2) Quadratic Classifiers

Quadratic classifiers are a set of classifiers implementing quadratic discrimination function, such as a circle, an eclipse or a parabola in feature space.

(3) Bayes Optimal Classifiers

As mentioned, when the probability density functions of the classes overlap, no classifier can classify without error. Bayes optimal classifiers can give the lower limit of the error a classifier can make.

Bayes optimal classifiers are based on the probability density functions of the classes. By finding the minimal error of the Bayes optimal classifier, we can find the theoretical minimal error any classifier can reach.

(4) Recursive Partitioning

Recursive partitioning is a classification method [Brieman et al., 1984]. Based on binary splits of selected decision variables, the training set is repeatedly divided into smaller groups. The selection of the decision variables is based on the "purity", defined by Gini criterion. The variable which maximizes the "purity" will be selected. In this way, the data set is divided into two subgroups. For each subgroup, this process is repeated until each leaf node contains no more than five subjects, or until all subjects are classified correctly (for the present research, it means all the patients are categorized the same as their right diagnosis). Based on the misclassification cost (for the present research, cost of classifying normal as infarct or infarct as normal) and complexity (the number of the leaf nodes), several decision trees are constructed. All the trees are tested by the 10-fold cross-validation. The trees with the least misclassification cost will be selected. The more amount of impurity reduced by that variable for the entire tree, the more important that variable is.

(5) Logistic Regression

Multiple logistic regression is a statistical method establishing the relationship between parameters and the interested phenomenon (for the present research, it tries to find the relationship between the ECG measurements and the presence of absence of infarction). It will produce a linear function:

$$LN(p/(1-p)) = B_0 + B_1 X_1 + B_2 X_2 + \ldots + B_n X_n,$$

where LN stands for the log-odd function, p is the probability of the phenomenon (for the present research, it is infarction), unknown coefficient, which will be estimated by this method, and Xi us the ith parameter (for the present research, it is ECG measurement).

The first stage is the selection of the optimal variables from all the possible useful variables. Two procedures are available to serve this stage: standard forward stepwise procedure and standard backward stepwise procedure. The standard forward stepwise procedure begins with no variables in the model and selects the most significant one to be added in the model, based on the evaluation of the significance of each variable. Then after "controlling" for the variable already in the model, the most significant variable among the variables not included in the model is selected to be added in the model. This procedure is repeated until all the significant variables are included in the model. The backward stepwise procedure begins with all the variables in the model. Then nonsignificant variables are removed until only significant variables are included in the model.

If there are interaction terms between those variables selected, the second stage is required. This stage will analyze the significance of interaction between them. The forward and/or backward stepwise procedure is used again to make sure that no significant variables are missed from the model and that all the variables in the model are significant.

2.4.3 Pattern Recognition Methods used in ECG Systems

The first generation of pattern recognition techniques was rule-based system. Pipberger developed a 12-lead system using syntactic rules for infarction detection in clinical data [Pipberger et al., 1961]. Belforte, Leblanc and etc. developed many ECG interpretation systems in this way [Belforte et al., 1979; Leblanc et al., 1989].

The second generation is the statistical pattern recognition technologies, which includes both clustering algorithms and discriminant analysis algorithms. Due to the

nonlinearly separable nature of discrimination between normal and ventricular beats, limitations of such technologies are inherent [Haisty et al., 1972]

2.4.4 Efforts on Standardization

To end the task of comparison of different methods, a standard digitized ECG database is needed. Two databases are the Massachusetts Institute of Technology-Beth Israel Hospital (MIT-BIH) database and the Common Standards for Quantitative Electrocardiograph (CSE) database, which proves to be the best ECG databases and are used worldwide.

The MIT-BIH database was the result of years of investigating methods for real-time ECG rhythm analysis. An extensive annotated digital ECG database was developed during the course of work. In 1980, the first version was distributed to the public. In 1988, after the evaluation of nearly 100 academic and industrial research groups worldwide, the second version was issued with a package of C-language software included. Later in 1992, the third version was issued with some minor correction of the annotation of 16 beats. Until now, this is the latest version. The source of the ECGs was the Holter recordings obtained by the Beth Israel Hospital Arrhythmia Laboratory between 1975 and 1979. Neither the number of the subjects, nor the number of patients was revealed. There were 48 records in the third version, each slightly over 30 minutes long. They can be divided into two parts: 23 records (numbered from 100 to 124, inclusive with some number missing) , serving as a representative sample of the variety of waveforms and artifact that an arrhythmia detector might encounter in routine clinical use; 25 records, including complex ventricular, junctional, and supraventricular arrhythmia and conduction abnormalities, which were rare but clinically important phenomena. Some of the records

in the part two presented significant difficulty to arrhythmia detectors. The original analog recording were made using nine Del Mar Avionics Model #445 two-channel recorders. During the digitization process, the analog recordings were played back on a Del Mar Avionics Model #660 unit and were filtered to limit analog-to-digital saturation and for anti-aliasing, using a passband from 0.1 to 100 Hz. The annotation process was preformed by 2 cardiologists independently. They mark their own labels on the paper printed for each record. All the discrepancies between the cardiologists were highlighted. Each discrepancy was then reviewed and resolved by consensus. The corrections were analyzed by an auditing program to make sure no missing or falsely detected beats [Moody, 1992].

CSE study (Common Standards for Quantitative Electrocardiograph) was supported by the European Community. The first part of CSE, dealing with the accuracy of waveform recognition in ECG interpretation systems, was completed in 1985. The second stage, on diagnostic interpretation, was completed in 1990. It included 1,220 well documented short (12- or 15- lead) ECG recordings, falling into seven main diagnostic categories, designed for evaluating diagnostic ECG analyzers. The data were collected from five European Centers. Three cardiologists checked the clinical information. A consensus was required for each case selected. The criteria to exclude ECGs were ECGs showing complete left or right bundle brunch or other major intraventricular conduction defects and those of poor technical quality [Willems et al., 1985].

Some similar databases are AHA database [AHA ECG Database, 2000], Ann Arbor Electrogram Libraries [Ann Arbor Electrogram Libraries, 2000], European ST-T Database [Taddei et al., 1987 & Taddei et al, 1989], Improve Data Library [Improve Data

Library, 2000], MGH Database [MGH, 2000],the 12 Lead ECG Library [12 Lead ECG Library, 2000].

The American Heart Association (AHA), with funding from the National Heart, Lung, and Blood Institute (NHLBI), sponsored the development of the AHA Database for Evaluation of Ventricular Arrhythmia Detectors during the late 1970s and early 1980s at Washington University (St. Louis). The first portions of the AHA Database were released in 1982, and it was completed in 1985. Until recently, the only available portion of the AHA database consisted of 80 recordings, which were divided into eight "classes" of ten recordings each, according to the highest level of ventricular ectopy present:

no ventricular ectopy (records 1001 through 1010)

isolated unifocal PVCs (records 2001 through 2010)

isolated multifocal PVCs (records 3001 through 3010)

ventricular bi- and trigeminy (records 4001 through 4010)

R-on-T PVC s (records 5001 through 5010)

ventricular couplets (records 6001 through 6010)

ventricular tachycardia (records 7001 through 701 0)

ventricular flutter/fibrillation (records 8001 through 8010)

The final thirty minutes of each recording are annotated beat-by-beat although supraventricular ectopic beats are not distinguished from normal sinus beats. Two versions of the database are available: the "short" version includes five minutes of unannotated ECG signals prior to the thirty-minute annotated segment of each recording, and the "long" version includes 2.5 hours of unannotated ECG signals prior to each annotated segment. At the time the AHA Database was created, a second set of 80

recordings was constructed according to the same criteria as the first set. This second set was intended for evaluations without any possibility that the detectors might have been "tuned" (optimized) for the test data; for this reason, this "test set" was unavailable until recently [AHA ECG Database, 2000].

The annotated recordings of intracardiac electrocardiograms in the Ann Arbor Electrogram Libraries were made and annotated by Dr. Janice Jenkins and her colleagues at the University of Michigan over a period of more than fifteen years. This collection of over 800 recordings, made during electrophysiology studies, was a uniquely valuable resource, particularly for developers and evaluators of implantable cardiac devices. Since resource, intracardiac electrocardiograms can reveal atrial activity much more clearly than typical surface ECGs, these recordings are also useful for basic research in cardiac electrophysiology [Ann Arbor Electrogram Libraries, 2000].

The European ST-T Database is a large collection of fully annotated excerpts of two-channel ambulatory ECG recordings, selected to exhibit transient ST and T-wave changes. The database consists of 90 recordings. The European ST-T Database CD-ROM also includes the VALE Database, an earlier single-channel ECG database created by the Pisa group. The VALE Database contains 35 three-hour recordings, annotated beat by beat.

This database consists of 90 annotated excerpts of ambulatory ECG recordings from 79 subjects. Myocardial ischemia was diagnosed or suspected for each subject [Tadder et al., 1987]; additional selection criteria were established in order to obtain a representative selection of ECG abnormalities in the database. The database includes 367 episodes of ST segment change, and 401 episodes of T-wave change, with durations ranging from 30

seconds to several minutes, and peak displacements ranging from 100 micro-volts to more than one millivolt.

Each record lasts two hours. Two cardiologists worked independently to annotate each record beat-by-beat and for changes in ST segment and T-wave morphology, rhythm, and signal quality. ST segment and T-wave changes were identified in both leads (using predefined criteria, which were applied uniformly in all cases), and their onsets, extreme, and ends were annotated. Annotations made by the two cardiologists were compared, disagreements were resolved by the coordinating group in Pisa [Tadder et al, 1989], and the reference annotation files were prepared; altogether, these files contain 802,866 annotations.

IMPROVE is a European Union concerted-action project with the goal of improving on-line assessment and management of patient state in critical care and operating theater environments. The project has developed a large collection of recordings of multiple physiologic signals made in critical care units, extensively annotated and supplemented by simultaneously acquired clinical information [Improve Data Library, 2000].

The Massachusetts General Hospital/Marquette Foundation Waveform Database contains 250 multi-channel recordings (3 ECG leads, ABP, PAP, CVP, respiration, and C02) acquired from anesthesia monitors. The recordings have varying lengths but are typically about 1.5 hours long [MGH Database, 2000].

The 12-lead ECG Library is a well-organized collection of 12-lead ECGS, available as images only [12 Lead ECG Library, 2000].

Besides the databases mentioned above, two more big databases are on the way. They are the MIMIC Database and the long-term ST Database .

The MIMIC Database was developed by MIT. It is a very large database of ICU recordings (The total size is around 50 GB). These recordings are typically 24 to 48 hours in length, and include 2 or 3 ECG signals, 2 to 4 pressure signals, respiration, and extensive clinical data on each subject. The long-term ST Database is an international effort to develop a database of two-channel 24-hour ECG recordings selected to document transient ischemic and non-ischemic ST changes. This project is coordinated by Franc Jager of the Laboratory of Biomedical Computer Systems and Imaging of the University of Ljubljana (Slovenia), and also includes the participation of the developers of the European ST-T Database.

Among them, except AHA database, Ann Arbor Electrogram Libraries, IMPROVE Data Library, MGH Database, the rest include myocardial infarction records.Only European ST-T Database revealed the number of patients includes. For the rest, no such information is revealed.

2.5 Signal Preprocessing

This part involves tasks such as filtering, removal of noises, annotation of each wave and maybe the detection of reversal of electrodes.

The most commonly used filtering is band pass filtering, usually ranging from 0.01 - 100 Hz. The choice of the band pass range will influence the later performance severely. [Vila et al., 2000] This choice is based on the standard of American Heart Association. This frequency range avoids disturbing variations in baseline and ST segments but allows

the regular frequency range of a T wave [Srikanth, 2000]. The removal of noises includes the removal of 50 or 60 Hz noises and any other interference recorded.

Annotation will be a critical part of the work. The experienced cardiologists will annotate each wave of a beat and/or the rhythm in the recording. Usually, P wave, QRS complex, T wave, and the onset and the end of P wave, QRS complex are annotated. For any classification task, such annotation will work as the standard to compare with the performance of FCG interpretation systems [Jenkins, 1998]. There is no fixed standard on the annotation method. In the database developed by Laguna [Laguna et al., 1997], the interface is called WAVE, a Unix-based software tool.

Although artificial beats are used in many studies [Haisty et al, 1972], in the present work, no such data are used.

2.6 QRS Detection

2.6.1 QRS Morphology

A normal QRS complex is composed of a Q wave, the negative wave at the onset of the complex, and R wave, the most prominent point in a beat, and S wave, another negative wave following R wave. In different leads, the shapes and the direction of QRS may vary. The main feature of the QRS complex is the sharp rise and fall of the complex, resulting from the higher frequency components in it.

2.6.2 Detection Methods

QRS detection is the beginning of the estimation of the fiducial points. The general methods include non-linear transformation and decision logic [Pahlm et al., 1984]. The non-linear transformation technologies include short-term energy calculation, calculation

of smoothed envelope, parametric modeling and maximizing the first difference between samples.

In ambulatory data processing, the most popular method, the moving window integrator algorithm, was proposed by Pan and Tompkins in 1985 [Pan et al., 1985]. Another category of algorithms are based on ANN because of the observation that the whole ECG signals are non-linear and generated by non-linear systems [Schimminger, 1998]. Rasiah [Rasiah et al., 1995] and Xue [Xue et al., 1992] developed such algorithms.

A new method is wavelet transform based algorithm. This kind of algorithm avoids the shortcomings of difficult choice of window length, as in the moving window methods. They involve a large amount of computation but show good accuracy. With the quicker speed of CPU this method will be a promising one [Li et al., 1995 & Vila et al., 2000].

2.7 T and P Wave Detection

T wave detection usually follows the detection of QRS complex. And the P wave of the next beat may merge with the T wave of the preceding beat when the heart rate is fast. By wavelet transform, it is not difficult to detect T wave [Vila et al., 2000]. For P wave, the duration of P wave is less than 0.12 second. The small amplitude P wave and the insufficient spectral information of P wave make the detection of P wave still difficult.

The J point, the junction between ST segment and QRS complex, is the angle peak formed by the ST and QRS complex. Points on the ST segments are called with reference to the number of millisecond beyond J point. Greenhut [Greenhut et al., 1989] used the tangent operator to detect J points.

2.8 Artificial Neural Network

For many years, scientists in different subjects, such as engineers, mathematics, physicists, physiologists, have been trying to develop machines exhibiting "intelligent" behavior. With the birth of first computer, people thought it captured some aspects of human brains. The idea behind computers is symbolic processing, a way of human information processing. But it is found that the performance is far from that of human beings.

- The value of a processing unit is predetermined by programs. It must follow
- some kind of functional relationship, not being able to respond as a different one to different input.
- It can not resist noise and has no ability to tolerate mistakes. In a short, if there is any deviation from the correct input, the result will be wrong.
- If some of the processing units are damaged, the whole program will crash.
- What is more, it has no ability to generalize. It cannot understand concept or make a conclusion based on known information.

Concurrent with the development of computers, however, has been research which develops models based on simplified animal brain structure. These models can learn from a training environment, not being determined by computer programs. Work on these so-called "neural networks" experienced a boom in 1960's, a low tide in 1970's and early 80's, and now a renaissance.

The starting point of artificial neural networks is that "in order to recreate some of processing capabilities of the brain it is necessary to recreate some of its architectural

features. Physiological research shows that human brains have 10^9 - 10^{10} basic processing units, neurons, which are connected following networks.

2.8.1 The Structure of a Real Neuron

Each neuron has three parts: dendrite, axon, and synapse. Signals are transmitted between neurons by electrical pulses (action potentials or 'spike' trains) travelling along the axon. These pulses impinge on the afferent neuron at terminals called synapses. These are found principally on a set of branching processes emerging from dendrites. Each pulse occurring at a synapse initiates the release of a small amount of chemical substance or neurotransmitter, which travels across the synaptic cleft and is then received at post-synaptic receptor sites on the dendritic side of the synapse. The neurotransmitter becomes bound to molecular sites here which, in turn, initiate a change in the dendritic membrane potential is post-synaptic-potential (PSP) change may serve to increase (hyperpolarise) or decrease (depolarize) the polarization of the post-synaptic membrane [Antanitus, 1998].

2.8.2. The Structure of Artificial Neuron

After simplification, the real neuron is abstracted as in the figure below.

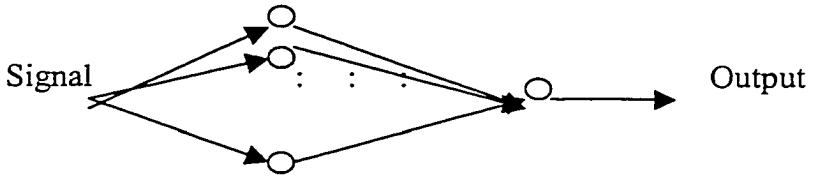

Figure 2.8 Structure of artificial neurons

Figure 2.8 shows the structure of artificial neurons. The information processing performed in this way may be crudely summarized as follows: signals (action potentials) appear at the unit's inputs (synapses). The effect each signal has may be approximated by multiplying the signal by some number or weight to indicate the strength of the synapse.

The weighted signals are now summed to produce an overall unit activation. If this activation exceeds a certain threshold the unit produces an output response. This functionality is captured in the artificial neuron known as the Threshold Logic Unit (TLU) originally proposed by McCulloch and Pitts [McCulloch et al., 1943]

Each neuron accepts input from dendrites and sends output by axons. Each neuron functions as a basic processing unit, a node. The dynamics of a node contains two functions, activation and threshold detection. First is activation and summation. The activation function for the node j, is

$$X_j = \sum_i W_{ij} \cdot Y_i$$

where X_j is the result of activation, W_{ij} is the weight from node i to node j. And Y_i is the output of node i. If there is no connection between two nodes, the weight will be 0.

Second, the threshold function will determine the output of a node. Depending on different network topology, it may be 0/1 or +1/-1. For Perceptron, it will be either 1 or 0. The most common threshold function is the sigmoid function since it is very similar to the behavior of biological neurons [Anthony and Bartlett, 1999].

The sigmoid function is

$$f(x) = \frac{1}{1+e^{-x}}$$

2.8.3 The Definition of Artificial Neural Nets

There are many different definitions of artificial neural nets, but until now there is no popularly accepted one. Here we present only a simple one. A neural network is an interconnected assembly of simple processing elements, units or nodes, whose functionality is loosely based on the animal neuron. The processing ability of the network

is stored in the inter-unit connection strengths, or weights, obtained by a process of adaptation to, or learning from, a set of training patterns [Anthony and Bartlett, 1999].

2.8.4 The Performance of Artificial Neural Nets

The performance of these models seems promising. They overcome some shortcomings of traditional computers and show some similar characters of animal brains. Typical modes of operation are as associative memories, retrieving complete patterns from partial data, and as pattern classifiers. The following explains some of their features.

The node parameters are trained to their final values by continually presenting members from a set of patterns or training vectors to the net, allowing the net to respond to each presentation, and altering the weights accordingly; that is, they are adaptive rather than preprogrammed systems.

Their action under presentation of input is often best thought of as the time evolution of a dynamical physical system, and there may even be an explicit description of this time evolution in terms of a set of differential equations. They are robust under the presence of noise on the inter-unit signal paths and exhibit graceful degradation under hardware failure. A characteristic feature of their operation is that they work by extracting statistical regularities or features from the training set [Leondes, 1997]. This characteristic allows the net to respond to novel inputs in a useful way by classifying them with one of the previously seen patterns or by assigning them to new classes.

Anyway, there is no simple correspondence between nodes and high level semantic objects. Rather, the representation of a 'concept' or 'idea' within the net is via the complete vector of unit activities, being distributed over the net as a whole, so that any given node may partake in many semantic representations.

2.8.5 Application of Artificial Neural Nets in ECG Analysis

Artificial neural networks have been widely accepted as excellent pattern recognizers [Aleksander and Stonham, 1979 & Bledsoe et al., 1959] and is one of the most important non-symbolic artificial intelligent methods in ECG analysis [Xue et al., 1989 & Lin and Chang, 1989]. During the several decades of development, many useful artificial neural network models were designed: Rosenblatt's Perceptron [Rosenblatt, 1962], which was proved to have very limited explanation ability by Minsky [Minsky et al., 1969] in 1969, bringing the low tide of artificial neural network development, and which was then renovated by Rumelhart [Rumelhart et al., 1985 and Rumelhart et al., 1986]. During the next 20 years, the research of artificial neural networks still went on although much national funding was cut out [Little, 1974 and Parker, 1982]. In 1975 Fukushima developed a model Cognitron [Fukushima, 1975], which involved intensive calculation. The Kohonen network impressed others with its amazing fault-tolerant ability [Kohonen, 1984]. Both models above are self-organizing, a very important characteristic of an artificial neural network. Freeman's research on chaos based on the physiological experiment of olfaction [Mandelbrot, 1988] has found many applications in expectation of multiple variables, a highly uncertain environment.

A group of physicists views the neural networks as dynamic systems. The process of the system is to reach a certain local minima. The most famous systems among them are the Hopfield Network designed by Hopfield, using the Hebb rule [Hebb, 1949] for weight setup in 1982 [Hopfield, 1982] and the spin glass model [Amit and Gutfreund, 1985].

In 1987, Grossberg, another physicist, designed the Adaptive Resonance Theory (ART) model [Carpenter and Grossberg., 1987; Grossberg, 1987 and Grossberg, 1988]. And later they further develop it into ART 2 [Carpenter and Grossberg, 1987]. It is an unsupervised learning model, which means the system will classify the inputs automatically according to certain criteria [Carpenter and Grossberg, 1987].

Generally speaking, neural networks are good for classifying small amounts of different patterns. When the number of different patterns increases, the performance of the network degrades quickly. Due to the nature of the algorithm, which distributes the total error among all the lower level nodes, the back propagation model is the most successful for ECG classification [Kuppuraj, 1995; Lippman, 1987]. According to a study using simulated ECG data sets, the delta-rule is the optimal paradigm [Kuppuraj, 1995].

The back propagation model suffers from the long training time and possible traps in local minima, not the optimal result, which also results from the nature of the algorithm [Magoulas et al., 1999]. Two parameters influence the behavior of the network greatly and there are many attempts to select the optimal values [Magoulas et al., 1999].

2.8.6 Application of Artificial Neural Nets in MI ECG Detection

Artificial neural networks have been widely accepted as excellent pattern recognizers [Aleksander et al., 1979, Bledsoe and Browning, 1959] and are widely used in myocardial infarction ECG Detection [Baxt, 1990; Baxt, 1991 , Baxt, 1992a; Baxt, 1992b; Baxt, 1994; Baxt et al., 1995; Baxt et al., 1996; Heden et al., 1994, Heden et al., 1996 & Heden et al., 1997; Harrison et al., 1991; Kennedy et al., 1997]. The perceptrons were used in all the above research. All have only one output nodes, with value between zero and one. A threshold is selected. The following table (Table 2.10) is a comparison of

the structures of these artificial neural networks.

Table 2.10 Structures of the Artificial Neural Networks used for MI Detection

Major Researcher	Structure of the Network (input node number X hidden node number X output node number)	Function
Baxt [Baxt, 1990]		Acute Cornary Occlusion
Baxt [Baxt, 1991]	20 x 10 x10 x 1 (2 hidden layers)	Chest Pain Presenting to Emergency Department
Baxt and Skora [Baxt et al., 1996]	20 x 10 x10 x 1 (2 hidden layers)	Extend the Previous Research to over 1000 Patients
Heden [Heden et al., 1994]	15 x 5 x 1	No Presence of Healed Inferior Myocardial Infarction
	15 x 5 x 1	No Presence of Healed anterior Myocardial Infarction
	30 x 9 x 1	Presence of Healed Inferior Myocardial Infarction
	30 x 9 x 1	Presence of Healed anterior Myocardial Infarction
Heden [Heden et al., 1996]	24 x 6 x 1	Healed Myocardial Infarction
Kennedy [Kennedy et al., 1997]	53 x 18 x 1	Acute Myocardial Infarction
Kennedy [Kennedy et al., 1997]	72 x 15 x 1	Acute Myocardial Infarction

There has been no uniform standard for the MI detection. The measurements selected vary from group to group. And the numbers of measurements also vary greatly, ranging from 15 [Heden et al., 1994] to 72 [Heden et al., 1997]. Usually they include the patient history, clinical symptoms, and ECG measurements. To avoid the inter-variation between the cardiologists who input the patient history and clinical symptoms, some research use only the ECG measurements as the inputs [Heden et al., 1994; Heden et al.,1996; Heden et al., 1997]. The following paragraphs list the inputs used by the above networks.

All of Heden's research listed here select only ECG measurements. In his research of 1994 [Heden et al.,], Heden selected Q amplitude, Q duration, R amplitude, S amplitude, and S duration of lead V2, V3, and V4 to train the network to identify there was no anterior myocardial infarction. He added another 15 parameters to train the network to identify the presence of myocardial infarction. They were ST-segment amplitude 1/6, ST-segment amplitude 2/6, ST-segment amplitude 3/6, ST-segment amplitude 4/6, ST-segment amplitude 5/6 of lead V2, V3 and V4. Q amplitude, Q duration, R amplitude, S amplitude, and S duration of lead II, III, and aVF were selected to train the network to identify there was no inferior myocardial infarction. Similarly, another 15 parameters were used for interior myocardial infarction detection. They were: ST-segment amplitude 1/6, ST-segment amplitude 2/6, ST-segment amplitude 3/6, ST-segment amplitude 4/6, ST-segment amplitude 5/6 of lead II, III and aVF.

Based on the previous research, Heden [Heden et al., 1996] selected 8 measurements from V2, V3, V4 to diagnose healed myocardial infarction: Q, R, S amplitude, Q and R duration, ST amplitude 1/6, ST amplitude 3/6, ST amplitude 5/6.

Later, in another research project, Heden trained the network to detect acute MI [Heden et al., 1997] by 6 measurements from 12 lead: ST-J amplitude, ST slope, ST amplitude 2/8, ST amplitude 3/8, positive T amplitude and negative T amplitude.

In the series of research conducted by Baxt since 1991, [Baxt, 1991; Baxt, 1992a; Baxt, 1992b, Baxt, 1994; Baxt et al., 1995, & Baxt et al., 1996], Baxt used the same network structure. The 20 inputs selected from 22 potential predictors were age, sex, left anterior location of pain, nausea and vomiting, diaphoresia, syncope, shortness of breath, palpitation, response to nitroglycerin, acute myocardial infarction, angina, diabetes,

hypertension, jugular venous distension, rales, 2-mm ST-segment elevation, 1-mm ST-segment elevation, ST-segment depression, T-wave inversion, significant ischemic change.

[Kennedy et al., 1997] used the most parameters among the research listed here, 53 inputs: ages in years (20+, 30+. 40+. 50+, 60+, 70+, 80+), smoker, ex-smoker, family history of ischaemic heart disease, diabetes mellitus, hypertension, hyperlipidaemia; further, is chest pain the major symptom: central chest pain, pain in left side of chest, pain radiating to neck or jaw, pain radiating to left arm, pain radiates to right arm, worse on respiration, pain related to posture, chest wall tenderness, pain described as sharp or stabbing; pain described as tight, heavy, gripping or crushing; sweating, shortness of breath, nausea, vomiting, syncope, episodic pain, duration of pain in hours (10+, 20+, 30+, 40+, 50+), history of angina, previous myocardial infarction, worse than usual angina/similar to previous acute myocardial infarction, fine crackles suggestive of pulmonary edema, added heart sounds, signs of hypoperfusion, new ST segment elevation, new pathological Q waves, ST segment or T wave changes suggestive of ischaemia, bundle branch block, old ECG features of myocardial infarction, and ECG signs of ischaemia known to be old. The effect of varying the number of hidden nodes was tested, and the optimal was 18.

Most of the networks use the traditional back propagation algorithm to train the network [Rumelhart et al., 1985 and Rumelhart et al., 1986], except one network used by Heden [Heden et al., 1997]. The two-layer perceptron was trained by the Langevin extension of the back propagation algorithm [Rognvaldsson, 1994].

All the research showed very promising results, which demonstrated that artificial neural networks can be a useful tool for my myocardial infarction diagnosis.

2.9 Summary

For several decades, ECG has been the most successful method to detect the early pathological changes of the heart. The pattern recognition methods used in myocardial infarction classification have included heuristic methods, statistical methods, and artificial neural networks. Based on previous research, artificial neural networks were the best classifiers for myocardial infarction detection, in terms of sensitivity and specificity [Baxt, 1990; Baxt, 1991; Baxt, 1992a; Baxt, 1992b; Baxt, 1994; Baxt and White, 1995; Baxt and Skora, 1996; Edenbrandt et al., 1993; Harrison et al., 1991; Heden et al., 1994; Heden et al., 1996; Heden et al., 1997; Kennedy et al., 1996; Kennedy et al., 1997]. So, we hypothesize that an artificial neural network-based ECG interpretation system may improve clinical myocardial infarction detection.

There were some weakness in the previous research (see the details in section 2.3). To improve that, the following design was made. First, the cardiologists involved in the present research were very experienced (one has 19 years of practice and the other has 22 years). Second, only ECG measurements were used, to avoid inter-observer variation and intra-observer varaition. Third, a large data set was used to make sure the neural network was well trained.

The following tables (Table 2.11 and Table 2.12) compare the present research with Baxt's research in 1990 and 1991 [Baxt, 1990 and Baxt, 1991].

Table 2.11 The Comparison between Present Research and Baxt's Research

	Present Research	Baxt's Research
Number of Layers	2	3
The Structure of the Network	20 x 10 x1	20 x 10 x 10 x 1
Initial Number of Parameters	20	22
Final Number of Parameters	20	20
Number of Patient s	137	300
Network Training Method	Back Propagation	Back Propagation
Experience of Cardiologists	Medical Residents in Postgraduate year 2 and 3 & Emergency Room Attending Faculty Physicians	One has 19 Years of Experience, the Other has 21 Years of Experience
Instant Decision Made?	Yes	No
Final Decision Established by	Subsequent Review of Patient Records and Follow-up Phone Interviews	Subsequent Review of Patient Records
Has Signal Pre-processing?	Yes	No
Inter-observer Variation	No	Yes
Intra-observer Varation	No	Yes
Sensitivity	97.2%	92.2%
Specificity	96.2%	50.7%

Table 2.12 Features Comparison between Present Research and Baxt's Research

Features	Present Research	Baxt's Research
T Wave Amplitude	Yes	No
R Wave Amplitude	Yes	No
The Slope of the 2 Sides of T Wave	Yes	No
ST Duration	Yes	No
ST-junction to T Max Amplitude	Yes	No
1/8 Segment Amplitude	Yes	No
2/8 Segment Amplitude	Yes	No
3/8 Segment Amplitude	Yes	No
4/8 Segment Amplitude	Yes	No
5/8 Segment Amplitude	Yes	No
6/8 Segment Amplitude	Yes	No
7/8 Segment Amplitude	Yes	No
8/8 Segment Amplitude	Yes	No
T Wave Duration	Yes	No
T Wave Positive Peak Amplitude	Yes	No
T Wave Negative Peak Amplitude	Yes	No
The Presence of Q Wave	Yes	No
Age	No	Yes
Sex	No	Yes
Left Anterior Location of Pain	No	Yes
Nausea and Vomiting	No	Yes
Diaphoresia	No	Yes
Syncope	No	Yes
Shortness of Breath	No	Yes
Palitation	No	Yes
Response to Nitroglycerin	No	Yes
Acute Myocardial Infarction	No	Yes
Angina	No	Yes
Diabetes	No	Yes
Hypertension	No	Yes
Jugular Venous Distension	No	Yes
Rales	No	Yes
2-mm ST-segment Elevation	Yes	Yes
1-mm ST-segment Elevation	Yes	Yes
ST-segment Depression	Yes	Yes
T-Wave Inversion	Yes	Yes
Significant Ischemic Change	No	Yes

CHAPTER 3

METHODOLOGY

3.1 Task

The overall goal of the present dissertation is to design an automated single lead ECG diagnosing system to detect the presence or absence of myocardial infarction. The system must satisfy the following criteria:

(i) Expandable: the system can be expanded to multi-lead systems for a more comprehensive diagnosis.

(ii) Modular: the system can work as a component to be embedded into other compatible diagnosing systems which do not have the ability for myocardial infarction detection.

(iii) Optimized: the system will implement the algorithms, which have the highest correction rate under the assumption that the hardware will not be a problem.

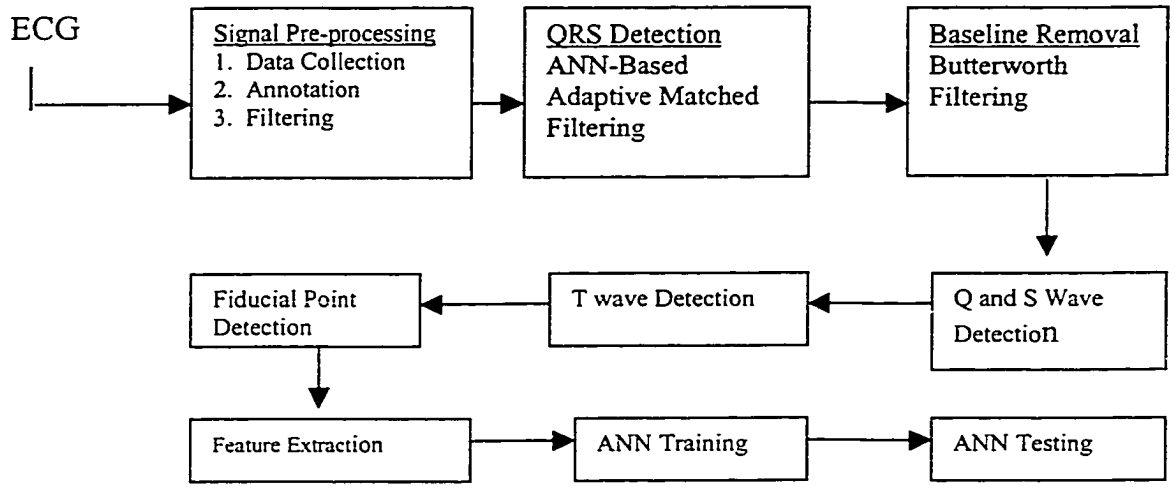

Figure 3.1 Block Diagram of the Myocardial Infarction Detection System

The subsystems include signal pre-processing, QRS detection algorithm, baseline removal, Q and S Wave Detection, T wave detection system, fiducial point detection, feature extraction, artificial neural network training, and artificial neural network testing for MI recognition.

The selection and implementation of each sub system is the result of close cooperation with experienced cardiologists. The close cooperation with cardiologist through the whole research project is also the trend of current ECG diagnosing systems [Sheffield, 1987 & Srikanth, 2000]. The algorithms practiced here are based on the survey of CSE [Leblanc et al., 1989 & Haisty et al, 1972], the system designed by Srikanth [Srikanth, 2000] and the latest technology in ECG analysis [Shaw et al., 1995; Laguna et al., 1996; Hu et al., 1997; Burattini et al., 1998; Frenkel et al., 1999; Garcia et al., 2000].

Around three thousand lines of code are written in MatLab. They can be divided into 9 modules: signal pre-processing module, QRS detection module, Baseline remocal module, Q and S wave detection module, T wave detection module, fiducial detection

module, feature extraction module, artificial neural network training module, and artificial neural network testing module. The communication between modules is very limited. No goto command is in the functions. Each basic function finishes only one task. The result of one function passes to other functions as data parameters only, leaving space for the later update and modification. For example, cheby2_coeffi routine generated the coefficients for the chebyshev type II low pass filter for a specific cut off frequency. If we want to generate a chebyshev type II low pass filter for another cut off frequency, we need only to change the input parameter in the routine. To draw the bode plot for the chebyshev type II filter requires the coefficients of the filter. The coefficients generated by the cheby2_coeffi routine can be fed into this routine (See the APPENDIX). The cohesion between the functions is high. This modular design makes the whole system compact and well-functioned.

3.2 Signal Pre-processing

3.2.1 Data Collection

The source of the ECGs was Holter recordings obtained by the Dynamic ECG Unit of the Beijing Hospital between 1988 and 2000. There were 137 records, in two leads, V1 and V5, with variant length. 53 records were in V1 leads and the remaining 84 were in V5. Each record was taken from a different patient. 62 records are 24-hour Holter recordings and the remaining 75 are short recordings of about 3 minutes. They can be divided into two parts: 15 records from the normal group, the remaining 122 records from patients who later had experienced MI, as verified by the patient history. Similar to the MIT-BIH database, professional recorders and scan systems were used for recording. Both cassette recorders and digital recorders were used. During the digitization process,

the analog recordings were played back on a Del Mar Avionics Model #363 unit and were filtered to limit analog-to-digital saturation and for anti-aliasing, using a passband from 0.01 to 100 Hz. The ECG records were annotated by two cardiologists independently. They marked their own labels on the paper printed for each record. All the discrepancies between the cardiologists were highlighted. Each discrepancy was then reviewed and resolved by consensus, meaning that both the cardiologists and the Dean reach the same diagnosis for the beats. The corrections were analyzed to make sure there were no missing or falsely detected beats.

The patients can be divided into two groups. One is the group consisting of the patients who came to the Dynamic ECG Unit without the prescription of doctors, and the other consisting of the patients who received treatment in the hospital and came to have the test according to the prescription. The basic selection criteria are (1) these patients had not been diagnosed by other methods as myocardial infarction certainly, (2) they had no myocardial infarction history before, (3) they had experienced some kind of uncomfortable symptoms such as short of breath, chest pain, sweating, etc., for at least one month. None of these patients were aware that their data were recorded for the present research, and their names were unknown to the researchers in the present research.

During observation at the hospital, 25 records had no real-time signal saturation spikes, no interchanged or loose electrodes, no broken lead wires, no interference from phone and, as told by the cardiologists in the department, the signals collected had no real-time signal saturation spikes, no interchanged or loose electrodes, no broken lead wires, no interference from phone lines. The data may contain noise such as electromagnetic interference, baseline sways and 50 Hz AC interference, introduced during the recording.

3.2.2 Annotation

To facilitate the research, fiducial points in each beat (starting point of Q, Q peak, R peak, S peak, ending point of S wave, J point, starting point of T wave, T peak, ending point of T wave) in the data set were annotated manually by two experienced cardiologists (19 years of experience and 22 years of experience in ECG diagnosing) and the Dean of the Dept. of Dynamic ECG Unit at the hospital. They marked their annotations on the recording paper. The dean double checked their work if there was conflict.

3.2.3 Filtering

For the rest of processing, first the entire signal was filtered by the Chebyshev low pass filter (fc= 100HZ, 6^{th} order). The selection of this cutoff frequency is consistent with the standard of American Heart Association [AHA, 2000]. And this frequency range avoids disturbing minor variations in baseline and ST segments and allows the regular frequency range of T waves, which is crucial to the present research, and affects only a little of the QRS complex [Srikanth, 2000].

Then, to get rid of the 50Hz noise, a notch filter designed by MatLab was used. Then the mean data were subtracted from the filtered data, to get rid of the DC component.

To get the accurate ECG measurement, we needed to process the baseline sway. In the present research, a high pass Butterworth filter was used to process the baseline drift.

3.3 QRS Detection

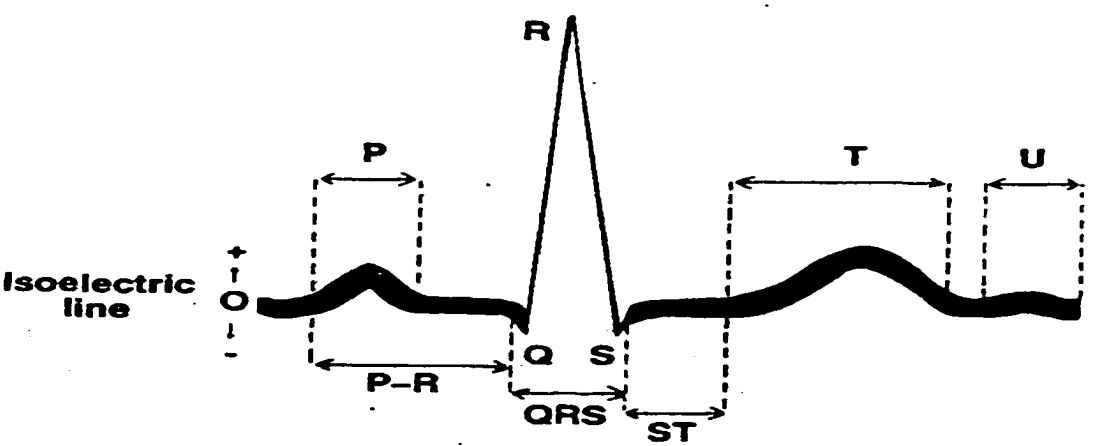

Figure 3.2 Normal ECG Beat with the Vital Intervals and Amplitudes Indicated. [Kelly, 1984]

Correct QRS detection is very important for any ECG automated analysis, not only because it reveals the heart rate information but also because it shows most changes during pathological changes. The QRS complex represents the depolarization of the ventricles. Once the QRS complex has been identified, the ST segment maybe examined for evidence of ischemia [Laguna et al., 1996]. Any error introduced in this stage will be passed and accumulated into later steps, so it is very important to detect the QRS as accurate as possible.

Pahlm and Sornmo gave a review of the method used for QRS complex detection [Pahlm et al., 1984]. Generally the signal first was filtered by a bandpass filter with a

center frequency of 10 to 17 Hz. Then the signal is squared and averaged over a number of samples to give an estimation of the local energy in the passband. The problems of this method are (1) the passband of the QRS complex in each signal is different. It even varies from beat to beat. (2) It is not easy to select the passband, making the QRS complex completely separate from the noise.

If the signal is known, a matched filter can maximize the signal-to-noise ratio. The optimal design of a matched filter requires the knowledge of both the signal and the correlation statistics of the noise. The signal and the noise in the ECG are both nonstationary, which makes it difficult to implement the matched filter for QRS detection.

Linear adaptive matched filters have been implemented for the QRS detection [Xue et al., 1988]. This kind of filter adjusts itself to compensate the changes in the signal and the noise. Compared with the performance of QRS detectors based on bandpass filtering and local energy estimation [Pan et al., 1985], the performance of linear adaptive matched filter was better in the presence of extreme noise.

Since the ECG is a nonlinear signal by nature, it is difficult to use a linear model to fully compensate the changes in the ECG. So, the performance of the linear adaptive matched filter is not optimal. Since artificial neural networks are nonlinear inherently, artificial neural network based adaptive matched filters may be potentially useful for the QRS detection. Relatively, it is a new application field of artificial neural networks since usually artificial neural networks are used for pattern recognition (in the present research, artificial neural networks also are used for the pattern recognition). Theoretically, an artificial neural network with a nonlinear hidden layer can approximate any nonlinear

function in the real world. However, this approximation may be limited by the number of nodes used in the network [Lippmann, 1987].

In the present research, 75 input nodes are used since it is hoped that the model will predict non-QRS portion (i.e., P wave, T wave and the rest information of the ECG) of the signal better than the QRS complex itself. With more hidden units, the computation increases. For the consideration of the learning speed, 15 hidden units are used.

The initial selection of the input node number was 200. To speed up the computation, 20 hidden units were used. Then a process was made to try the best selection of the input node number. 100, 90, 80, 70, and 75 were tested. The selection was based on the correction rate. The correction rate is defined as the correctly classified beats. The selection of 75 was the best. And then fix the input node number as 75, different number of the hidden units were tested. 20, 15, and 10 were tested. 15 was the best. Based on the above process, the network has 75 input nodes and 15 hidden nodes. This network is different from the network in section 3.7.

A PC with Pentium III 800M Hz CPU, 128MB memory, and 20 GB hard disk was used to generate the above result.

3.3.1 Matched Filter and Whitening Filter

For signal detection, the goal is to detect the presence of a signal s(t) from received signal, x(t), which includes both s(t) and noise, n(t).

$$x(t) = s(t) + n(t)$$

A finite impulse response digital filter which has an impulse response $h(t) = s(t-t_0)$ is used as the matched filter.

If n(t) is a white noise random process, the matched filter will have optimal performance. Unfortunately, for the QRS detection problem in the ECG signal, the background noise is colored. Thus, there is correlation between the noise components, such as the P and T waves. So a whitening filter is needed. A linear adaptive autoregressive (AR) model is selected (To improve the performance of this model, nonlinear coefficients are adopted. See the next section). It is assumed that the data sampled from the colored noise in the ECG signal at time t can be predicted by a linear combination of previous q data samples.

$$n_t = \sum_{i=1}^{q} u_i n_{t-1} + \varepsilon_t$$

where {uil i=l, . . . , q} is the set of AR parameters, and et is the modeling error, which approximates white noise gradually if the model is correct. The selection of q is quite important since the QRS complex exists only in a very short time during the whole beat, and the main frequency component of the complex is higher. The proper value of q will enable the whitening filtering to not predict the QRS complex s(t). After the original

$$y(t) = x(t) - \sum_{i=1}^{q} u_i x_{t-1} = s(t) - \sum_{i=1}^{q} u_i s_{t-1} + \varepsilon_t = s_1(t) + \varepsilon_t$$

ECG signal x(t) is passed through the whitening filter, the output is

where $s_l(t)$ is the distorted signal after passing through the whitening filter. As long as the q is small enough so the higher frequency components in s(t) are not modeled by the set of AR parameters, the detection of $s_l(t)$ is equivalent to the detection of s(t).

3.3.2. Adaptive Linear Whitening Filter and Artificial Neural Network-Based Nonlinear Whitening Filter

The design of this adaptive linear filter is based on the work of Xue et al. [Xue et al., 1990]. An adaptive least mean square (LMS) algorithm [Widrow et al., 1985] is selected to computer the set of AR parameters, to cope with the time varying nature of the background noise in QRS detection.

$$u_{t+1} = u_t + 2\mu e_t x_t$$

Where u is the step size which controls the search step, and

$$e_t = x_t^H u_t$$

is the instantaneous error of the whitening filter. A momentum term is added to reduce

$$u_{t+1} = u_t + 2\mu e_t x_t + \alpha(u_t - u_{t-1})$$

the magnitude of random fluctuation.

The problem with this model is that the nature of the background noise in QRS detection of the ECG is nonlinear. The performance of a linear model is limited. An artificial neural network based nonlinear whitening filter may be the method to accurately model the nonlinear relationship among the samples of background noise processes.

The present research will use a two-layer artificial neural network, with a nonlinear hidden layer, to remove noise adaptively. Each of the hidden units produces a nonlinear

$$z_i = f(\sum_{j=1}^{M} W_{ij} y_{t-j} + b_j)$$

result, which will be passed to the next layer for the final output, according to the rule:

where f() is a sigmoid function defined as

$$f(x) = \frac{1}{1+e^{-x/T}}$$

the value of T controls the nonlinearity of the function. The smaller the value of T, the more nonlinear the function. The W_{ij} are the weights, which connect the input units to the hidden units, and the b_js are the bias terms. The output of the nonlinear whitening filter is

$$y_0 = y_t - y\hat{}$$

$$y_t - \sum_{i=1}^{q} u_i z_{t-i} = y_t - \sum_{i=1}^{q} u_i f(\sum_{j=1}^{M} W_{ij} y_{t-j} + b_j)$$

a linear combination of the outputs of the hidden units.

The generalized delta rule is used here to update the weights. The hidden layer weights are updated as

$$W_{t+1}^{j} = W_t^j + 2\mu\delta_j x_t + \alpha(W_t^j - W_t^{j-1})$$

Where W_{jt} is the weight vector connected from the input units to the jth hidden units; δ is the error term from the upper layer; α is the step size of a momentum term. The output will be single, not limited by the range between 0 and 1.

The LSM error of this filter is

$$e = E\{(y_t - \sum_{i=1}^{q} u_i f(\sum_{j=1}^{M} W_{ij} y_{t-j} + b_j))^2\}$$

A template is needed for the matched filter. The template is selected by an artificial neural network based nonlinear adaptive filter. First the network will be trained for about 30 QRS complex. The template vector is

$$QRS = \frac{1}{4}\sum_{i}^{4} QRS_i(t)$$

The whitened QRS template is

$$WQRS(t)_k = QRS(t)_k - \sum_{i=1}^{q} u_i f(\sum_{j=1}^{M} WijQRS(t)_{k-j} + b_j$$

After both the whitened signal and the whitened template have been obtained, matched filtering is performed. The output of the matched filter is

$$y_m(t) = \sum_{i=1}^{L} WQRS_t y_w(t-i)$$

After the data are output from the matched filter, it is sent to the subsystems of squaring, moving average, and threshold checking [Pan et al., 1985].

The basic steps in the moving window integrator are differentiator, squaring algorithm, and summations. The ECG output from the filter is differentiated to provide the QRS-complex slope information. In the present work, a five-point differentiator with the transfer function was used [Srikanth, 2000].

$$H(z) = (1/8T) * \{(-z^{-2} - 2z^{-1} + 2z^{1} + z^{2})\}$$

The difference equation was

$$y(n) = (1/8T) * \{-x(n-2) - 2x(n-1) + 2x(n+1) + x(n+2)\}$$

Where x(n) is the filtered ECG signal.

The next step is the squaring function, point by point.

$$z(n) = [y(n)]^2$$

This squaring process amplifies the output of the derivative, emphasizing higher frequencies, intensifies the slope of the frequency response of the derivative, and helps to restrict false positives caused by T waves with higher than usual energies. Next step is the moving window integration to obtain waveform feature information apart from the slope of the R wave [Proakis et a., 1995].

$$w(n) = (1/N) * \{z(n-(N-1)) + z(n-(N-2)) + \cdots + z(n)\}$$

where N is the number of samples in the width of the integration window and z(n) are the squares of filtered values.

The width of the window is determined by trial and error. The QRS complex duration usually is about one-sixth of a second (≈150 ms). In the present work, sampling rate are 128 Hz and 360 Hz, so the window length of 20 samples or 55 samples is chosen. Moving window integrator output contains information about both the slope and the width of the QRS complex. The upward slope of the moving window integrator for each beat is found to correspond to the QRS complex [Pan and Tompkins, 1985].

The last step is threshold checking. The parameters include mean baseline amplitude (after removing QRS complexes), mean amplitude, maximum and minimum amplitudes of ECG signal and moving window integrator output, and so on.

The R point is defined as the top of the rising arm of the moving window integrator. The detection of the S point is based on the duration, especially the zerocrossing of slope and angle. The following equation shows how to calculate the angle between two lines, given their start and end points are provided

Where d1=data(i)-data(i-1) and d2=data(i+1)-data(i)

$$\vartheta(i) = a\tan((d1+d2)/(1-d1*d2)) * (180/pi)$$

3.4 Baseline Removal

A high pass Butterworth filter, third order, with cut off frequency of 0.6 Hz is used to remove the baseline because most the frequency components in the baseline are below 0.5 Hz [Davis, 2001]. This step is quite essential for the correct detection of ST segment amplitude. The amplitude of a ST segment is often quite small but quite important for the

diagnosis. The amplitudes of different portions of ST segments have been used as parameters for MI detection [Heden et al., 1994; Heden et al., 1996; Heden et al., 1997].

3.5 T Wave Detection

3.5.1 J Point

After the detection of Q point, R point, and S point, the next step is to detect the J point. The J point is defined as the junction between a QRS complex and its ST segment. The detection of a J point is also based on changes in the angle and changes in the direction of the slope, which shall be small, compared to S wave detection.

3.5.2 T Wave

The mathematical definition of a local maximum or minimum (here is the peak of T wave) is that the value of the first order derivative at that point is zero. Another very direct way to understand it is that there are at least two descending points on either side of the peak point as well as a sign change in slope. Another criterion used is that amplitude of the T wave peak should be above a threshold amplitude, based on R amplitude. The end of T wave is defined as the amplitude gradually drops to the baseline.

Since for MI detection the information in P waves is not important, P waves are not detected in the present research.

3.6 Feature Extraction

Until now, there is no uniform optimal set of classification features. And even for the same research group, different sets of features have been tested. The number of features varies greatly, from around 10 to around 100. Some of them use features from 12 leads, whereas others use just some leads. Some use the information combining clinical

tests, ECG features and patient history, whereas some only use ECG features or only case history [Baxt, 1991; Henden et al, 1994; Heden et al., 1996; Heden et al., 1997; Kennedy et al., 1996, Kennedy et al., 1997; Jonsbu et al., 1993].

For this system, the main task is to determine if the patient has MI and if the patient has potential to have myocardial infarction later. The parameters were based on previous research [Heden et al., 1994; Heden et al., 1996; Heden et al., 1997] and close discussion with experienced cardiologists. To avoid inter-observation variability and intra-observation variablity, only ECG measurements were included. There are 4 stages in the development of myocardial infarction (See the details in Chapter 2). In stage 1, the T wave becomes sharp and high and Q-T interval is longer than normal, so the T wave amplitude, R wave amplitude, the slope of the 2 sides of the T wave, and Q-T interval were selected as features. In stage 2, the S-T segment elevates, so the ST-junction to T max amplitude is measured. In stage 3, the S-T segment develops to a monophasic curve, so the S-T slope was selected as a feature. In stage 4, the T wave inverts, so the T wave direction was measured. In Heden's research, he selected 1/6 ST segment amplitude, 3/6 ST segment amplitude, and 5/6 segment amplitude and the T wave positive peak amplitude and T wave negative peak amplitude were also selected. Here, we modify the 1/6 to 1/8, hoping to get more information from S-T segments. The S-T duration and T wave duration were common features for research on myocardial infarction, so they are also included.

The following features are selected:

Table 3.1 Features Selected for Myocardial Infarction Classification

Feature1	T wave amplitude	Feature 2	R wave amplitude
Feature 3	the slope of the 2 sides of T wave	Feature 4	Q-T interval
Feature 5	S-T slope	Feature 6	S-T duration
Feature 7	ST-junction to T max amplitude	Feature 8	1/8 ST segment amplitude
Feature 9	2/8 ST segment amplitude	Feature10	3/8 ST segment amplitude
Feature11	4/8 ST segment amplitude	Feature12	5/8 ST segment amplitude
Feature13	6/8 ST segment amplitude	Feature14	7/8 ST segment amplitude
Feature15	8/8 ST segment amplitude	Feature16	T wave direction
Feature17	T wave duration	Feature18	T wave positive peak amplitude
Feature19	T wave negative peak amplitude	Feature20	the presence of Q wave

The following figure is the waveform example.

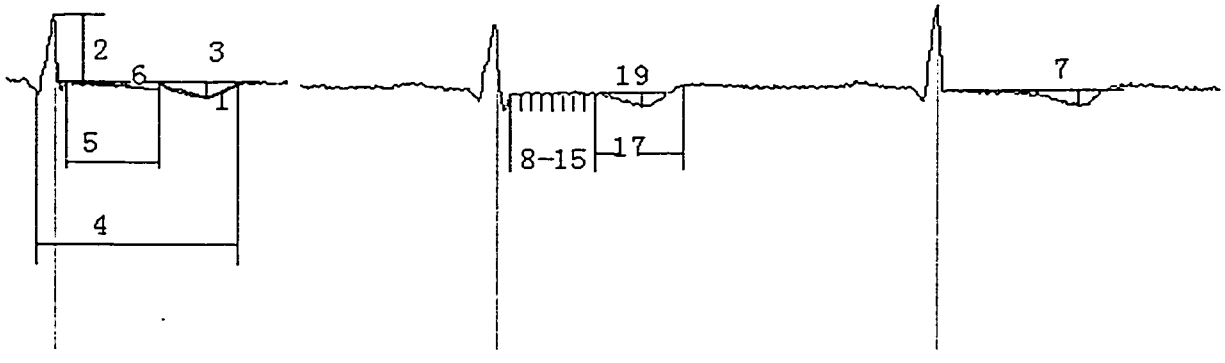

Figure 3.3 Features

Baxt also selected 20 features; most of them were patient symptoms. Only 4 of them were ECG measurements (see Table 2.12). The present research selected only ECG measurements to avoid intra-observer variation and inter-observer variation.

3.7 Classification

A two-layered BP network was used for the detection of myocardial infarction. It is a network with 20 input units and 1 output unit, which classify if there is myocardial infarction or not. The number of hidden units was tested. The more hidden units, the more complex pattern may be captured, and the more computation required for each case,

and the longer time is needed for the diagnosing. The compromise between a better performance and quicker speed has to be made. Initially 10 hidden units were selected. This selection is based on previous experience; usually ½ of the number of the input nodes shall be enough for the learning. The performance of the networks with different hidden units was tested (see Chapter 4). 10, 15, and 5 hidden units were tested. The criteria to measure the performance is the correction rate (The number of correctly classified beats /The total number of beats). Sometimes, a network with too many hidden units will not yield optimal results since the network is "over-trained", which means the difference the network can discern is too small, making the whole performance degrade. The structure of the final network is shown in the following figure. Based on the correction rate, the best of the three network structures was select as the structure for the present research.

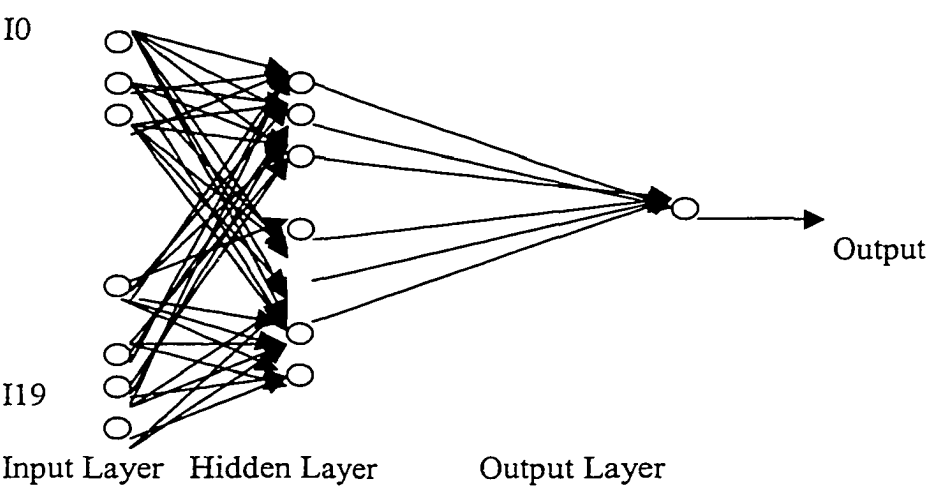

Figure 3.3 Structure of the Neural Network

Compared with Baxt's research in 1990 and 1991, the present research used one less layer, speeding up the calculation (see Table 2.11). The meanings of each parameters are listed below:

Table 3.2 Meaning of Each Node in the Neural Network of this Dissertation

Input node	Value Type	Meaning
I0	Binary	I0=1 if amplitude of T/R >0.25; else 10=0
I1	Binary	I1= 1 if QT interval >0.45 second; else I1=0
I2	Binary	12=1 if both of the base angles of the triangle formed by baseline and T wave are less than 35 degrees; else 12=0
I3	Binary	I3=1 if the amplitude difference between ST-j junction and the maximum of T wave is more than 0.1 mm; else I3=0
I4	Binary	I4= 1 if ST slope changes; else I4=0
I5	Binary	I5=1 if T wave is inverted; else I5=0
I6	Binary	I6=1 if Q wave is present; else I6=0
I7	Real	T wave duration
I8	Real	ST duration
I9	Real	ST slope
I10	Real	1/8 ST segment amplitude
I11	Real	2/8 ST segment amplitude
I12	Real	3/8 ST segment amplitude
I13	Real	4/8 ST segment amplitude
I14	Real	5/8 ST segment amplitude
I15	Real	6/8 ST segment amplitude
I16	Real	7/8 ST segment amplitude
I17	Real	8/8 ST segment amplitude
I18	Real	T wave positive peak amplitude
I19	Real	T wave negative peak amplitude

3.8 Training and Testing

The training and the testing are 2-fold methods (see the details in Chapter 2). Half of the data were randomly selected, with the aid of a program, to train the network until the error is within the limit (here 99.9% is selected). And the other half was used for testing. The method is that all the beats were assigned a number between 0 and 2512 randomly. The program produced 1256 pseudo-random numbers between 1 and 2512. These beats were used for training and the remaining were used for testing. Then those two parts of the data switched. The data originally used for training were used for testing

the neural network in the second round; the part of data used for testing firstly were used for training the network. The results of the network of both rounds were recorded.

During the testing stage, the weights between layer were adjusted by the Hebb rule to minimize the error between the network output and the desired output [Hebb, 1949]. The weight update rule is the general delta rule. When the error is less than 0.01, the training stops and the weights at that time will be used for later testing.

One task during the testing stage was to find the best number of hidden layer units. There is no standard for the optimal performance of a perceptron. Here the number of correctly recognized beats was used as the measurement. Since the choice of hidden unit number is unlimited, what would be tested in the present research was only a very small set and the best one selected was based on the correction rate (the number of correctly classified beats / the number of total beats).

During testing, each case in the testing data set was tested and the result was recorded. If the output of the network was different from the diagnosis made before, that result was wrong, and it was recorded.

3.9 Statistical Analysis

According to the comparison between the network results and the diagnosis, the following parameters will be measured:

False Positive (FP): The output of the network shows the patient has myocardial infarction, while the diagnosis is negative.

False Negative (FN): The output of the network shows the patient does not have myocardial infarction, while the diagnosis is positive.

True Positive (TP): The output of the network shows the patient has myocardial infarction, while the diagnosis is also positive.

True Negative (TN): The output of the network shows the patient does not have myocardial infarction, while the diagnosis is also negative.

Sensitivity (Se) and Specificity (Sp) were calculated based on the above measurements.

$Se = TP/(TP+FN)$ and $Sp = TN/(TN+FP)$

Sensitivity and specificity were used to compare with the results of previous research (see Table 5.3) to verify the correctness of the hypothesis in the present research. If the sensitivity and specificity of present research (of T test) were not worse than the results shown in Table 5.3, we can conclude that the hypothesis in present research is true.

CHAPTER 4

RESULTS

4.1 Introduction

A single lead ECG diagnosing system, which incorporates intensive usage of ANNs, is designed in the present dissertation. It is a multi-component system. The performance and analysis of the performance of the sub-systems is presented in this chapter. These sub-systems are signal preprocessing unit, QRS detection unit, baseline removal unit, T wave detection unit, feature extraction unit, and classification unit. The signal-preprocessing unit includes 3 parts: data collection, annotation, and filtering. The present system is designed to detect the presence of myocardial infarction solely based on the patient's Holter ECG recordings.

4.2 Signal Pre-processing

The signal preprocessing unit in the present dissertation completes the following tasks: collecting clinical ECG data, annotating each beat, and low pass (fc=100 Hz) and 50 Hz notch filtering of the signal. The source of the ECGs was the Holter recordings obtained by the Dynamic ECG unit of a clinical hospital between 1988 and 2000. The leads used were V1 and V5. Classification of beats is made by a team of two experienced cardiologists. Similar to the methods used in the MIT-BIH Database, a consensus is

required before an annotation is fixed. When there is discrepancy, the Dean of the department doublechecked it, and all the three discussed it to reach a consensus. Marking is made on the printed ECG recordings. Altogether 137 recordings were collected. 62 were 24 hours recordings and 75 were 3 minutes recordings. The data can be divided into two groups: normal subjects and myocardial patients later. The data may contain noises, such as electromagnetic interference, baseline sways and 50 Hz AC interference, introduced during recording. The Chebyshev 2nd type of low pass filter is selected to get rid of the high frequency components. A notch filter is then used to get rid of the 50 Hz AC interference.

4.2.1 Data Collection

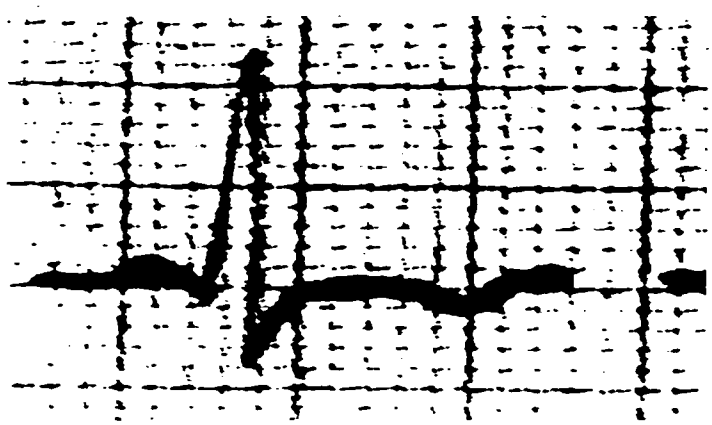

Figure 4.1 A Segment of the Clinical Myocardial Infarction ECG Data

The ages of subjects range from 42 to 87. The ratio between male and female is around 55:45. All subjects, whether their ECGs exhibit myocardial infarction or not, did not have myocardial infarction history before. Due to the consideration of physicans' subject opinions on the clinical systems, other indications, such as rales, syncope, jugular venous distention, response to trinitroglycerin, nausea and vomiting, age, sex, history of hypertension, diabetes mellitus, and angina, were not selected as the measurements used in the present research.

The sampling frequencies of the clinical data were 128 Hz and 360 Hz. Two leads, V1 and V5, were selected in the clinical data. During the course of myocardial infarction, these leads demonstrate significant ST elevation or damping.

4.2.2 Annotation

The starting point of Q wave, Q wave peak, R wave peak, S wave peak, the ending point of S wave, J point, the starting point of T wave, T peak, and ending point of T wave are annotated and the presence of myocardial infarction for each segment was labeled. Two very experienced cardiologists and the Dean of the Dept. of the hospital took charge of the annotation. Figure 4.2 is the annotated clinical ECG of the raw clinical data in figure 4. 1.

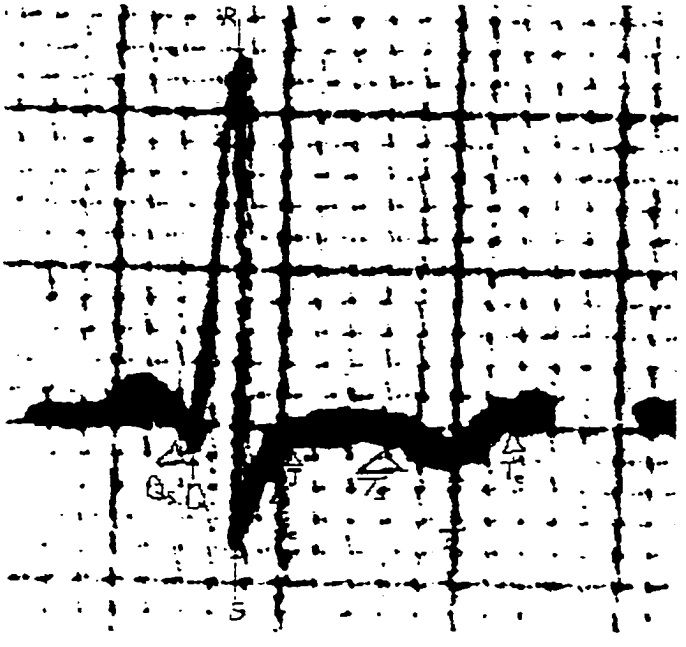

Figure 4.2 Annotated Clinical ECG Data of Figure 4.1

4.2.3 Filtering

Most information in biological signals, such as ECGS, is in the region of low frequency. Figure 4.3 is a typical normal ECG sampled at 360 Hz. Fig 4.4 is the Power Spectrum Density plot of the signal shown in the Figure 4.3. It clearly shows the frequency components of that ECG.

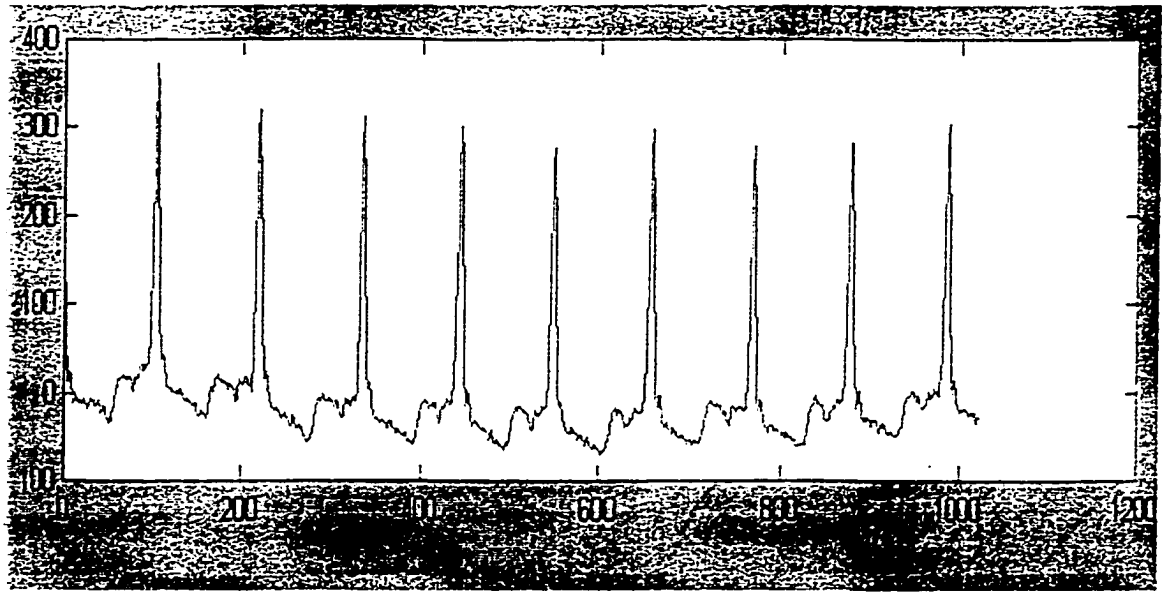

Figure 4.3 A Normal ECG

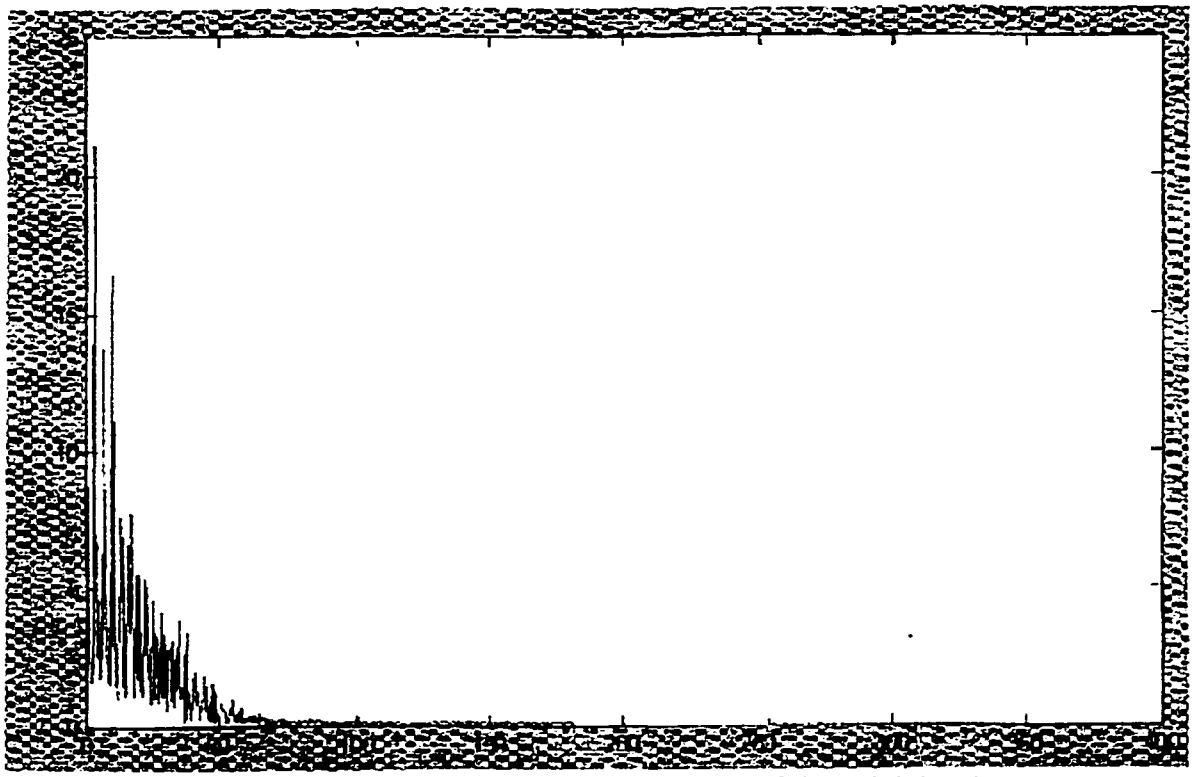

Figure 4.4 The Power Spectrum Density of the ECG in Fig. 4.3

The proportion of the energy of frequency below 100 Hz is 0.9446. The cut-off frequency of 100 Hz is selected for the low pass filtering. This frequency affects only a little of the QRS complex and avoids disturbing minor variations in baseline and ST segments and allows the regular frequency range of T waves [Srikanth, 2000], which is crucial to the present research.

An ideal low pass filter shall have the vertical transition band at the cut-off frequency, which is impossible to realize. All the low pass filters are just approximations of it. The higher order of the filter, the sharper transition band and the better approximation of an ideal low pass filter. The higher order of the filter, the more computation and the longer calculation time. A designer must make a balance between these factors. The characteristics of the major filters differ greatly. The Butterworth fitter provides the best tailor approximation for an ideal low pass filter at $\Omega=0$ and $\Omega=$infinite.

The Chebyshev filter has a much sharper transition band than the Butterworth has. The first type of the Chebyshev filter has a flat stop band and ripples in the pass band. On the other hand, the second type of the Chebyshev filter has a flat pass band and ripples in the stop band [Proakis et al., 1995]. MatLab® software provides the function to calculate the minimum orders of certain filters to meet some specific requirements. To satisfy the requirement of current research, the least order needed for a butterworth filter is 25, while that of a Chebyshev filter is only 6. For the present research, the frequency components in low frequency region are very important. Attenuation in the pass band is not desirable. So, a 2^{nd} type Chebyshev filter of 6^{th} order is selected, which shows good performance.

Figure 4.5 compares the frequency responses of the Butterworth filter, the 1^{st} type and 2^{nd} type Chebyshev filter of the same order, 6. From that, we can see clearly, the performance of the 2^{nd} type Chebyshev is the best because its frequency response drops almost vertically at around 100 Hz. The ripping of the filtering could affect some features.

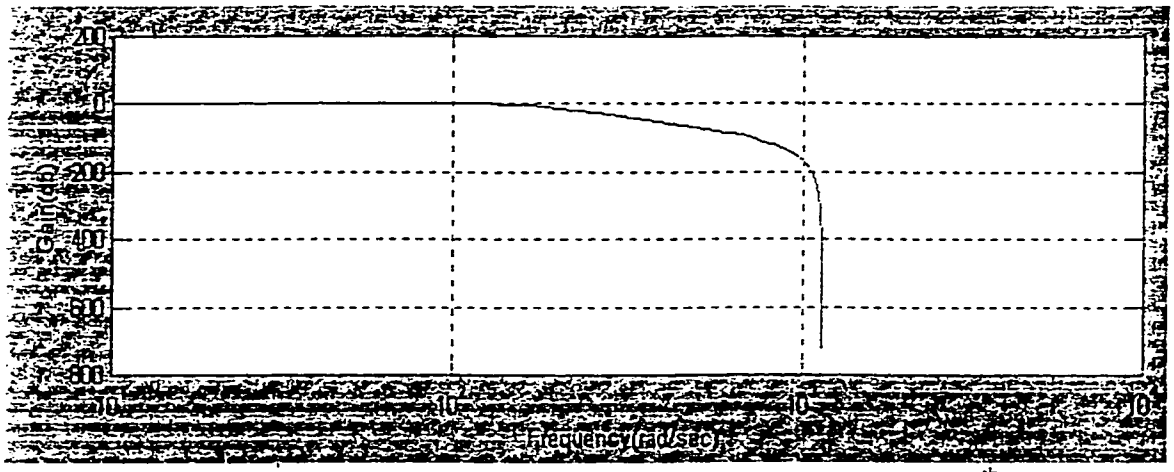

Figure 4.5(a) The Frequency Response of Butterworth Filter of 6th Order

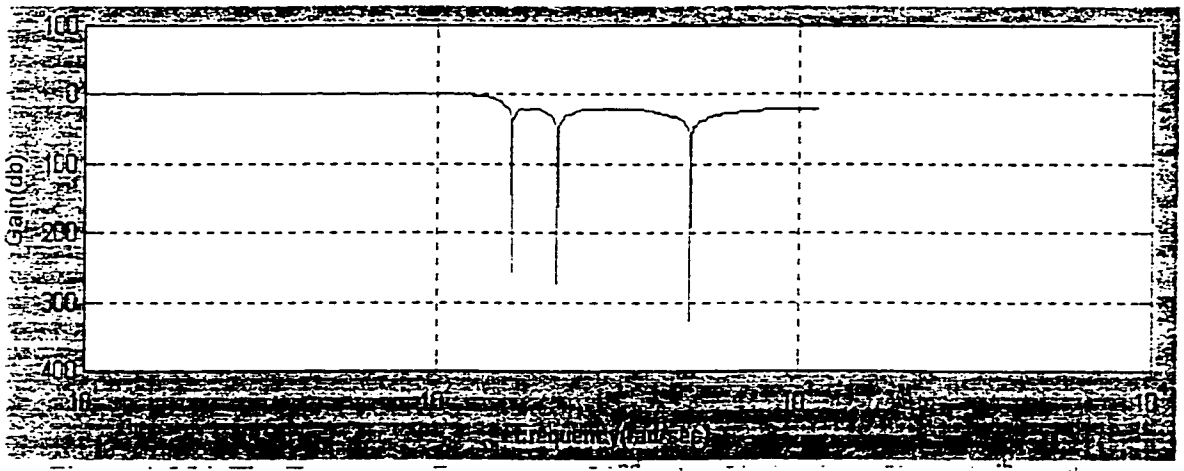

Figure 4.5(b) The Frequency Response of 2nd Type Chebyshev Filter of 6th Order

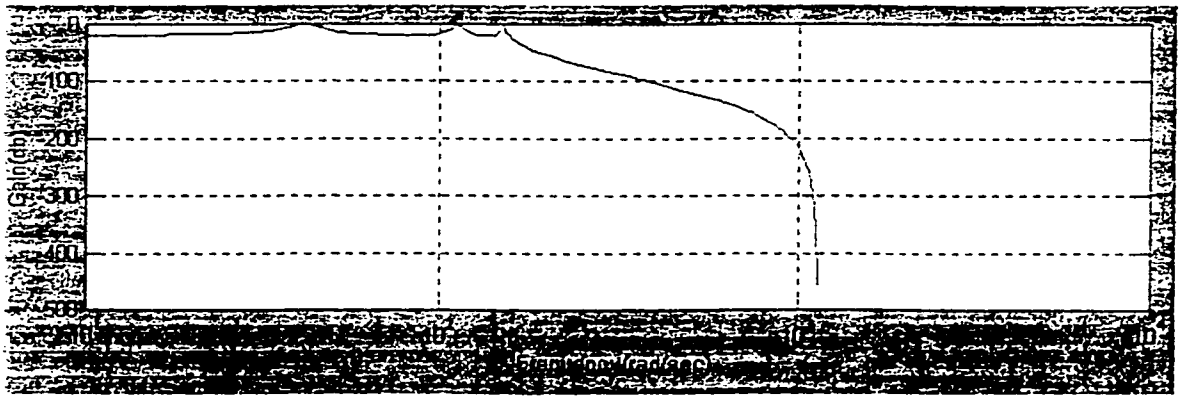

Figure 4.5(c) The Frequency Response of 1st Type Chebyshev Filter of 6th Order

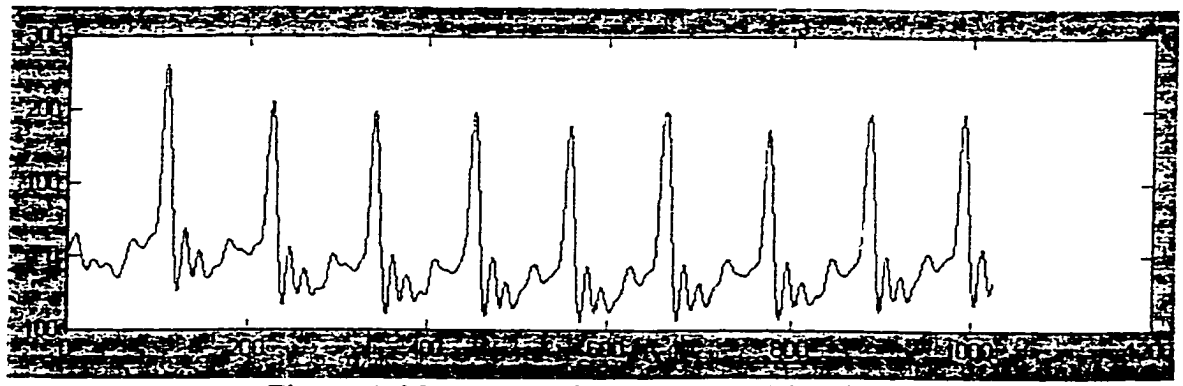

Figure 4.6 The Data after Low Pass Filtering

Figure 4.6 shows the result after applying the filter to the data shown in Figure 4.3. Compared with the ECG in Figure 4.3, the ECG in 4.6 retains the geometric characteristics of those in the original data, which is very important to the accuracy of the myocardial infarction detection.

By checking the Power Spectrum Density of the signal shown in Figure 4.6, we can see that all the frequency components over 100 Hz are eliminated. And the proportion of the energy of frequency below 100 Hz increases from 0.9446 to 0.9785.

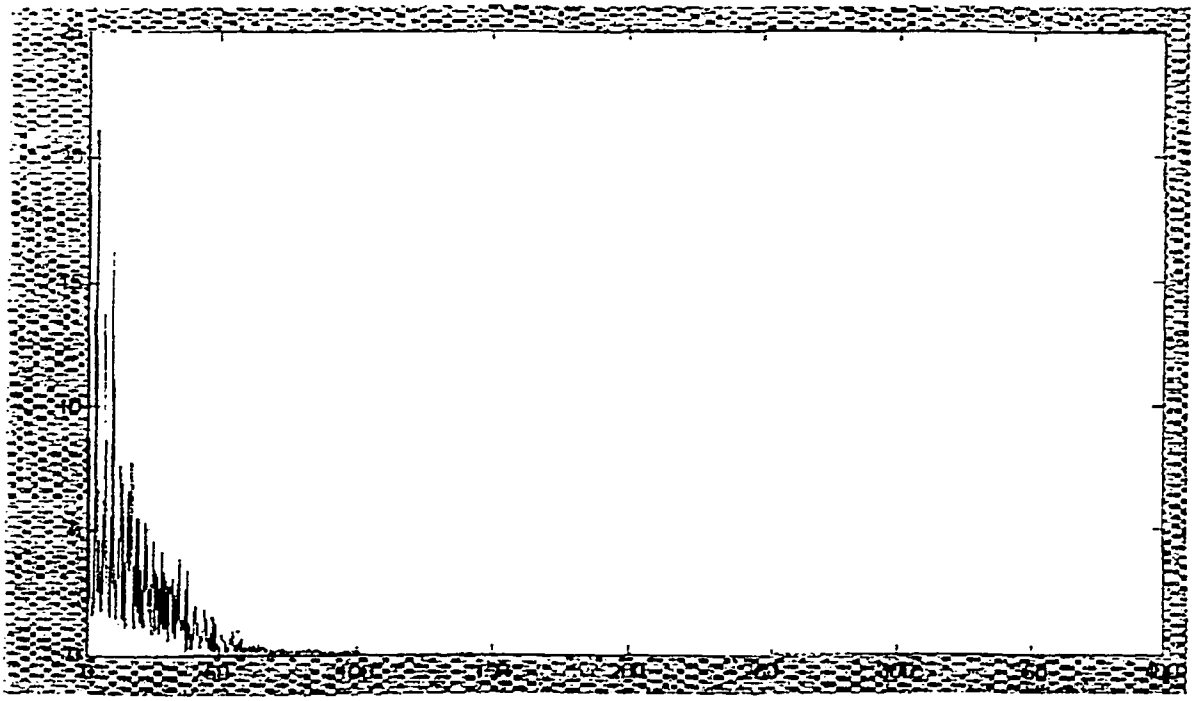

Figure 4.7 The Power Spectrum Density of the ECG in Fig. 4.6

Since the clinical data were collected in China, the AC interference is 50 Hz. To eliminate the 50 Hz noises, a notch filter designed by MatLab was used. A Butterworth of 4^{th} order is designed to implement such function. Figure 4.8 showed the Frequency response of it. The mean data will be subtracted from the filtered data, to eliminate the DC component.

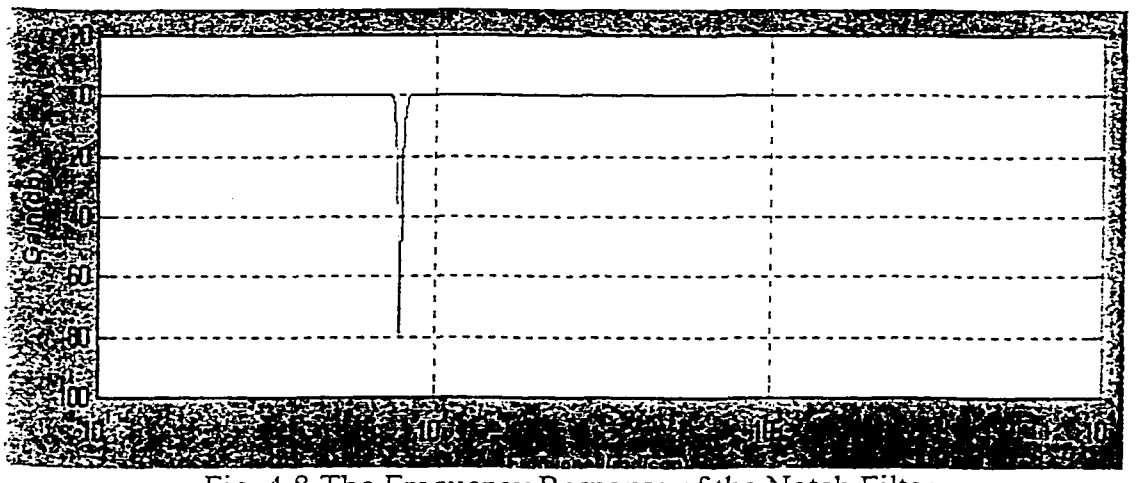

Fig. 4.8 The Frequency Response of the Notch Filter

4.3 QRS Detection, Baseline Removal, T wave Detection, and Fiducial Points

QRS detection is the key part of the present research. It is composed of several different components: the artificial neural network-based nonlinear whitening filter, the linear adaptive matched filter, the template generator, the blocks of squaring, moving average, and the threshold checking.

The selection of the current algorithms in the present research has been illustrated in details in Chapter 3, and the equations applied are also in Chapter 3. This unit involves intensive usage of artificial neural networks. The artificial neural network-based nonlinear whitening filter is essential to the good performance of the matched filter since the optimal performance of a matched filter assumes the input signal is white. However, neither the QRS sections in the ECGs nor the input signal is white. The artificial neural network-based template bank updates itself dynamically to trace the change in the ECGS. The linear adaptive matched filter has shown good results in the previous research [Xue et al., 1988]. The artificial neural network-based nonlinear adaptive matched filter provides nonlinearity to match the nonlinear nature of ECGs.

After QRS detection, a high pass Butterworth filter of 4^{th} order with cut off frequency 0.6 Hz was used to get rid of the baseline drift.

Then, J point and T wave detection was made, which completed the fiducial point detection. The following table (Table 4.1) shows the results of fiducial point detection.

Table 4.1 Results of Fiducial Points

Total number of beats	2512
Correct R point Detection	2469
Correct Q point Detection	2389
Correct S point Detection	2160
Correct Detection of the Starting point of QRS complex	2085
Correct Detection of the Ending point of QRS complex	2034
Correct Detection of the Starting point of T Wave	2016
Correct Detection of the T Wave Peak	2054
Correct Detection of the Ending point of T Wave	2003
Correct Detection of the J Point	2012

4.4 Feature Extraction

Twenty features, derived solely from ECGs, were selected as the inputs for the neural networks. These features contain most of the information predicting the myocardial infarction. The following table showed the values of these 20 features.

Table 4.2 Values of Features Extracted

Feature	Max	Min	Mean
T wave amplitude	0.9 millivolts	0.1 millivolts	0.5 millivolts
R wave amplitude	2.8 millivolts	0.1 millivolts	2.0 millivolts
Degree of left side of T wave	58	-51 (inverted T waves)	13.5
Degree of right side of T wave	53	-46 (inverted T waves)	10.7
Q-T interval	0.43 seconds	0.36 seconds	0.41 seconds
S-T duration	0.13 seconds	0.08 seconds	0.10 seconds
S-T slope degrees	47 degrees	-36 degrees	9 degrees
1/8 ST segment	0.87 millivolts	0.07 millivolts	0.54 millivolts
2/8 ST segment	0.79 millivolts	0.09 millivolts	0.52 millivolts
3/8 ST segment	0.81 millivolts	0.11 millivolts	0.60 millivolts
4/8 ST segment	0.63 millivolts	0.05 millivolts	0.47 millivolts
5/8 ST segment	0.71 millivolts	0.06 millivolts	0.51 millivolts
6/8 ST segment	0.74 millivolts	0.06 millivolts	0.50 millivolts
7/8 ST segment	0.72 millivolts	0.08 millivolts	0.54 millivolts
8/8 ST segment	0.69 millivolts	0.10 millivolts	0.52 millivolts
T wave duration	0.14 seconds	0.09 seconds	0.12 seconds
T wave positive peak amplitude	0.83 millivolts	0.12 millivolts	0.55 millivolts
T wave negative peak amplitude	-0.90 millivolts	-0.05 millivolts	-0.62 millivolts

T wave direction is quite important for myocardial infarction detection. 2210 beats had inverted T waves.

4.5 Classification

During the classification stage, a two-layer back-propagation network was used. For the total of 2512 beats, each myocardial infarction beat is used to train the network for later identification. The 2-fold methods, as mentioned in the chapter 3, were used to train and test the neural network. Half of the randomly selected beats were used for training and the remaining half were used for testing. Then those two parts of data were switched (see the details of the methods in Chapter 2 and Chapter 3).

The selection of the number of hidden units would influence the performance of the neural network greatly. In the present research, 10, 5, and 15 were selected as the possible number of hidden units. Table 4.3 showed the results of the experiment.

Table 4.3 Results of Three Different Neural Networks

The number of hidden units	The percentage of correctly recognized beats
10	85%
5	79%
15	82%

So, the network with 20 input units, 10 hidden units and 1 output unit was selected as the structure of the current research.

4.6 Statistical Analysis

The result of this research is promising: 2135 beats were correctly classified. The following statistical measurements were recorded: false positive, false negative, true positive and true negative.

Table 4.4 Statistical Measurements for the Selected Neural Network

Statistical Measurements	Number of Beats
True Positive	1914
True Negative	221
False Positive	215
False Negative	162

Sensitivity = TP/(TP+FN)=1914/(1914+162)=1914/2076 =92.2%

Specificity = TN/(TN+FP)=221/(221+215)=221/436=50.7%

CHAPTER 5

DISCUSSION

Myocardial infarction is a kind of disease with low incidence, but a very high cost must be paid for misdiagnosis. Due to the nature of myocardial infarction detection, the diagnosis of myocardial infarction remains a challenge. Previous research shows that an automated diagnosis system based on an artificial neural network is a promising aid for the detection of myocardial infarction [Baxt., 1991; Baxt, 1992a; Baxt, 1992b; Baxt, 1994; Baxt and White, 1995; Baxt and Skora, 1996; Heden et al., 1994; Heden et al., 1996; Heden et al., 1997; Kennedy et al., 1996; Kennedy et al., 1997].

The present research is trying to identify the presence of myocardial infarction from a single lead ECG by an artificial neural network-based computer system, formulated on the hypothesis that an artificial neural network based ECG interpretation system may improve clinical diagnosis of myocardial infarction.

The present research included 137 patients. Among them, 15 were normal and the remaining 122 experienced myocardial infarction later. The neural network used for myocardial infarction classification in the present research had 20 inputs, 10 hidden units and 1 output node. A total of 2512 beats were tested by 2-fold method. Among them, 2135 beats were correctly classified. The sensitivity and specificity of present research were 92.2% and 50.7% respectively.

Compared with the results of the research groups led by Baxt, Heden, and Kennedy, the present research overcame some weakness: (i) The cardiologists were more experienced. One cardiologist in the present research had 22 years of experience and the other had 19 years. Their average performance shall be better than that of medical residents in postgraduate 2 and 3 years [Baxt, 1991; Baxt, 1992a; Baxt, 1992b; Baxt, 1994; Baxt and White, 1995; Baxt and Skora, 1996]. (ii) Similar to the research of Heden [Heden et al., 1994; Heden et al., 1996; Heden et al., 1997], only ECG measurements were used as parameters, avoiding inter-observation variability and intra-observation variability of physician in Baxt's research [Baxt, 1991; Baxt, 1992a; Baxt, 1992b; Baxt, 1994; Baxt and White, 1995; Baxt and Skora, 1996].

The weakness of the present research is that (i) all the patients were from one hospital, the portability of the neural networks can not be tested.(ii) the specificity is low compared with that of other researchers.

The result of present research is comparable with the results of other researchers. Table 5.3 showed the comparison. By T test, the present result was as good as ($P<0.05$) the results listed in Table 5.3, in terms of sensitivity. From previous research, the sensitivity of cardiologists ranged from 55.4% [Heden et al., 1997] to 83.5% (Table 2.8). The present result, 92.2% was significantly higher than those of the cardiologists. For the specificity, the present result was lower than those of cardiologists [Baxt, 1990; Baxt and Skora, 1996; Heden et al., 1996].

After studying the figures in Chapter 4, Dr. Steven Jones suggested that the coefficients of the filter were wrong. He advised me to create a 50 Hz sine wave and let the filter filter this wave. If there is significant attenuation in the signal, the coefficients

were wrong. I tested and found the signal attenuate significantly. For the cutoff frequency to be half of the sampling frequency, the parameter in the low pass filter function should be 1. I calculated the parameter and found it was only 0.25.

The low specificity resulted from the wrong coefficients of the low pass filter in the first block. We made a further study by using MIT-BIH database. We used 500 normal beats and 7 myocardial infarction beats. The following table (Table 5.1) shows the results of classification by the filter used in this dissertation.

Table 5.1 The Results of Applying the Old Filter to the MIT-BIH Database

True Positive	True Negative	False Positive	False Negative
6	278	222	1

Sensitivity = True Positive / (True Positive + False Negative) = 6/7 = 85.7%

Specificity = True Negative / (True Negative + False Positive) = 278/500 = 55.6%

In the MatLab routine, the cut off frequency is normalized to the ratio between 0 and 1, with 1 meaning half of the sampling frequency. So, the cut off frequency should be multipled 2 then divided by the sampling frequency. Due to the typing error, the cut off frequency was divided by 2 and then divided by the sampling frequency. It resulted in a four-fold difference, meaning that the cut off frequency used in the previous chapters was 25 Hz, instead of 100Hz. The following figures (Figure 5.1(a) and Figure 5.1(b)) showed the ECG data before and after the filter. After we correct the mistake, the specificity increases significantly and the rippling effect in Figure 4.6 is eliminated. Table 5.2 shows that the result after applying the new filter.

Table 5.2 The Results of Applying the New Filter to the MIT-BIH Database

True Positive	True Negative	False Positive	False Negative
6	412	88	1

Sensitivity = True Positive / (True Positive + False Negative) = 6/7 = 85.7%

Specificity = True Negative / (True Negative + False Positive) = 412/500 = 82.4%

This specificity is in the same range of the results shown in Table 5.3. After this study, we can conclude that artificial neural network-based ECG interpretation system can improve the detection of myocardial infarction.

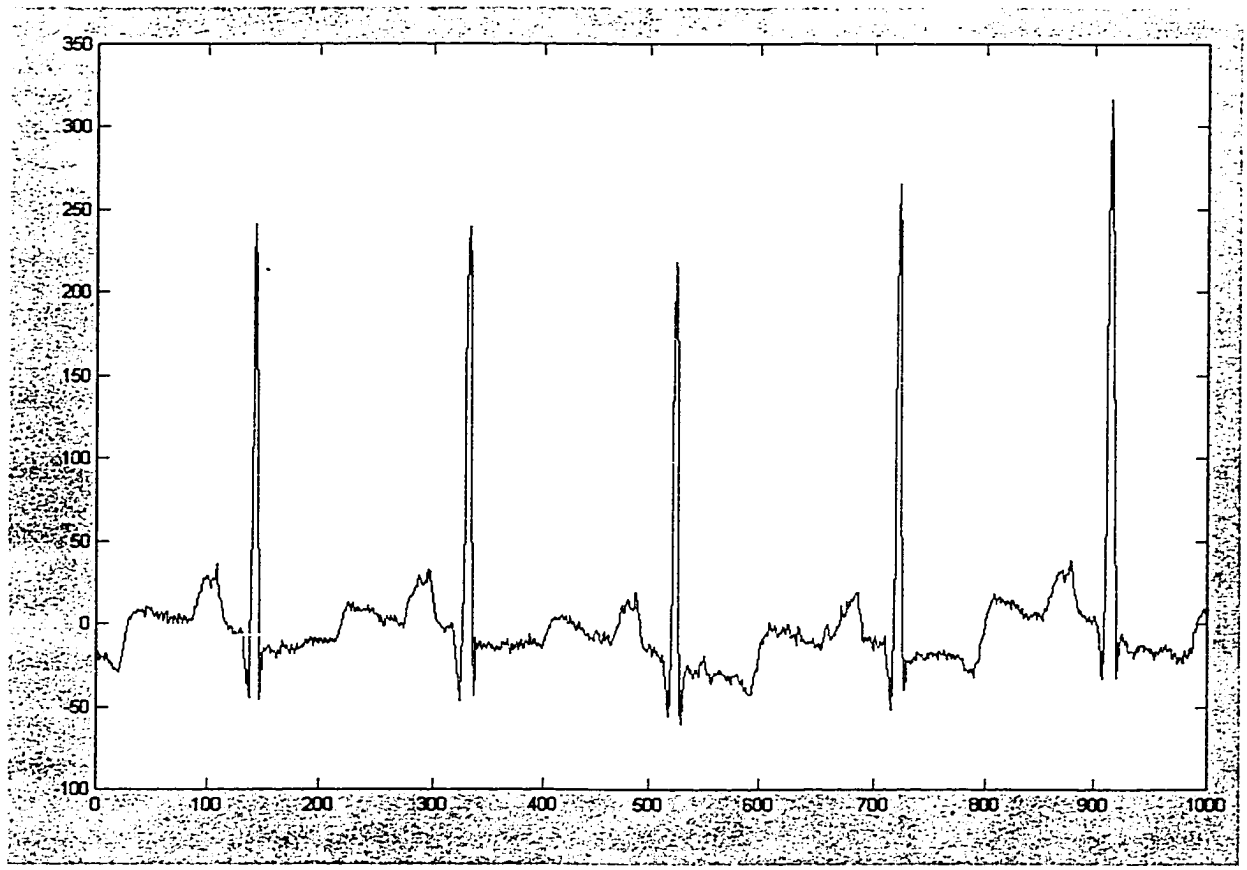

Figure 5.1(a) The ECG Data before Applying the New Filter

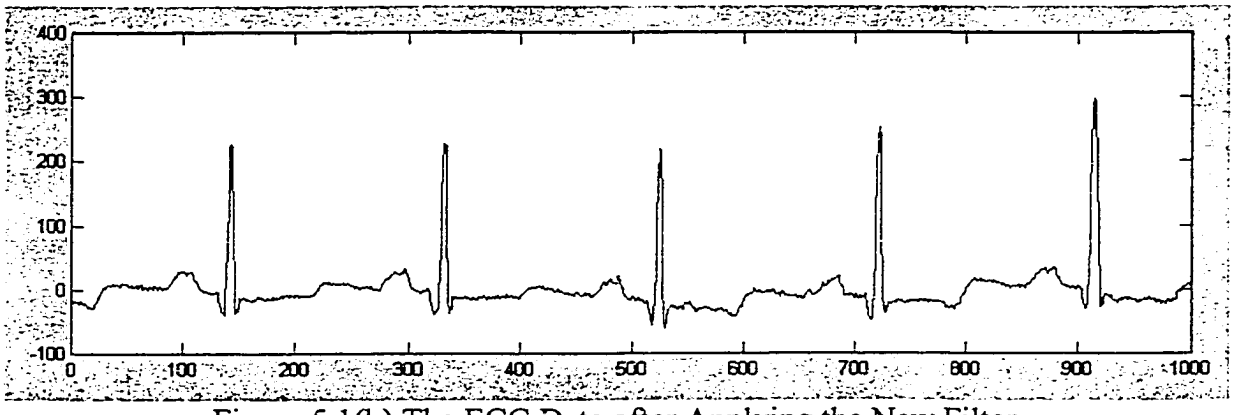

Figure 5.1(b) The ECG Data after Applying the New Filter

Table 5.3 The Results Comparison of the Present Research with Other Researchers

Major Researchers	Results
Zhou Present Dissertation	Sensitivity: **92.2%** Specificity: **50.7%**
Hart and Wyatt [Hart et al., 1988]	Sensitivity: 73% Specificity: 68%
Baxt [Baxt, 1990]	Sensitivity: 92% Specificity: 96%
Harrison, Marshall & Kennedy [Harrison et al., 1991]	Sensitivity: 88% Specificity: 88%
Baxt [Baxt, 1991]	Sensitivity: 97% Specificity: 96%
Baxt and Skora [Baxt et al., 1996]	Sensitivity: >95% Specificity: >95%
Edenbrant [Edenbrant et al., 1993]	Sensitivity: 63% Specificity: 97%
Hu [Hu et al., 1993]	Sensitivity: 81% Specificity: 78%
Devine & Macfarlane [Devine et al., 1994]	Sensitivity: 97% Specificity: 88%
Heden [Heden et al., 1994]	Sensitivity: 81% Specificity: 97.5%
Heden [Heden et al., 1996]	Sensitivity: 81.4% Specificity: 94.8%
Heden [Heden et al., 1997]	Sensitivity: 97% Specificity: 88%
Kennedy [Kennedy et al., 1997]	Sensitivity: 91.2% Specificity: 90.2%

The sensitivity of the present research showed a much better result than that of cardiologists, which is usually around 80%. Although the results of artificial neural networks are much better than those of the physicians, the importance of cardiologists' diagnosis cannot be ignored, due to the still-low correction rate (the number of correctly recognized beats / the number of total beats) of the artificial neural network (the correction rate of present research is 85%). However, we can conclude that, an artificial neural network can be a useful aid for the cardiologists' diagnosis of presence of myocardial infarction.

The structures of the neural networks influence the performance of the network greatly. The more nodes, or the more hidden layers, the more computation and the slower the speed. The design of the neural network is the art making balance to achieve best result. Table 5.4 compared the structures of previous researches with the present dissertation.

Table 5.4 The Neural Network Structure Comparison

Major Researcher	Structure of the Network (input node number X hidden node number X output node number)	Function
Zhou Present Dissertation	20 x 10 x 1	Presence of Myocardial Infarction
Baxt [Baxt, 1990]		Acute Cornary Occlusion
Baxt [Baxt, 1991]	20 x 10 x10 x 1 (2 hidden layers)	Chest Pain Presenting to Emergency Department
Baxt and Skora [Baxt et al., 1996]	20 x 10 x10 x 1 (2 hidden layers)	Extend the Previous Research to over 1000 Patients
Heden [Heden et al., 1994]	15 x 5 x 1	No Presence of Healed Inferior Myocardial Infarction
	15 x 5 x 1	No Presence of Healed anterior Myocardial Infarction
	30 x 9 x 1	Presence of Healed Inferior Myocardial Infarction
	30 x 9 x 1	Presence of Healed anterior Myocardial Infarction
Heden [Heden et al., 1996]	24 x 6 x 1	Healed Myocardial Infarction
Kennedy [Kennedy et al., 1997]	53 x 18 x 1	Acute Myocardial Infarction
Kennedy [Kennedy et al., 1997]	72 x 15 x 1	Acute Myocardial Infarction

From Table 5.4, the present research used the least number of input nodes to detect the presence of myocardial infarction.

The objective of the present research is to present an integrated automated ECG diagnosing system, which can be used for clinical Holter data, with the capacity to expand to multi-lead ECG interpretation systems and to be included in other ECG interpretation systems, which do not detect myocardial infarction. So we make the system expandable, modularized, and optimized. The whole system of the present research can be viewed as a black box; the input to the system is a clinical Holter ECG; the output of

the system is the classification. To expand the system, no program modification is required, just connecting the systems to right input (see the mechanism in Figure 5.1). The whole system can be divided into 9 modules. Each module implements the function described in the diagram (see Figure 3.1). Between each module, the only communication is the passing of the results. The selection of algorithms in the present research is based on the previous research and the close cooperation with experienced cardiologists [Baxt., 1991; Baxt, 1992a; Baxt, 1992b; Baxt, 1994; Baxt and White, 1995; Baxt and Skora, 1996; Heden et al., 1994; Heden et al., 1996; Heden et al., 1997; Kennedy et al., 1996; Kennedy et al., 1997; Sheffied, 1987; Leblanc et al., 1989; Haisty et al., 1972; Shaw et al., 1995; Laguna et al., 1996; Hu et al., 1997; Burattini et al., 1998, Frenkel et al., 1999; Garcia et al., 2000; Srikanth, 2000; Xue et al., 1988; Xue et al., 1989; Xue et al., 1990; Xue et al., 1992]. The selection criterion is the correction rate. The algorithms with highest correction rates were selected.

The system consists of 9 blocks: signal pre-processing block, QRS detection block, baseline removal block, Q and S wave detection block, T wave detection block, fiducial point detection block, feature extraction block, artificial neural network training block, and artificial testing block.

The present system reached a promising result; the sensitivity is significantly higher than ($P<0.05$) those of cardiologists and specificity (after correcting the mistake of the old filter) is as good as those of cardiologists (see Table 5.3). However, according to the opinions of the cardiologists who cooperated in the current research, the correction rate is still too low, not acceptable as the only tool for myocardial infarction.

Future work may (1) expand the current system to multi-lead system, such as the

routine 12-lead, system to diagnose myocardial infarction, (2) embed this system to the diagnosing equipment which do not have the function of myocardial infarction detection.

Due to the modular design of the present system, it is not too complex to complete the above two tasks. Figure 5.2 shows the mechanism to finish task 1. For example, n=12. The ECG input will contain 12 leads ECG. Each lead is fed into one system, from system 1 to system 12. The output of each system is the diagnosis of whether the patient has myocardial infarction beat in that lead. The more leads used, the more information is revealed.

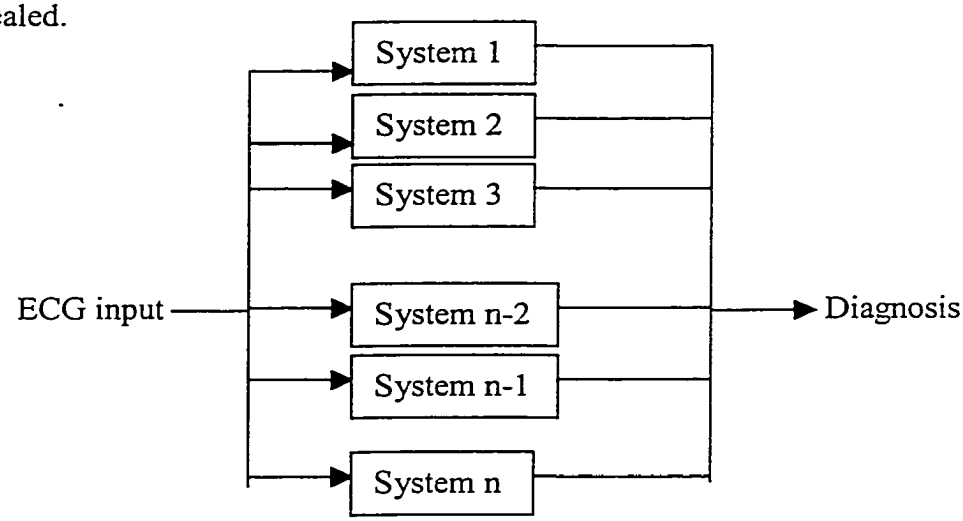

Figure 5.2 Mechanism to Make a Multi-lead System

For task 2, since the whole system is a single input, single output system, the interface with other systems is very flexible. The whole system can be embedded into other systems as a component.

APPENDIX

MATLAB ROUTINES

```
%%%%%%%%%%%%%%%%%%%%%%%%%%%%%%%%%%%%
function [num, denum] = cheby2_coeffi( level, cut_off, sam_freq)
% It generates the numerator and denominator for the second type chebyshev filter
% level controls the level of the filter
% cut_off is the cut off frequency
% sam_freq is the sampling frequency of the signal
% num is the numerator of the coefficient
% denum is the denominator of the coefficient
%%%%%%%%%%%%%%%%%%%%%%%%%%%%%%%%%%%%
function [mag, phase, w]=cheby2_bode( level, cut_off, fs)
% It generates the bode plot of the second type chebyshev filter
% mag is the magnitude response
% phse is the phase response
% w contains the frequencies, in radians/sec, at which the bode response is evaluated
% level is the orderof the filter
% cut_off is the cut_off frequency of the filter
% fs is the sampling frequency
%%%%%%%%%%%%%%%%%%%%%%%%%%%%%%%%%%%%
function [signal] = read_data(size)
% It read data from the file
% signal is the vector read from the file
% size controls the amount of data read from the file
%%%%%%%%%%%%%%%%%%%%%%%%%%%%%%%%%%%%
function [] = plot_data(data)
% It plots the data
%%%%%%%%%%%%%%%%%%%%%%%%%%%%%%%%%%%%
function [pxx, f] = plot_psd(b, fs)
% plot_psd draws the rough power spectrum density of the signal.
% b is the signal
% fs is the sampling frequency
% pxx is the approximate psd vector
% f is the frequency
%%%%%%%%%%%%%%%%%%%%%%%%%%%%%%%%%%%%
function [ratio] = percentage_psd(psd, freq, low, high)
% percentage_psd calculates the percentage of certain frequency period
% in the rought power spectrum density.
% freq is the vector of the same length of psd, at which the power spectrum density of
% the signal is estimated
% psd is the approximate psd vector
% low the lower boundary of the frequency period
% high is the higher boundary of the frequency period
```

```
%%%%%%%%%%%%%%%%%%%%%%%%%%%%%%%%%%%%%%%%%%%%
function [num, denum] = butter_coeffi(level, cut_off, sam_freq)
% It generates the numerator and denominator for the butterworth filter
% level controls the level of the filter
% cut_off is the cut off frequency
% sam_freq is the sampling frequency of the signal
% num is the numerator of the coefficient
% denum is the denominator of the coefficient
%%%%%%%%%%%%%%%%%%%%%%%%%%%%%%%%%%%%%%%%%%%%
function [mag, phase, w] = butter_bode(level, cut_off, fs)
% It generates the bode plot of the butterworth filter
% mag is the magnitude response
% phse is the phase response
% w contains the frequencies, in radians/sec, at which the bode response is evaluated
% level is the orderof the filter
% cut_off is the cut_off frequency of the filter
% fs is the sampling frequency
%%%%%%%%%%%%%%%%%%%%%%%%%%%%%%%%%%%%%%%%%%%%
function [num, denum] = cheby1_coeffi(level, cut_off, sam_freq)
% It generates the numerator and denominator for the first type chebyshev filter
% level controls the level of the filter
% cut_off is the cut off frequency
% sam_freq is the sampling frequency of the signal
% num is the numerator of the coefficient
% denum is the denominator of the coefficient
%%%%%%%%%%%%%%%%%%%%%%%%%%%%%%%%%%%%%%%%%%%%
function [mag, phase, w] = cheby1_bode(level, cut_off, fs)
% It generates the bode plot of the first type chebyshev filter
% mag is the magnitude response
% phse is the phase response
% w contains the frequencies, in radians/sec, at which the bode response is evaluated
% level is the orderof the filter
% cut_off is the cut_off frequency of the filter
% fs is the sampling frequency
%%%%%%%%%%%%%%%%%%%%%%%%%%%%%%%%%%%%%%%%%%%%
function [signal, i ] = filter(signal, num, denum)
% If filters the signal to get the new signal
% signal in input is the raw signal to be processed
% num is the numerator of the filter coefficients
% denum is the denominator of the filter coefficients
% i is the size of the signal
```

```
% signal in output is the signal after filtering
%%%%%%%%%%%%%%%%%%%%%%%%%%%%%%%%%%%%%%%%
function [num, denum] = notch_coeffi(level, cut_off, sam_freq)
% It generates the numerator and denominator for the notch filter
% level controls the level of the filter
% cut_off is the cut off frequency
% sam_freq is the sampling frequency of the signal
% num is the numerator of the coefficient
% denum is the denominator of the coefficient
%%%%%%%%%%%%%%%%%%%%%%%%%%%%%%%%%%%%%%%%
function [mag, phase, w] = notch_bode(level, cut_off, fs)
% It generates the bode plot of the notch filter
% mag is the magnitude response
% phse is the phase response
% w contains the frequencies, in radians/sec, at which the bode response is evaluated
% level is the orderof the filter
% cut_off is the cut_off frequency of the filter
% fs is the sampling frequency
%%%%%%%%%%%%%%%%%%%%%%%%%%%%%%%%%%%%%%%%
function [QRSTemplate] = Template( QRS)
% It generates the new QRS template based on the old QRS
% QRS is the input QRS vector
% QRSTemplate is the average the latest four QRSs
%%%%%%%%%%%%%%%%%%%%%%%%%%%%%%%%%%%%%%%%
function [white_QRS]=whiten_QRS(QRSTemplate, u, q, w, m, b)
% It whites the QRS template to prepare for the matched filter
% QRSTemplate is the template of QRS
% u is the AR parameters
% q is the summation parameter
% w is the weight
% m is the weight update summation parameter
% b is the momentum
% white_QRS is the white QRS
%%%%%%%%%%%%%%%%%%%%%%%%%%%%%%%%%%%%%%%%
function [y]=whiten_signal( ecg, q, u, w, m, b)
% It whites the ecg signal
% ecg is the raw ecg data after the filtering
% q is the summation parameter
% u is the AR parameters
% q is the summation parameter
% w is the weight
```

```
% m is the weight update summation parameter
% b is the momentum
% y is the whited signal
%%%%%%%%%%%%%%%%%%%%%%%%%%%%%%%%%%%%%%%%%%%%%
function [total_signal]=connect(signal1, signal2)
% It concatenates signal1 and signal2, in this order, to form total_signal
% signal1 is the one input signal
% signal2 is the other input signal
% total_signal is the concatenation of signal1 and signal2.
%%%%%%%%%%%%%%%%%%%%%%%%%%%%%%%%%%%%%%%%%%%%%
function [signal]=sigmoid(signal, t)
% It generates the signal using sigmoid function
% signal in input is the form of a vector
% t is the parameter contorlling the non-linearity of the function.
% signal in the output is the output of the sigmoid function
%%%%%%%%%%%%%%%%%%%%%%%%%%%%%%%%%%%%%%%%%%%%%
function [newAR]=AR_coeffi(AR, step_size, error, momentum, signal)
% It generates the new auto-regressive parameter based on the previous paramters
% AR is the old auto-regressive paramters, a vector
% step_size controls the search step
% error is the instantaneous error
% momentus is used to reduce the random fluctuation
% signal here is the ecg
% newAR is the new auto-regressive parameter
%%%%%%%%%%%%%%%%%%%%%%%%%%%%%%%%%%%%%%%%%%%%%
function [error]=instant_error(signal, h, u)
%It calculates the instantaneous error of the whiten filter
% signal is the signal to be processed by the filter
% h is the order of signal
% u is the current auto-regressive parameter
%%%%%%%%%%%%%%%%%%%%%%%%%%%%%%%%%%%%%%%%%%%%%
function [new_weight] = weight_update(weight, step_size, error, momentum)
% It calcuates the new weight for the hidden layer
% weight is the current weight vector
% step_size controls the search step
% error is the instantaneous error
%momentum is used to reduce the random fluctuation
% new_weight is the new weight
function [output] = matched_filter(whiteQRS, white_signal, l)
% It generates the signal passing the matched filter
% whiteQRS is the QRS after passing the whiten filter
```

```
% white_signal is the signal after passing the whiten filter
% l is the summation parameter
% output is the signal after passing the matched_filter
%%%%%%%%%%%%%%%%%%%%%%%%%%%%%%%%%%%%%%%%%%%%%%%%%%%%%%%%
function [y]=difference(ecg)
% It generates signal according to 5 point difference equation
% ecg is the input signal
% y is the output according to the equation y(n)=1/8*{-x(n-2)-2x(n-1)+2x(n+1)+x(n+2)}
%%%%%%%%%%%%%%%%%%%%%%%%%%%%%%%%%%%%%%%%%%%%%%%%%%%%%%%%
function [z]=square(y)
% It generates point to point sqaure of y
% y is the input signal
% z is the square of y
%%%%%%%%%%%%%%%%%%%%%%%%%%%%%%%%%%%%%%%%%%%%%%%%%%%%%%%%
function [w]=moving_window_integration(z, n)
% It generates the moving window integration of z
% z is the signal to be processed
% n is the window length
% w is the signal passing the moving window integration
%%%%%%%%%%%%%%%%%%%%%%%%%%%%%%%%%%%%%%%%%%%%%%%%%%%%%%%%
function [slope] = angle(data)
% It calculates the slope of each point in data
% data is the input signal
% slope is the slope of each point in data
%%%%%%%%%%%%%%%%%%%%%%%%%%%%%%%%%%%%%%%%%%%%%%%%%%%%%%%%
function [Qs, Q, R, S, Se, Ts, Tp, Tn, Te, J, Tleft_angle, Tright_angle, Qindex, Teindex,
Seindex, Tsindex] = fiducial(ecg)
% It calculates the fiducial points of ecg
% ecg is the input signal
% Qs is the starting point of QRS
% Q is the peak of Q wave
% R is the peak of R wave,
% S is the peak of S wave,
% Se is the ending point of QRS
% Ts is the starting point of T wave
% Tp is the positive peak of T wave
% Tn is the negative peak of T wave
% Te is the ending point of T wave
% J is the J point
% Tleft_angle is the angle formed by the leftside
% Tright_angle is the angle formed by the rightside
```

```
% Qindex is the index of Q wave
% Teindex is the index of T wave
% Seindex is the index of ending point of QRS
% Tsindex is the index of starting point of T wave
%%%%%%%%%%%%%%%%%%%%%%%%%%%%%%%%%%%%%%%%%%%%%%%%%%%%%%%%%%%%
function [featureQT] =featureQT(Teindex, Qindex, fs)
% It calculates the QT interval
% Teindex is the ending point of T wave
% Qindex is the index of Q wave
% fs is the sampling frequency
% featureQT is the QT interval
%%%%%%%%%%%%%%%%%%%%%%%%%%%%%%%%%%%%%%%%%%%%%%%%%%%%%%%%%%%%
function [featureST]=featureST(Tsindex, Seindex, fs)
% It calculates the ST duration
% Tsindex is the index of strating point of T wave
% Seindex is the index of ending point of S wave
% fs is the sampling frequency
% featureST is the ST duration
%%%%%%%%%%%%%%%%%%%%%%%%%%%%%%%%%%%%%%%%%%%%%%%%%%%%%%%%%%%%
function [1ofst, 2ofst, 3ofst, 4ofst, 5ofst, 6ofst, 7ofst, 8ofst]=features(Seindex, Tsindex,
ecg)
% It calculates the 1/8 of ST segment, 2/8 of ST segment, to 8/8 of ST segment
% Seindex is the ending point index of S wave
% Tsindex is the starting point index of T wave
% ecg is the ecg
% 1ofst is 1/8 of ST segment
% 2ofst is 2/8 of ST segemnt
% 3ofst is 3/8 of ST segment
% 4ofst is 4/8 of ST segment
% 5ofst is 5/8 of ST segment
% 6ofst is 6/8 of ST segment
% 7ofst is 7/8 of ST segment
% 8ofst is 8/8 of ST segment
%%%%%%%%%%%%%%%%%%%%%%%%%%%%%%%%%%%%%%%%%%%%%%%%%%%%%%%%%%%%
function [y]=derivative( data, order)
% It calculates the derivative of data input
% data is the input data to be processed
% order is the order of the derivative
% y is the output
%%%%%%%%%%%%%%%%%%%%%%%%%%%%%%%%%%%%%%%%%%%%%%%%%%%%%%%%%%%%
function [index]=ascendcheck(data)
```

```
% It detects the rising point in the data
% data is the input
% index is the index of rising point
%%%%%%%%%%%%%%%%%%%%%%%%%%%%%%%%%%%%%%%%%%%%
function [flag]=under(a, b)
% It compares the value of a and b
% a is the one input parameter for comparison
% b is the other input parameter for comparison
% flag = 1 if a<b, else flag=0
%%%%%%%%%%%%%%%%%%%%%%%%%%%%%%%%%%%%%%%%%%%%
function [flag]=check_region(i, range)
% It detects if i is between the range
% i is the input number for comparison
% range is a vector containing the boundaries
% flag is 0 if the input number is not in the range; or flag is 1
%%%%%%%%%%%%%%%%%%%%%%%%%%%%%%%%%%%%%%%%%%%%
function [flag, index]=smallpeak(ecg)
% It finds the small peak in the ecg and returns the index of the peal
% ecg is the input signal
% flag is 0 when it did not find small peak; it is 1 when smallpeak is found
% index is the index of the peak
%%%%%%%%%%%%%%%%%%%%%%%%%%%%%%%%%%%%%%%%%%%%
function [index]=descendcheck(data)
% It detects the falling point in the data
% data is the input signal
% index is the index of falling point
%%%%%%%%%%%%%%%%%%%%%%%%%%%%%%%%%%%%%%%%%%%%
function [index]=surecurve(ecg)
% It detects the curve peak point of ecg
% ecg is the input signal
% index is the index of the peak point
%%%%%%%%%%%%%%%%%%%%%%%%%%%%%%%%%%%%%%%%%%%%
function [code]=localpeak(ecg, threshold)
% It detects the local peak in the data compared to the threshold
% ecg is the input signal
% threshold is the parameter controlling the size of the peal
% code is 0, meaing no local peak is found; it is 1 when the local peak is found

function [code]=localvalley(ecg, threshold)
% It detects the local valley in the ecg compared to the threshold
% ecg is the input signal
```

```
% threshold controls the size of valley
% code is 0 when there is no local valley; when the local valley is found, code is 1.
%%%%%%%%%%%%%%%%%%%%%%%%%%%%%%%%%%%%%%%%%%%%%%%%%%%%%
function [e] = upward(mwi)
% It detects the upward slope of moving window integration output
% mwi is the moving window integration output
% e is the vector containing upward slope
%%%%%%%%%%%%%%%%%%%%%%%%%%%%%%%%%%%%%%%%%%%%%%%%%%%%%
function [r]=r(ecg)
% It detects the R wave peak in the ecg
% ecg is the input signal
% r is the vector containing the R wave peak index
%%%%%%%%%%%%%%%%%%%%%%%%%%%%%%%%%%%%%%%%%%%%%%%%%%%%%
function [c] = signchange(data)
% It detects if there is sign change in the data
% data is the input signal
% c is 0 when there is no sign change; c is 1 when there is sign change.
%%%%%%%%%%%%%%%%%%%%%%%%%%%%%%%%%%%%%%%%%%%%%%%%%%%%%
function [c]=straightline(data, parameter)
% It detects if the data is a straight line in the range controlled by parameter
% data is the input signal
% parameter controls the tiny fluctuation of the line
% c is 0 when the line is not a straight line; else it is 1.
%%%%%%%%%%%%%%%%%%%%%%%%%%%%%%%%%%%%%%%%%%%%%%%%%%%%%
function [c] =testcurve(data)
% It detects if the data forms a curve
% data is the input signal
% c is 1 when the data forms a curve; else, it is 0
%%%%%%%%%%%%%%%%%%%%%%%%%%%%%%%%%%%%%%%%%%%%%%%%%%%%%
function [featureT]=featureT(Tsindex, Teindex)
% It calculates the T wave duration
% Tsindex is the index of the starting point of T wave
% Teindex is the index of the ending point of T wave
% featureT is the T wave duration
%%%%%%%%%%%%%%%%%%%%%%%%%%%%%%%%%%%%%%%%%%%%%%%%%%%%%
function [flag]=below_region(i, range)
% It detects if i is below range
% i is the input number
% range is the threshold
% flag is 0 when i is less than range; else it is 1
%%%%%%%%%%%%%%%%%%%%%%%%%%%%%%%%%%%%%%%%%%%%%%%%%%%%%
```

```
function [f0, f1, f2, f3, f4, f5, f6, f7, f8, f9, f10, f11, f12, f13, f14, f15, f16, f17, f18, f19]
= feature_extraction(ecg)
% It extracts features from ecg
% ecg is the input signal
% f0 is the first feature
% f1is the second feature
% f2 is the third feature
% f3 is the fourth feature
% f4 is the fifth feature
% f5 is the sixth feature
% f6 is the seventh feature
% f7 is the eighth feature
% f8 is the ninth feature
% f9 is the tenth feature
% f10 is the eleventh feature
% f11 is the twelfth feature
% f12 is the thirteenth feature
% f13 is the fourteenth feature
% f14 is the fifteenth feature
% f15 is the sixteenth feature
% f16 is the seventeenth feature
% f17 is the eighteenth feature
% f18 is the nineteenth feature
% f19 is the twentieth feature
%%%%%%%%%%%%%%%%%%%%%%%%%%%%%%%%%%%%%%%%%%%%%%%%%%%%
function [class] = classification(f0, f1, f2, f3, f4, f5, f6, f7, f8, f9, f10, f11, f12, f13, f14,
f15, f16, f17, f18, f19)
% It classify beats according to their features
% f0 is the first feature
% f1is the second feature
% f2 is the third feature
% f3 is the fourth feature
% f4 is the fifth feature
% f5 is the sixth feature
% f6 is the seventh feature
% f7 is the eighth feature
% f8 is the ninth feature
% f9 is the tenth feature
% f10 is the eleventh feature
% f11 is the twelfth feature
% f12 is the thirteenth feature
```

```
% f13 is the fourteenth feature
% f14 is the fifteenth feature
% f15 is the sixteenth feature
% f16 is the seventeenth feature
% f17 is the eighteenth feature
% f18 is the nineteenth feature
% f19 is the twentieth feature
% class is the vector containing the classification
```

BIBLIOGRAPHY

1. 12 Lead ECG Library, http://homepages.enterprise.net/djenkins/ecghome.html, 2000.

2. AHA ECG Database, http://www.healthcare.ecri.org, 2000.

3. Aleksander, I. and T.J. Stonham. Guide to pattern recognition using random-access memories. Computers and digital techniques, 2:29 - 40, 1979.

4. Alonsozana, G. L., Christenson, R. H. The Case for Cardiac Troponin T: Marker for Effective Risk Stratification of Patients with Acute Cardiac Ischemia. Clinical Chemistry, Vol. 42, 803-808, 1996.

5. American Heart Association News Letter, http://www.americanheart.org/statistics , 1999.

6. Amit, D.J. and H. Gutfreund. Spin-glass models of neural networks. Physical Review A, 32:1007 - 1018, 1985.

7. Ann Arbor Electrogram Libraries, http://electrogram.com, 2000.

8. Antanitus, D. S., A Theory of Cortical Neuron-Astrocyte Interaction http://www.antanitus.com/hypothesis/index.html, 1998.

9. Anthony, M & Bartlett, P. L. Neural Network Learning : Theoretical Foundations. Cambridge Univ. Pr, 1999.

10. Antman, E. M., Tanaaijovic, M. J., Thompson, B. et al. Cardiac-Specific Troponin I levels to predict the Risk of Mortality in Patients with Acute Coronary Syndromes. New England Journal of Medicine. Vol. 335, 1342-1349, 1996.

11. Baxt, W. G. Use of an Artificial Neural Networks for the Data Analysis in Clinical Decision-Making: the Diagnosis of Acute Coronary Oclusion, Neural Computation, Vol. 2, No. 4, 480-489, Winter,1990.

12. Baxt, W. G., Use of an Artificial Neural Networks for the Diagnosis of Myocardial Infarction, Annals of Internal Medicine, Vol. 115, No. 11, 843-848, Dec. 1st 1991.

13. Baxt, W. G., Improving the Accuracy of an Artificial Neural Network using Multiple Differently Trained Networks, Neural Computation, Vol. 4, No. 5, 772-780, Sep., 1992a.

14. Baxt, W. G., Analysis of Clinical Variables Driving Decision in an Artificial Neural Network to Identify the Presence of Myocardial Infarction, Annals in Emergency Medicine, Vol. 21, 1439-1444, Dec., 1992b.

15. Baxt, W. G., A Neural Network Trained to Identify the Presence of Myocardial Infarction Bases Some Decisions on Clinical Associations That Differ from Accepted Clinical Teaching, Medical Decision Making, Vol. 14, No.3, 217-222, July 1 1994.

16. Baxt, W. G., White, H. Bootstrapping Confidence Intervals for Clinical Input Variable Effects in a Network Trained to Identify the Presence of Acute Myocardial Infarction, Neural Computation, Vol. 7, No. 3, 624-638, May 1st, 1995.

17. Baxt, W. G., Skora, J. Prospective Validation of Artificial Neural Network Trained to Identify Acute Myocardial Infarction, Lancet, Vol. 347, 12-15, Jan. 6 1996

18. Belforte, G.,Mori, R. D., and Ferraris, F., A Contribution to the Automatic Processing of Electrocardiogram Using Syntactic Methods, IEEE trans. on Biomed. Engr., Vol. 26, 125-136, 1979.

19. van Bemmel, J. H. Zywietz, Chr., Kors, J. A. Signal Analysis for ECG Interpretation, Methods of Information in Medicine, Vol. 20, 317-329, No. 4, 1990.

20. Bledsoe, W.W. and I. Browning. Pattern recognition and reading by machines. In Proceedings of the Eastern Joint Computer Conference, 225 - 232. 1959.

21. Bishop, C. M., Neural Networks for Pattern Recognition, Oxford University Press, 1995.

22. Bortolan, G., Willems, J. L., Diagnostic ECG Signal Classification based on Neural Networks. Journal of Electrocardiology, Vol. 26, 75-79, supp.1993.

23. Bounds, D. G., Lloyd, P. J., Mathew, B. G. A Comparison of Neural Network and Other Pattern Recognition Approaches to the Diagnosis of Low Back Disorder. Neural Networks. Vol.3 583-591, 1990.

24. Breslow, W. J., Miller, C. G., Parker, S. D. Changes in T-wave Morphology Following Anesthesia and Surgery: A Common Recovery-room Phenomenon. Anesthesiology, Vol. 64, 398-402, 1986.

25. Brest, A. N. & Moyer, J. H.: Cardiovascular Disorders. 1968.

26. Brieman, L., Friedman, J. H., Olshen, R. A., Stone, C. J. Classification and Regression Trees. Wadsworth, Belmont, CA, 1984.

27. Brown, C. S., Bertolet, B. D. Cardiac Tronopin: See You Later CK! [Editorial]. Chest, Vol. 111, No. 1,2-4, 1997.

28. Burattini, L., Zareba, W., Couderc, J. P., Konecki, J. A., Moss, A. J. Optimizing ECG Signal Sampling Frequency for T-Wave Alternans Detection., Computers in Cardiology, Vol. 25, 721-724, 1998.

29. Carpenter, G. and S. Grossberg. A massively parallel architecture for a self-organizing neural pattern recognition machine. Computer Vision, Graphics, and Image Processing, 37:54 - 115, 1987a.

30. Carpenter, G. A. and Grossberg,.S. ART 2: self-organization of stable category recognition codes for analog input pattern. Applied Optics Vol. 26, No. 23, 4919 – 4930, 1987b.

31. Chung, E. K. Principles of Cardiac Arrhythmias 4th ed. Baltimore, MD: Williams & Wilkins, 1989.

32. Clos, K. J., Chen, K., Langerderfer, R. A. Use of Neural Networks in Detecting Cardiac Diseases from Echocardiographic Images. IEEE Engineering in Medicine and Biology Magazine. Vol. 9, 58-60, 1990.

33. Conn, H. L. Jr & Horwitz, O.: Cardiac and Vascular Diseases. 1971.

34. Davis, D., Quick and Accurate 12-Lead Ecg Interpretation, Lippincott Williams & Wilkins Publishers, 3rd Edition, 2001.

35. Del Mar Medical, http://www.delmarmedical.com/Products/accuplus.html, 2000.

36. Devine, B., Macfarlance, P. W. Detection of Electrocardiographic 'Left Ventricular Strain' using Neural Nets. Medical & Biological Engineering & Computing. Vol. 31, No. 4, 343-348, 1993.

37. Ebell, M. H., Flewrlling,D. Flynn, C. A. A Systematic Review of Troponin T and I for Diagnosing Acute Myocardial Infarction. The Journal of Family Practice, Vol. 49, No. 6, 550-556, 2000a.

38. Ebell, M. H., White, L. L., Weismantel, D. A Systematic Review of Troponin T and I Values as a Prognostic Tool for Patients with Chest Pain. The Journal of Family Practice, Vol. 49, No. 8, 746-753, 2000b.

39. Eberhart, R. C., Dobbins, R. W., Hutton, L. V. Neural Network Paradigm Comparisions for Appendictis Diagnosis. In: Proceedings of Fourth Annal IEEE Symposium on Computer-Based Medical Systems, 298-304, 1991.

40. Edenbrandt, L., Heden, B., Pahlm, O. Neural Networks for Analysis of ECG Complexes, Journal of Electrocardiology, Vol 26, 74, supp.1993.

41. Elghazzawi, Z., Geheb, F. Critique of Arrhythmia Detectors Based on Heuristic Rules. Biomedical Instrumentation and Technology, Vol. 31, No. 3, 263-271, 1997.

42. Frenkel, D., Nadal, J. Ischemic Episode Detection using an Artificial Neural Network Trained with Isolated ST-T Segments. Computers in Cardiology, Vol. 26, 53-56, 1999.

43. Fukushima, K., Cognitron: a self-organizing multilayered neural network. Biological Cybernetics, 20:121 - 136, 1975.

44. Garcia, J., Sornmo, L., Olmos, S., Laguna, P. Automatic Detection of ST-T Complex Changes on the ECG using Filtered RMS Difference Series: Application to Ambulatory Ischemia Monitoring. IEEE trans. on Biomedical Engineering, Vol. 47, No. 9, 1195-1201, 2000.

45. GE Medical Systems, http://www.mei.com/products/, 2000.

46. Goldman, L., Cook, E. F., Brand, D. A., *et al.* A Computer Protocol to Predict Myocardial Infarction in Emergency Department Patients with Chest Pain. New England Journal of Medicine. Vol 318, 797-803, 1988.

47. Greenhut, S. E., Chadi, B. H., Lee, J. W., Jenkins, J. M. and Nicklas, J. M., An Algorithm for the Quantification of ST-T Segment Variability, Computers and Biomedical Research, Vol 22, 339-348, 1989.

48. Grossberg, S., Competitive learning: from interactive activation to adaptive resonance. Cognitive Science, 11:23 - 63, 1987.

49. Grossberg, S., Nonlinear neural networks: Principles, mechanisms, and architectures. Neural Networks, 1:17 - 61, 1988.

50. Guyton, A. C. & Hall, J. E. Textbook of Medical Physiology, 9th Edition, W.B. Saunders Company, ISBN 0-7216-5944-6, 1996.

51. Haisty, W. K., Batchlor, C., Cornfield, J., and Pipeberger, H. V., Discriminant Function Analysis of RR intervals: an Algorithm for on-line Arrhythmia Diagnosis, Computers and Biomedical Research, Vol 5, 247, 1972.

52. Harrison, R. F., Marshall, S. J., Kennedy, R. L. The Early Diagnosis of Heart Attacks: a Neurocomputational Approach. In: Proceeding of the International Joint Conference on Neural Networks (1991). Vol. I, 1-5.

53. Hart, A., Wyatt, J. Connectionist Models in Medicine: an Investigation of their Potential. In: Proceedings of AIME'89 (2nd European Conference on Artificial Intelligence in Medicine, London, 1989). Heidelberg: Springers, 115-124, 1989.

54. Hebb, D.O., The Organization of behavior. John Wiley, 1949.

55. Heden, B., Edenbrandt, L., Haisty, W. K. & Pahlm, O., Artificial Neural Networks for the Electrocardiographic Diagnosis of Healed Myocardial Infarction, The American Journal of Cardiology, Vol. 74, No. 1, 5-8, July 1, 1994.

56. Heden, B., Ohlsson, M., Rittner, R., Pahlm, O., Haisty, W. K., Peterson, C. and Edenbrandt, L. Agreement Between Artificial Neural Networks and Experienced Electrocardiographer on Electrocardiogy Diagnosis of Healed Myocardial Infarction Journal of the American College of Cardiology, Vol. 28, No. 4, 1012-1016, 1996.

57. Heden, B., Ohlin, H., Rittner, R., and Edenbrandt, L. Acute Myocardinal Infarction Detected in the 12-lead ECG by Artificial Neural Networks, Circulation, Vol. 96, No. 6, 1798-1802, 1997.

58. Hiraiwa, A. Shimohara, K., Tokunaga, Y. EEG Topography Recognition by Neural Networks. IEEE Engineering in Medicine and Biology Magazine. Vol. 9, 39-42, 1990.

59. Hopfield, J.J,. Neural networks and physical systems with emergent collective computational properties. Proceedings of the National Academy of Sciences of the USA, 79:2554 - 2588, 1982.

60. Hu, Y. H., Tompkins, W. J., Urrusti, J. L. Applications of Artificial Neural Networks for Analysis of ECG Signal Detection and Classification. Journal of Electrocardiology, Vol. 26, 66-73, supp. 1993.

61. Hu, Y. H., Palreddy, S., Tompkins, W. J. A Patient-Adaptable ECG Beat Classifier Using a Mixture of Experts Approach. IEEE trans. on Biomedical Engineering, Vol 44, No. 9, 891-900, 1997.

62. Hudson, D. L., Cohen, M. E., Anderson, M. F., Determination of Testing Efficacy in Carcinoma of the Lung using a Neural Network Model. Symposium on Computer Application in Medical Care 1988 Proceeding: 12th Annual Symposium, Washington, D. C. Vol. 12, 251-256, 1988.

63. Improve Data Library, http://www.vtt.fi/tte/samba/projects/improve/improve.htm, 2000.

64. Jenkins.D.,ECGdatabase, http://www.homepages.enterprise.net/djenkins/ecghome.htm#contents, 1998.

65. Jonsbu, J., Aase, O., Rollag, A., Liestol, K., Erikssen, J. Prospective Evaluation of an EDB-based Diagnostic Program to be Used in Patients Admitted to Hospital with Acute Chest Pain. European Heart Journal. Vol 14, No. 4, 441-446, 1993.

66. Jurlander, B., Clemmensen, P., Wagner, G. S., Grande, P. Very Early Diagnosis and Risk Stratification of Patients Admitted with Suspected Acute Myocardial Infarction by the Combined Evaluation of a Single Serum Value of Cardiac Troponin-T, Myoglobin, and Creatine Kinase MB. European Heart Journal, Vol. 21, No. 5, 2000.

67. Katz, A. M. Physiology of the Heart. 5th ed. New York: Raven Press, 1977.

68. Kaufman, J. J., Chiabera, A., Hatem, M., *et al.* A Neural Network Approach for Bone Fracture Healing Assessment. IEEE Engineering in Medicine and Biology Magazine. Vol. 9, 23-30, 1990.

69. Kelly, S. J., ECG Interpretation: Identifying Arrhythmia, Philadelphia: J. B. Lippincott Co., 1984.

70. Kennedy, R. L., Burton, A. M., Fraser, H. S., McStay, L. N., Harrison, R. F., Early Diagnosis of Acute Myocardial Infarction (AMI) Using Clinical and Electrocardiographic Data at Presentation: Derivation and Evaluation of Logistic Regression Models, European Heart Journal, Vol. 17, No.8, 1181-1191, 1996.

71. Kennedy, R. L., Harrison, R. F., Burton, A. M., Fraser, H. S., Hamer, W. G., MacArthur, D., McAllum, R. And Steedmsn, D. J., An Artificial Neural Network System for Diagnosis of Acute Myocardial Infarction (AMI) in the Accident and Emergency Department: Evaluation and Comparison with Serum Myoglobin Measurements, Computer Methods and Programs in Biomedicine, Vol. 52, No.2, 93-103, 1997.

72. Kohonen, T., Self-organization and associative memory. Springer Verlag, 1984.

73. Komreich, F., Montague, T. J., Rautaharju, P. M. Body Surface Potential Mapping of ST Segment Changes in Acute Myocardial Infarction: Implications for ECG Enrollment Criteria for Thrombolytic Therapy. Circulation, Vol. 87, 773-782, 1993.

74. Kuppuraj, R. N. CORDOC - A Hybrid AI Approach to ECG Interpretation. Ph. D. Dissertation, Louisiana Tech University, 1995.

75. Laguna, P., Jane, R., Olmos, S., Thakor, N. V., Rix, H., Caminal, P. Adaptive Estimation of QRS Complex Wave Features of ECG Signal by the Hermite Model, Medical & Biological Engineering & Computing, Vol.34, No.1, 58-68, 1996.

76. Laguna, P., Mark, R. G., Goldberg, A., and Moody, G. B., A Database for Evaluation of Algorithms for Measurement of QT and other Waveform Intervals in the ECG, Proceedings of Computers in Cardiology, Vol.24, 673-676, 1997.

77. Lazzara, R. "Basic Electrophysiology". In Bellet's Essentials of Cardiac Arrhythmias, ed. R. H. Helfant, 16-34. Philadelphia, PA: W.B. Saunders, Co., 1979.

78. Leblanc, A. R., Quantitative Analysis of Cardiac Arrhythmia, CRC Critical Reviews in Biomedical Engineering, Vol. 14, 1-60, 1989.

79. Lee, H. S., Corss, S. L., Garthwaite, P., Dickie, A., Ross, I., Walton, S., Jennings, K. Comparison of the value of novel rapid measurement of myoglobin, creatine kinase, and creatine kinase-MB with the electrocardiogram for the diagnosis of acute myocardial infarction. British Heart Journal. Vol. 71, No. 4, 311-315. 1994.

80. Leondes, C. T. (Editor) Algorithms and Architectures (Neural Network Systems Techniques and Applications Series , Vol. 1), Academic Pr, 1997.

81. Li, C., Zheng, C. and Tai, C. Detection of ECG Charactersitic Points using Wavelet Transforms, IEEE Trans. on Biomed. Engr., Vol. 42, 21-28. 1995.

82. Lin, K. & Chang, W. H. Classification of QRS Pattern by an Associative Memory Model. Proc. IEEE Engg. In Med. & Biol. Soc. 11th Annual International Conference, Track 14 - Neural Networks. 2017-2018, 1989.

83. Lippman, R. P. An Introduction to Computing with Neural Nets. IEEE ASSP Magazine, Vol 4, No 2, 4-22, 1987.

84. Little, W.A., The existence of persistent states in the brain. Mathematical Biosciences, 19:101 - 120, 1974.

85. Macfarlane, P. W., and Lawrie, T. D. V., An Introduction to Automated Electrocardiogram Interpretation, Published by Butterworths & Co. Ltd, 1974.

86. Macfarlane, P. W., and Lawrie, T. D. V., Comprehensive Electrocardiology, Vol.3 Oxford : Pergamom Press, 1989: 1543-1552.

87. Magoulas, G. D., Vrahatis, M. N. & G. S. Androulakis, Improving the Convergence of the Backpropagation Algorithm Using Learning Rate Adaption Methods, Neural Computation 11, 1769-1796, 1999.

88. Malr, J., Genser, N., Morandell, D., Maler, J. et al. Cardiac-Specific Troponin I in the Diagnosis of Myocardial Injury and Infarction. Clin Chim Acta. Vol. 245, 19-38, 1996.

89. Mandelbrot, B.B., The Fractal Geometry of Nature. W. H. Freeman & Co., 1988.

90. Marconi, L., Scalla, F., Ridella, S., Arrigo, P., Manal, C., Mela, G. S. An Application of Back Propagation to Medical Diagnosis. Proceedings of the International Joint Conference on Neural Networks, San Diego. Vol. 2, 255-262, 1988.

91. McCulloch, W. and Pitts, W. A logical calculus of the ideas immanent in nervous activity. Bulletin of Mathematical Biophysics, 7:115 - 133. 1943.

92. MGH Database, http://www.mgh.harvard.edu, 2000.

93. Michaelides, A. P., Triposkiadls, F. K., Boudoulas, H. New Coronary Artery Disease Index Based on Exercise Induced QRS Changes. American Heart Journal, Vol. 120, 292-302, 1990.

94. Minsky, M. and S. Papert. Perceptrons. MIT Press, 1969.

95. Moody, G. M., MIT-BIH Arrhythmia Database Directory, 3th ed, Harvard University-MIT Division of Health Sciences and Technology, 1992.

96. Murphy, M. J., Berding, C. B. Use of Measurements of Myoglobin and Cardiac Tropinins in the Diagnosis of Acute Myocardial Infarction. Critical Care Nurse, Vol. 19, No. 1, 58-66, 1999.

97. Pahlm, O. & Sornmo, L. Software QRS Detection in Ambulatory Monitoring - A Review. Medical & Biological Engineering & Computing. Vol. 22, 289-297, 1984.

98. Pan, J. and Tompkins, W., A Real Time QRS Detection Algorithm, IEEE trans.on Biomedical Engineering. Vol. 32, 230-236, 1985.

99. Parker, D. B., Learning-logic. Technical Report 581-64, Office of Technology Licensing, Stanford University, 1982.

100. Pipberger, H. V., Arms, R. J. and Stallman, F. W., Automatic Screening of Normal and Abnormal Electrocardiograms by Means of a Digital Computer, Proceedings of Society for Experts in Biology and Medicine, Vol.106, 130, 1961.

101. Pozen, M. W., D'Agostino, R. B., Selker, H. P., Sytokowski, P. A., Hood, W. B., A Predictive Instrument to Improve Coronary Care Unit Admission Practices in Acute Ischaemic Heart Disease. New England Journal of Medicine. Vol. 310, 1273-1278, 1984.

102. Proakis, J. G., Manolakis, D. G., Digital Signal Processing: Principles, Algorithms and Applications, 3rd Edition, Prentice Hall, 1995.

103. Rasiah, A. I., Togneri, R. and Attikiouzel, Y. QRS Detection using Morphological and Rhythm Information, IEEE International Conference on Neural Networks, 1995.

104. Rognvaldsson, T. On Langevin Updating in Multilayer Perceptrons. Neural Computation, Vol. 6, No. 5, 916-926. 1994.

105. Rosenblatt, F., Principles of Neurodynamics: Perceptrons and the Theory of Brain Mechanisms. Spartan Books, 1962.

106. Rumelhart, D. and D. Zipser. Feature discovery by competitive learning. Cognitive Science, 9:75 - 112, 1985.

107. Rumelhart, D.E., G.E. Hinton, and R.J. Williams. Learning representations by back-propagating errors. Nature, 323:533 - 536, 1986.

108. Salto, K., Nakano, R. Medical Diagnosis Expert System Based on PDP Model. Proceedings of the International Joint Conference on Neural Networks, San Diego. Vol. 2, 255-262, 1988.

109. Schimminger, T., Analysis and Modeling of ECG Signals Using Nonlinear Methods, Ph.D. Dissertation, Technische University Dresden, Denmark, http://circhp.epfl/ch/~schimmin/uni/beleg/body.html, 1998.

110. Shaw, G. R., Savard, P. On the Detection of QRS Variations in the ECG. IEEE trans. on Biomedical Engineering, Vol. 42, No. 7, 736-741, 1995.

111. Sheffield, L. T., The Role of Computerized ECG Interpretation in Clinical Trials, Journal of Electrocardiology - Supplemental Issues, 37-44, 1987.

112. Smith, J. W., Everhart, J. E., Dickson, W.C., Knowler, W. C., Johannes, R. S. Using the ADAP Learning Algorithm to Forecast the Onset of Diabetes Mellitus. Symposium on Computer Application in Medical Care 1988 Proceeding: 12th Annual Symposium, Washington, D. C. Vol. 12, 251-256, 1988.

113. Srikanth, T., Ph. D. dissertation, Bottom-Up Design of Artificial Neural Network for Single Lead Electrocardiogram Beat and Rhythm Classification, 2000.

114. Taddei, A., Benassi, A., Biagini, A., Bongiorni, M.G., Contini, C., Distante, G., Landucci, L., Mazzei, M.G., Pisani, P., Roggero, N., Varanini, M., Marchesi, C. ST-T change analysis in ECG ambulatory monitoring: a European standard for performance evaluation. Computers in Cardiology, Vol.14, 63-68, 1987.

115. Taddei, A., Biagini, A., Distante, G., Marchesi, C., Mazzei, M.G., Pisani, P., Roggero, N., Zeelenberg, C. An annotated database aimed at performance evaluation of algorithms for ST-T change analysis. Computers in Cardiology, Vol.16,117-120, 1989.

116. Timmis, A. D. Early Diagnosis of Acute Myocardial Infarction: Electrocardiography is Still Best. British Medical Journal, Vol. 301, 941-942, 1990.

117. Vila, J. A., Gang, Y., Presedo, J. M. R., Fernanadez-Delgado, M., Barro, S., and Malik, M., A New Approach for TU Complex Characterization, IEEE trans. On Biomed. Engr., Vol. 47, 764-772, No. 6, June 2000.

118. Weiner, D. A., Exercise Testing for the Diagnosis and Severity of Coronary Diseases. Jounal of Cardiac Rehabilitation, Vol. 1, 438-444, 1981.

119. White, H., Neural Network Learning and Statistics. AI Expert Magazine. 1989 (Dec) 48-52.

120. Widrow, B., Stearns, S. D. Adaptive Signal Processing. Englewood Cliffs, NJ: Prentice Hall, 1985.

121. Willems, J. L., Quantitative Electrocardiography -- Standardization and Performance Evaluation, Electrocardiography -- Past and Future, Ed: Coumel. P. and O, B. Garfein, 329-342, New York: The New York Academy of Science, 1990.

122. De Winter, R. J., Koster, R. W., Sturk, A., Sanders, G. T. Value of Myoglobin, Troponin T, and CK-MB in Ruling out Acute Myocardial Infarction in the Emergency Room. Circulation, Vol. 12, 3401-3407, 1995.

123. De Winter, R. J., Lijmer, J. G., Koster, R. W., Hoak, F. J., Sanders, G. T. Diagnostic Accuracy of Myoglobin Concentration for the Early Diagnosis of Acute Myocardial Infarction. Annals of Emergency Medicine, Vol. 35, No. 2, 113-120, 2000.

124. Wong, S. S. Strategic Utilization of Cardiac Markers for the Diagnosis of Acute Myocardial Infarction. Ann Clin Lab Sci. Vol. 26, 301-312, 1996.

125. Xue, Q., Hu, Y. H. & Tompkins, W. J. Adaptive Matched Filtering for ECG Detection. Proc. Ann. Int. Conf. IEEE Eng. Med. & Biol. Soc. 10th Annual International Conference, 145-146, 1988.

126. Xue, Q., Hu, Y. H. & Tompkins, W. J. A Neural Network Weight Pattern Study with ECG Pattern Recognition. Proc. IEEE Eng. In Med. & Biol. Soc. 11th Annual International Conference, Track 14 - Neural Networks. 2023-2024, 1989.

127. Xue, Q., Hu, Y. H. & Tompkins, W. J. Training of ECG signals in Neural Network Pattern Recognition. Proc. IEEE Eng. In Med. & Biol. Soc. 12th Annual International Conference, 1465-1466, 1990.

128. Xue, Q., Hu, Y. H. and Tompkins, W. J., Neural-network-based Adaptive Matched Filtering for QRS Detection, IEEE trans. on Biomed. Engr. Vol. 39, 317-329, 1992.

129. Yoon, Y. O., A Desktop Neural Network for Dermatology Diagnosis, Journal of Neural Network Computation. 43-52, 1989.

130. Yusuf, S., Pearson, M., Sterry, H. et al. The Entry ECG in the Early Diagnosis and Prognostic Stratification of Patients with Suspected Acute Myocardial Infarction. European Heart Journal, Vol. 5, 690-696, 1984.